Study of the nonlinear properties and propagation characteristics of the uterine electrical activity during pregnancy and labor

Ahmad Diab

Par **Ahmad DIAB**

Study of the nonlinear properties and propagation characteristics of the uterine electrical activity during pregnancy and labor

Thèse présentée en cotutelle pour l'obtention du grade de Docteur de l'UTC

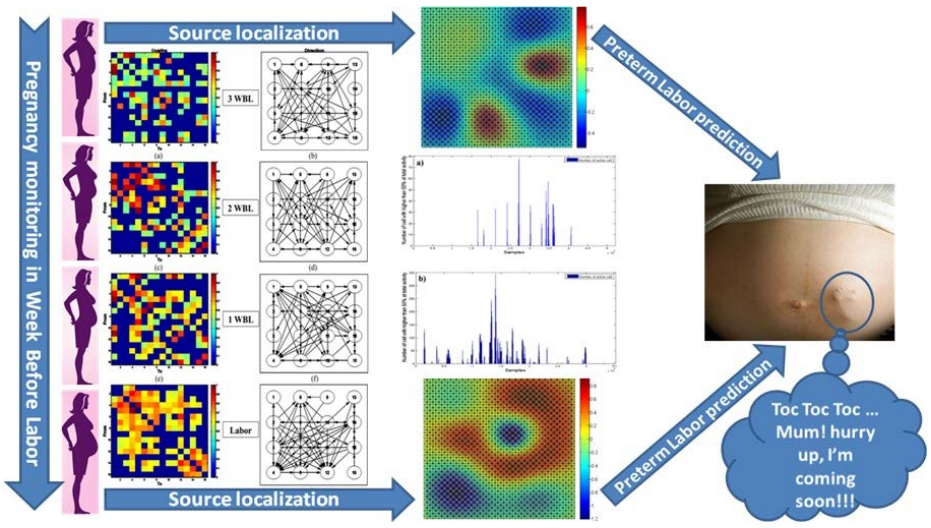

Soutenue le 11 juillet 2014
Spécialité : Biomécanique, Bio-ingénierie

D2140

Université de technologie de Compiègne & Reykjavik University

Thesis to receive the PhD degree in "**Biomedical Signal Processing**" issued by

Ecole Doctorale des Sciences pour l'Ingénieur (UTC)
&
School of Science and Engineering (RU)

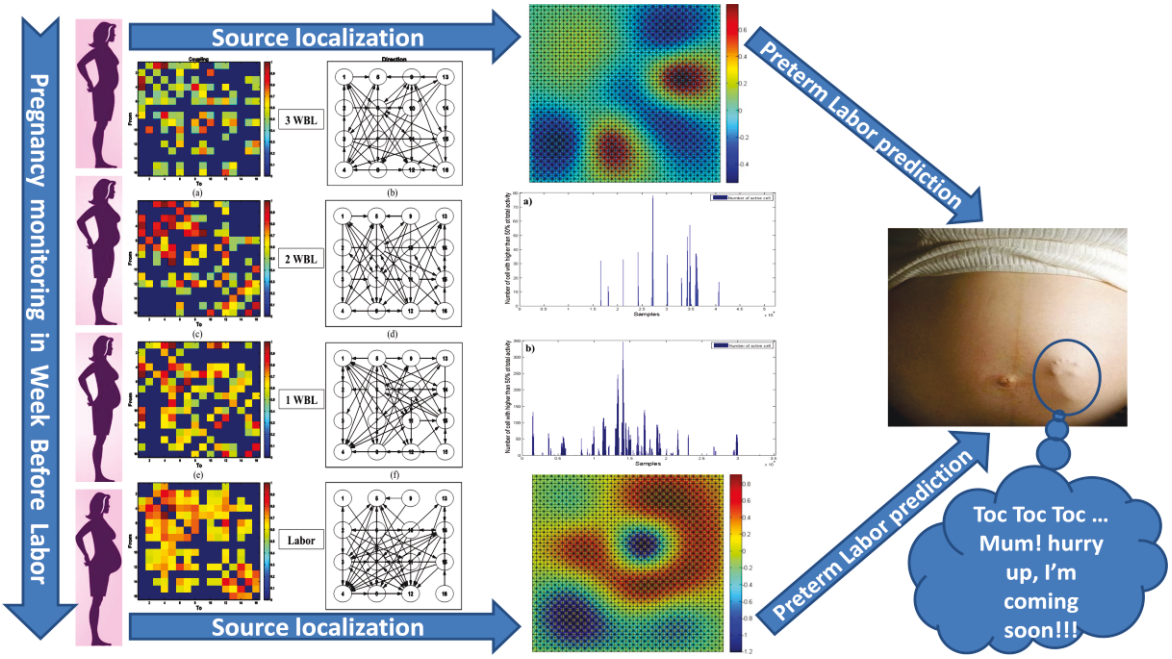

Presented and publicly defended 11 July 2014 by

Ahmad DIAB

Study of The Nonlinear Properties And Propagation Characteristics Of The Uterine Electrical Activity During Pregnancy And Labor

Examining committee Members

Catherine MARQUE	Prof., Université de Technologie de Compiègne	***Supervisor***
Brynjar KARLSSON	Prof., Reykjavik University	***Supervisor***
Fabrice WENDLING	Prof., LTSI, Université de Rennes1	***Reviewer***
Massimo MISCHI	Associate Prof., Eindhoven University of Technology	***Reviewer***
Mohamad KHALIL	Prof., Université Libanaise, Liban	***Examiner***
Þóra STEINGRIMSDOTTIR	Prof., Landspitali University Hospital	***Examiner***
Sofiane BOUDAOUD	Assistant Prof., Université de Technologie de Compiègne	***Examiner***

To…

Résumé Français

Titre:

Etude théorique et expérimentale de la propagation de l'EMG utérin: application clinique.

Contenu:

L'objectif global de notre étude à long terme est la prédiction précoce de l'accouchement prématuré. Nous devons donc tout d'abord comprendre le mécanisme du travail. Jusqu'à présent, le fonctionnement de l'utérus n'est pas clairement expliqué. Son évolution, de la grossesse vers l'accouchement, pose toujours de nombreuses questions. Pour être en mesure de prédire l'accouchement prématuré, nous devons tous d'abord comprendre le fonctionnement normal de l'utérus et la façon dont il se maintient au repos pendant toute la grossesse, et pour ensuite contracter et expulser le bébé pendant le travail.

L'objectif de notre recherche est de pouvoir extraire des signaux EMG utérin (Electrohysterogramme, EHG) certains paramètres qui pourraient nous aider à comprendre ce qui se passe dans l'utérus lors du passage de la grossesse au travail. Cette compréhension peut nous conduire à une interprétation physiologique de l'origine de l'accouchement prématuré. Ces paramètres extraits pourraient être inclus dans un système de diagnostic qui serait utilisé pour la surveillance de la grossesse et la prédiction de l'accouchement prématuré.

Le travail est un processus physiologique défini comme des contractions utérines régulières accompagnées par l'effacement et la dilatation du col de l'utérus. Dans l'accouchement normal, les contractions utérines et la dilatation du col sont précédées par des changements biochimiques dans le tissu conjonctif du col utérin. Un travail normal aboutit à la naissance d'un fœtus à terme. Selon la définition de l'Organisation mondiale de la Santé (World Health Organization (WHO) en anglais), l'accouchement prématuré est une accouchement avant 37 semaines de gestation ou moins de 259 jours d'aménorrhée. Chaque naissance survenant après 22 semaines d'aménorrhée et avant 37 semaines est définie comme une naissance prématurée. Une naissance survenant avant 22 semaines d'aménorrhée est considérée comme un avortement par le WHO. L'accouchement prématuré est un sujet d'actualité. En effet, 44000 naissances sont prématurées parmi 750000 naissances en France [1]. L'accouchement prématuré est toujours la complication obstétricale la plus fréquente pendant la grossesse,

avec 20% des femmes enceintes à haut risque d'accouchement prématuré. Aux États-Unis, plus d'un demi million de bébés, soit 1 sur 8, naissent prématurément chaque année.

L'un des principaux problèmes auquel fait face le monde obstétrical dans le développement d'un traitement efficace, est que les causes de l'accouchement prématuré ne sont pas connues dans 40% des cas [2]. La pathogénie de l'accouchement prématuré spontané n'est pas claire: les contractions prématurées spontanées peuvent être causées par une activation précoce du travail normal ou par d'autres causes pathologiques inconnues.

Plus le travail prématuré est détecté tôt, plus il est facile de l'empêcher. Avec un diagnostic précis, on pourrait éviter de traiter les femmes qui ne vont pas donner naissance avant terme [3, 4]. Si l'accouchement prématuré est détecté tôt, les médecins spécialistes peuvent tenter d'arrêter le processus de travail, ou en cas d'échec, ils sont mieux préparés à prendre soin du bébé qui sera né prématurément.

La détection optimale du travail implique de trouver des marqueurs indiquant que le travail va se produire, mais aussi de prédire si il entraînera effectivement une naissance prématurée (accouchement prématuré), pour éviter un traitement inutile d'un nombre significatif de patientes. En outre, ces marqueurs doivent être observées le plus tôt possible, afin que les cliniciens aient le temps pour l'intervention. Par exemple, lorsque la décision est de garder le fœtus "in utero", il semble plus facile de prévenir le début de travail que de l'arrêter. De même, quand une rupture prématurée des membranes se produit, un délai in utéro est précieux afin que l'administration de corticostéroïdes puisse avoir un effet sur la maturation des poumons du fœtus. Même un changement notable dans le dynamique du col peut ne pas être un indicateur fiable du véritable travail. En effet, un grand pourcentage de femmes avec des changements cervicaux établis n'ont pas accouché avant terme alors qu'elles n'étaient pas traitées par des tocolytiques [5].

Beaucoup de travail a été fait sur le sujet de la détection d'accouchement prématuré en utilisant l'EHG [6-10]. Ils sont principalement basés sur les caractéristiques d'excitabilité de l'utérus (caractérisation temporelle et fréquentielle d'une seule voie d'EHG). Le signal EHG est formé de deux composants, une onde basse fréquence, qui est corrélé a la pression intra-utérin (IUP), et une onde de haute fréquence, qui est également divisé en deux composantes de fréquence, de basse fréquence (nommée Fast Wave low (FWL) en anglais) et de haute fréquence (nommé Fast Wave High (FWH) en anglais). FWL et FWH sont supposés être liées à la propagation et à l'excitabilité des EHG respectivement [11]. Beaucoup de travaux ont

porté sur l'analyse des domaines temporel [12-14], fréquentiel [6, 15, 16], temps-fréquence [4, 17, 18], et non linéaire [10, 15] de l'EHG. Par contre les travaux concernant la propagation et la direction du signal EHG sont limitée à quelques études [19-27]. Ces méthodes ne sont toutefois pas utilisées actuellement dans la pratique clinique en raison d'une forte variance des résultats obtenus, avec un taux de prédiction insuffisante. A notre connaissance, aucune étude de localisation de source n'a été faite sur l'EHG.

Dans cette thèse, nous voulons mettre l'accent sur la dynamique de l'activité électrique (direction de propagation, localisation de source). Par conséquent, notre travail est concentré sur le développement et l'amélioration de l'analyse de l'excitabilité, de la propagation, et de la localisation de source du signal EHG. Nous avons utilisé une matrice de 4x4 électrodes pour avoir une image plus complète de l'utérus et des mécanismes contractiles sous-jacents. Nous avons essayé dans ce travail d'améliorer les performances des méthodes non linéaires et de caractérisation de la propagation, en testant leur sensibilité à différentes étapes de prétraitement et à différentes caractéristiques des signaux, telles que la fréquence d'échantillonnage, la stationnarité, le contenu fréquentiel... Nous avons également choisi d'étudier la direction de la propagation. Et finalement nous avons développé une nouvelle approche d'analyse des signaux EHG par la localisation de leurs sources.

Ces analyses devraient permettre l'identification de paramètres pertinents cliniquement. Des études cliniques à grande échelle seront alors nécessaires pour la compréhension de la relation entre les paramètres dérivés du signal EHG et les processus conduisant à l'accouchement.

Notre contribution dans le domaine de l'analyse EHG est structurée autour de quatre thèmes principaux: l'analyse non linéaire monovariée de l'EHG, l'analyse bivariée de la propagation de l'EHG et de sa direction, l'implantation d'un outil de localisation des sources de l'EHG et l'amélioration du protocole expérimental développé dans notre laboratoire sur les rates enceintes.

Ce manuscrit est organisé comme suit:

- **Chapitre 1**: nous présentons dans ce chapitre l'état de l'art sur les bases anatomique et physiologique de l'activité utérine. Nous présentons également la définition de l'accouchement prématuré et les caractéristiques de l'EHG. Ensuite, nous présentons les différentes études d'excitabilité et de propagation qui ont été faites précédemment à

partir de l‟EHG. Enfin, nous décrivons le protocole expérimental utilisé pour recueillir les signaux utilisés dans ce travail.

- **Chapitre 2**: Il présente le travail effectué sur la caractérisation non linéaire du signal EMG utérin afin de l'utiliser pour la classification des contractions de grossesse et de travail. Nous testons quatre méthodes d'analyse de la non-linéarité: Réversibilité du temps (Time reversibility, *Tr*), exposants de Lyapunov (Lyapunov exponents, *LE*), Entropie de l'échantillon (Sample Entropy, *SampEn*), et variance des vecteurs de retard (Delay vecteur variance, *DVV*). Ces méthodes sont testées tous d'abord sur des signaux générés par un modèle non linéaire synthétique classique. Dans ce modèle, le degré de complexité, qui représente la non-linéarité de ce modèle, peut être réglé et nous permet de tester les méthodes dans des conditions de complexité contrôlées. Nous étudions l'effet de la variation de complexité sur l'évolution des performances des quatre méthodes. Nous testons aussi la robustesse des méthodes en ajoutant du bruit, avant d'appliquer les méthodes sur les signaux synthétiques. Nous appliquons également les méthodes aux signaux, avec différentes valeurs de SNR, pour voir quelle méthode est la moins sensible au bruit. La technique de "surrogates" est généralement utilisée pour détecter la présence de non-linéarité dans les signaux. Cette technique a permis de mettre en évidence la présence de non-linéarité dans les signaux EHG. Le degré de non-linéarité peut également être estimé en utilisant le Z-score associé à l'utilisation des surrogates, mais l‟utilisation de surrogates est lourde en terme de temps de calcul. Dans notre étude, nous étudions l'effet de l'utilisation des surrogates sur la performance des méthodes testées sur des signaux synthétiques, ainsi que sur le taux de classification des signaux réels. Après avoir testé et validé les méthodes non linéaires sur des signaux synthétiques, nous les comparons avec des méthodes linéaires en les appliquant sur des signaux EHG réels. Nous testons également, à la fin de ce chapitre, la sensibilité des méthodes non linéaires à la fréquence d'échantillonnage et aux contenus fréquentiels des signaux EHG.
- **Chapitre 3**: Il présente l'étude bivariée. Nous essayons ici d'améliorer les performances des méthodes de détection de couplage pour améliorer la classification des contractions de grossesse et de travail. La nouvelle idée dans ce chapitre est d‟étudier par ces méthodes non seulement la valeur du couplage entre les signaux, mais aussi la direction de ce couplage. Nous commençons notre étude par l'hypothèse que la synchronisation augmente en passant de la grossesse à l'accouchement. Les contractions de grossesse sont censées être inefficaces et locales (faible propagation),

tandis que les contractions de travail sont censées se propager à l'ensemble de l'utérus dans une courte durée (propagation rapide). Nous comparons deux méthodes non linéaires, le coefficient de corrélation non linéaire (h^2), la synchronisation générale (H) et une méthode linéaire la causalité de Granger (GC), sur des signaux synthétiques générés par le modèle de Rössler dans des conditions différentes .

Ce genre de signaux synthétiques permet de mieux comprendre le comportement des méthodes dans des conditions variées et contrôlées. Cependant, ils ne sont pas très représentatifs des signaux réels. Pour cela, nous avons donc également testé les méthodes sur un modèle plus physiologique nouvellement développé dans notre laboratoire. Ce modèle peut générer une propagation d'onde plane et une propagation d'onde circulaire pour les potentiels d'action. Nous appliquons dans ce chapitre les méthodes sur des signaux simulés à l'aide de ce modèle, pour vérifier si elles peuvent détecter la bonne direction de l'onde propagée.

La dernière étape de ce chapitre est d'appliquer les méthodes testées et validées en utilisant des signaux synthétiques et simulés, sur les signaux EHG réels. Nous les appliquons sur un groupe de contractions réelles de grossesse et un autre groupe de contractions de travail pour voir la capacité des méthodes à différencier entre ces deux groupes. Pour étudier l'évolution de la synchronisation de l'utérus pendant la grossesse, nous appliquons également les méthodes sur 8 groupes de signaux regroupés en termes de semaines avant le accouchement (Week Before Labor, WBL) et allant de 7 WBL jusqu‟au travail. Nous avons amélioré les résultats en utilisant une approche de filtrage-fenêtrage comme prétraitement des signaux.

- **Chapitre 4**: Dans ce chapitre, nous abordons l'étude de la localisation de source des signaux EHG, ce qui nécessite la résolution d'un problème direct et d'un problème inverse. Par conséquent, nous avons implémenté un nouvel outil de localisation de source EHG basé sur la boîte à outils d‟accès libre « Fieldtrip ». Nous résolvons le problème direct en utilisant la méthode des éléments de frontière (Boundary Element Method, en Anglais, BEM), et le problème inverse en utilisant la méthode d'estimation de la norme minimale (Minimum Norme Estimate, en Anglais, MNE). Nous validons notre méthode en utilisant des signaux simulés par le modèle physiologique avec différentes positions de source. Puis nous appliquons cet algorithme de localisation à des signaux EHG réels, pour la localisation des source(s) d‟une contraction de grossesse et d‟une contraction de travail, enregistrées sur la même femme, ce qui nous permet d‟obtenir des résultats préliminaires sur des signaux réels.

- **Annexe**: Nous avons développé une matrice d'électrodes à succion pour améliorer le protocole de l'expérimentation animale préalablement développé dans notre laboratoire. Ces expérimentations seront utilisées pour enregistrer les signaux EMG de l'utérus de rate, qui à leur tour, serviront à valider le modèle d'EHG physiologique développé dans notre équipe ainsi que nos méthodes de traitement pour l'analyse de la propagation. L'avantage de l'utilisation de l'utérus de rate est qu'il est formé de deux couches bien organisées de fibres musculaires, une couche de fibres musculaires superficielles longitudinales et une couche interne circulaire, ce qui n'est pas le cas dans l'utérus humain. Donc, la validation du modèle et des méthodes peut être fait facilement à cause de la direction de propagation qui peut être prévue avec l'utérus de rate, ce qui n'est pas possible avec l'utérus de femme.
- Une conclusion générale et une discussion de cette thèse sont présentées à la fin avec des propositions pour les travaux futurs possibles.

Les résultats obtenus dans cette thèse nous ont permis d'écrire 2 articles de revues publiés, 1 article de revue accepté avec des modifications (en cours d'une révision finale), 2 articles de revues soumis, 5 conférences internationale publiés, 2 conférences internationale soumis, et 1 conférence nationale publiée.

Références:

[1] P. Johnson, "Suppression of preterm labour," *Drugs*, vol. 45, no. 5, pp. 684-692, May. 1993.

[2] H. Ruf, M. Conte, and J.P. Franquelbalme, "L'accouchement prématuré," in *Encycl. Med. Chir.*, 1988, Elsevier: Paris, pp. 12.

[3] J. M. Denney, J. F. Culhane, and R. L. Goldenberg, "Prevention of preterm birth," *Womens Health (Lond Engl),* vol. 4, pp. 625-38, Nov 2008.

[4] H. Leman, C. Marque, and J. Gondry, "Use of the electrohysterogram signal for characterization of contractions during pregnancy," *IEEE Trans. Biomed. Eng.,* vol. 46, pp. 1222-9, Oct 1999.

[5] J. Linhart, G. Olson, L. Goodrum, T. Rowe, G. Saade, and G. Hankins, "Pre-term labor at 32 to 34 weeks' gestation: effect of a policy of expectant management on length of gestation," *Am. J. Obstet. Gynecol.*, vol. 178, 1998.

[6] C. Marque, J. Duchêne, S. Leclercq, G. Panczer, and J. Chaumont, "Uterine EHG processing for obstetrical monitoring," *IEEE Trans. Biomed. Eng.*, vol. 33, no. 12, pp. 1182-7, Dec. 1986.

[7] S. Mansour, D. Devedeux, G. Germain, C. Marque, and J. Duchêne, "Uterine EMG spectral analysis and relationship to mechanical activity in pregnant monkeys," *Med. Biol. Eng. Comput.*, vol. 34, no. 2, pp. 115-21, Mar. 1996.

[8] M.P. Vinken, C. Rabotti, M. Mischi, and S.G. Oei, "Accuracy of frequency-related parameters of the electrohysterogram for predicting preterm delivery: a review of the literature," *Obstet. Gynecol. Surv.*, vol. 64, no. 8, pp. 529-41, Aug. 2009.

[9] R.E. Garfield, W.L. Maner, L.B. MacKay, D. Schlembach, and G.R. Saade, "Comparing uterine electromyography activity of antepartum patients versus term labor patients," *American Journal of Obstetrics and Gynecology*, vol. 193, no. 1, pp. 23-29, Jul. 2005.

[10] M. Hassan, J. Terrien, B. Karlsson, and C. Marque, "Comparison between approximate entropy, correntropy and time reversibility: Application to uterine electromyogram signals," *Medical engineering & physics (MEP)*, vol. 33, no. 8, pp. 980-986, oct. 2011.

[11] D. Devedeux, C. Marque, S. Mansour, G. Germain, and J. Duchêne, "Uterine electromyography: a critical review," *Am. J. Obstet. Gynecol.*, vol. 169, no. 6, pp. 1636-53, Dec. 1993.

[12] J. Gondry, C. Marque, J. Duchêne, and D. Cabrol, "Electrohysterography during pregnancy: preliminary report," *Biomed. Instrum. Technol.*, vol. 27, no.4, pp. 318-24, 1993.

[13] I. Verdenik, M. Pajntar, and B. Leskosek, "Uterine electrical activity as predictor of preterm birth in women with preterm contractions," Eur. J. Obstet. Gynecol. Reprod. Biol., vol. 95, no. 2, pp. 149-53, Apr. 2001.

[14] C. Sureau, "Etude de l'activité électrique de l'utérus au cours du travail," *Gynecol. Obstet.*, vol. 555, pp. 153-175, Apr-May. 1956.

[15] G. Fele-Žorž, G. Kavšek, Ž. Novak-Antolič, and F. Jager, "A comparison of various linear and non-linear signal processing techniques to separate uterine EMG records of term and pre-term delivery groups," *Med. Biol. Eng. Comput.*, vol. 46, no. 9, pp. 911-22, Sep. 2008.

[16] M.P.G.C. Vinken, C. Rabotti, M. Mischi, J.O.E.H. van Laar, and S.G. Oei, "Nifedipine-induced changes in the electrohysterogram of preterm contractions: feasibility in clinical practice," *Obstetrics and gynecology international*, vol. 2010, no. 2010, pp. 8, Apr. 2010.

[17] M. Khalil, and J. Duchêne, "Detection and classification of multiple events in piecewise stationary signals: Comparison between autoregressive and multiscale approaches," *Signal Processing*, vo. 75, no. 3, pp. 239-251, Jun. 1999.

[18] M. Hassan, J. Terrien, B. Karlsson, and C. Marque, "Interactions between Uterine EMG at Different Sites Investigated Using Wavelet Analysis: Comparison of Pregnancy and Labor Contractions," *EURASIP J. on Adv. in Sign. Process.*, vol. 2010, no. 17, pp. 9, Feb. 2010.

[19] J. Duchêne, C. Marque, and S. Planque, "Uterine EMG signal: Propagation analysis," in *12th Annual International Conference of the IEEE Engineering in Medicine and Biology Society (IEEE-EMBC)*, Philadelphia, Pennsylvania, USA, Nov. 1990, pp. 831-832.

[20] M. Hassan, J. Terrien, C. Muszynski, A. Alexandersson, C. Marque, and B. Karlsson, "Better pregnancy monitoring using nonlinear propagation analysis of external uterine electromyography," *IEEE Trans. Biomed. Eng.*, vol. 60, no. 4, pp. 1160-1166, Apr. 2013.

[21] C. Rabotti, M. Mischi, J.O.E.H van Laar, G.S Oei, and J.W.M Bergmans, “Inter-electrode delay estimators for electrohysterographic propagation analysis,” *Physiol. Meas.*, vol. 30, no.8, pp. 745-61, Jun. 2009.

[22] M. Lucovnik, W. L. Maner, L. R. Chambliss, R. Blumrick, J. Balducci, Z. Novak-Antolic, and R. E. Garfield, "Noninvasive uterine electromyography for prediction of preterm delivery," Am J Obstet Gynecol, vol. 204, pp. 228 -238 2011.

[23] E. Mikkelsen, P. Johansen, A. Fuglsang-Frederiksen, and N. Uldbjerg, “Electrohysterography of labor contractions: propagation velocity and direction,” Acta obstetricia et gynecologica Scandinavica, vol. 92, no. 9, pp. 1070-1078, 2013.

[24] L. Lange, A. Vaeggemose, P. Kidmose, E. Mikkelsen, N. Uldbjerg, and P. Johansen, “Velocity and Directionality of the Electrohysterographic Signal Propagation,” PLoS ONE, vol. 9, no. 1, pp. e86775, 2014.

[25] T.Y. Euliano, D. Marossero, M.T. Nguyen, N.R. Euliano, J. Principe, and R.K. Edwards, “Spatiotemporal electrohysterography patterns in normal and arrested labor,” Am. J. Obstet. Gynecol., vol. 200, no. 1, pp. 54.e1–54.e7, 2009.

[26] H. de Lau, C. Rabotti, R. Bijloo, M.J. Rooijakkers, M. Mischi, and S.G. Oei, “Automated conduction velocity analysis in the electrohysterogram for prediction of imminent delivery: a preliminary study,” Computational and Mathematical Methods in Medicine, vol. 2013, 7 pages, 2013.

[27] C. Rabotti, M. Mischi, G.S. Oei, and J.W.M. Bergmans, “Noninvasive Estimation of the Electrohysterographic Action-Potential Conduction Velocity,” IEEE Trans. on Biomedical Engineering, vol. 57, no. 9, pp. 2178-2187, 2010.

Contents

General introduction

The global long term objective of our study is the early prediction of term or preterm labor as well as making better prediction of when premature labor is not imminent. Any improvement in better assessing the risk of premature labor is a major public health issue as prematurity is one of the largest causes of preventable mortality and morbidity in the developed world.

If we want to be able to accurately assess and there for more appropriately treat premature labor, we first have to understand mechanism underlying labor. The exact mechanisms of functioning of the uterus are still not well understood. The details of its evolution and transition from pregnancy to labor are still an open question in physiology. To be able to predict the preterm labor, we should first try to understand the normal functioning of the uterus and how it operates while remaining quiescent during the whole pregnancy and then how it jumps into action to push the baby out during labor.

The aim of the work presented in this thesis is to extract some parameters from the uterine EMG (Electrohysterogramme, EHG) signals that could help us in understanding what happens to the uterus when going from pregnancy to labor. This understanding can lead us to a physiological interpretation of the cause of term and preterm labor. These extracted parameters can possibly be integrated to other parameters in a diagnosis system that can be clinically useful for pregnancy monitoring and preterm labor prediction.

Labor is a physiologic process defined as regular uterine contractions accompanied by cervical effacement and dilatation. In the normal labor, the uterine contractions and cervix dilatation are preceded by biochemical changes in the cervical connective tissue. A normal labor leads to the birth of a fetus at term. According to the definition of the World Health Organization (WHO), preterm delivery is a delivery at a gestational age less than 37 completed weeks or less than 259 days of amenorrhea. Every birth occurring after 22 weeks of amenorrhea and before 37 weeks is defined as a premature birth. A birth occurring before 22 weeks of amenorrhea is considered as an abortion by WHO. Preterm labor is a topical issue because out of 750,000 births in France, 44,000 are premature [1]. Preterm labor is still the most common obstetrical complication during pregnancy, with 20% of all pregnant women at high risk of preterm labor. In the United States, more than half a million babies - that is 1 of 8- are born premature each year.

One of the major problems facing the obstetrical world through the development of an effective treatment, is that the causes of premature labor are not known in 40 % of cases [2]. The pathogenesis of spontaneous preterm labor is not well understood: spontaneous preterm contractions may be caused by an early activation of the normal labor process or by other (unknown) pathological causes.

The earlier preterm labor is detected the easier it is to prevent it and with accurate diagnosis we can avoid treating women that are not going to give birth pre-term [3, 4]. If preterm labor is detected early, medical personnel can attempt to stop the labor process, or if unsuccessful, are better prepared to handle the premature infant.

Optimal prediction of labor implies finding markers indicating that the labor will occur, but also predicting whether it will actually result in a premature birth (premature labor), to avoid unnecessary treatment of significant number of patients. Moreover, these markers must be observed as early as possible, so clinicians will have time for intervention. For example, when the decision is to keep the fetus "in utero", it seems easier to prevent the onset of labor than to stop it. Similarly, when a premature rupture of membranes occurs, a delay is valuable so that the administration of corticosteroids can have effect on fetal lung maturation. Even noticeable dynamic cervical change may not be an accurate indicator of true labor, as a large percentage of women with established cervical change do not deliver preterm when not treated with tocolytics [5].

A lot of work has already been done on preterm labor prediction by using EHG [6-10] as this is one of the few indicators that are accessible and representative of the underlying muscular activity of uterine contractions. It is therefore a very promising signal if one aims to understand what is going on in real time.

The EHG is composed of two components, a low wave, which is synchronous to the intra uterine pressure (IUP), and a fast wave, which is also divided into two frequency components, Fast Wave Low (FWL) and Fast Wave High (FWH). FWL and FWH are thought to be related to the propagation and the excitability of EHG respectively [11].,

Many studies of the EHG have been performed and in the past they have mainly based on uterine excitability aspects (time and frequency characterization of one or two EHG leads). A lot of work has already been done for the analysis of the time [12-14], frequency [6, 15, 16], time-frequency [4, 17, 18], nonlinear [10, 15] domains of such "local" EHG signals. None of

these methods are however not currently used in routine practice due to a high variance of the results obtained and an insufficient prediction rate.

The EHG signals were proven to be nonlinear similarly to all electrophysiological signals from human body. Therefore a more investigation of nonlinear methods are needed to respect the nonlinearity of EHG signals and to add additional information to those obtained by linear method from EHG signal in order to increase the labor prediction rate.

Fewer and more recent studies have been performed on aspects relating to the origin of uterine contractions and the propagation of the contractile activity between the different parts of the uterus. EHG propagation and direction investigation is limited to just a few studies [19-27]. To our present knowledge, no study has ever been aimed at localizing the actual sources of uterine EMG as the one we present in this work.

In this thesis we plan to focus also on the dynamics of the electrical activity (direction of propagation, source localization). Our work is focused on developing and improving the analysis of EHG excitability, propagation, and source localization. We therefore used signals from a 4x4 matrix of electrodes to give us a much more complete image of the uterus and its underlying contractile mechanisms. We tried in this work to improve the performance of nonlinear and propagation methods, by testing their sensitivity to different pre-processing steps and signal characteristics like sampling frequency, stationarity, and frequency content… We also decided to study the direction of the propagation. We finally developed a new way of analyzing EHG signals by localization of their sources.

This analysis could permit the identification of clinically relevant parameters. Extensive clinical studies will then be required for understanding the relation between the parameters derived from the EHG signal and the processes leading to labor.

Our contribution to the field of EHG analysis is structured around four main themes: monovariate nonlinear analysis, bivariate analysis of propagation and its direction, implementation of an EHG based source localization tool and the improvement of the rat experimental protocol developed in our laboratory (**Figure 1**).

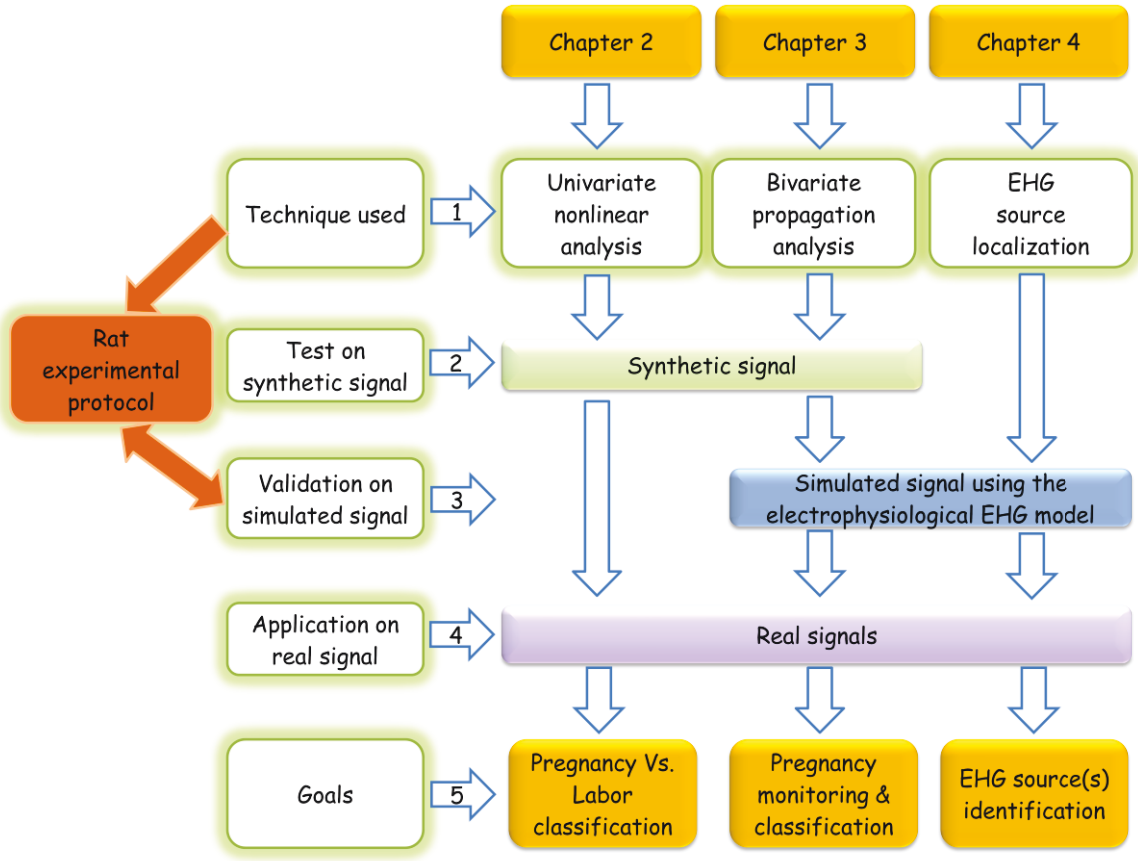

Figure 1: An organization chart that summarizes the work done during this thesis.

This monograph is organized as follows:

- **Chapter 1**: we present the state of the art of anatomical and physiological background of the uterine activity. We present also the definition of preterm labor and the characteristics of EHG. Then we present the different excitability and propagation studies that have been done in the past. At the end we describe the experimental protocol used to obtain the signals used throughout this work.
- **Chapter 2**: presents the work done on the nonlinear characterization of uterine EMG signal in order to use it for the classification of pregnancy and labor contractions. We test four nonlinearity analysis methods: Time reversibility (Tr), Lyapunov exponents (LE), Sample Entropy (SampEn) and Delay vector variance (DVV). These methods will be first tested on signals generated by a classical synthetic nonlinear model. In this model, the degree of complexity, which represents the nonlinearity of this model, can be tuned to test the methods in controlled conditions. We investigate the effect of varying complexity on the evolution of the four methods. We also test the robustness of methods by adding noise before applying the methods to the synthetic signal. We

also apply the methods on signals with different SNR values to test which method is the least sensitive to noise. Surrogate technique is usually used to detect the presence of nonlinearity in signals. This technique has evidenced the presence of nonlinearity in EHG signals. The degree of non-linearity can also be estimated by using the z-score associated with the use of surrogates, but computing is thus time consuming. In our study we investigate the effect of the use of surrogate on the performances of the tested methods on synthetic signals, as well as on the classification rate for real signals. After testing and validating the methods on synthetic signals we apply and compare them with linear methods on real EHG signals. We will test also at the end of this chapter the sensitivity of nonlinear methods to the sampling frequency and to the frequency contents of EHG signals.

- **Chapter 3**: presents the bivariate study. We try here to improve the performances of coupling detection methods to improve the classification of pregnancy and labor contractions. The new idea in this chapter is that we study by these methods, not just the coupling value between signals, but also the direction of the coupling. We start our study from the hypothesis that the synchronization increases from pregnancy to labor. Pregnancy contractions are supposed to be inefficient and to remain local (small propagation) while labor contractions are supposed to propagate to the whole uterus in a short time (fast propagation). We compare two nonlinear methods, nonlinear correlation coefficient (h^2), general synchronization (H) and one linear method Granger causality (GC), on synthetic Rössler signals in different conditions.

  This kind of synthetic signals permits to better understand the behavior of the methods under varied conditions. However, they are not very representative of the real signals. We thus also tested the methods on a more physiological model newly developed in our laboratory. This model can generate a planar wave propagation and a circular wave propagation of action potential. We apply in this chapter the methods on signals simulated by this model, to investigate if they permit to detect the right direction of the given propagated wave.

  The final step in this chapter is to apply the methods, tested and validated by using synthetic and simulated signals, on real EHG signals. We apply them on pregnancy and labor groups of real contractions to see the capability of methods in differentiating between these two groups. To study the evolution of uterine synchronization during pregnancy, we also apply the methods on 8 groups of signal regrouped in terms of

week before labor (WBL) and going from 7 WBL to labor. We proposed to improve the results by using a filtering-windowing approach.

- **Chapter 4**: in this chapter we tackle the study the EHG source localization, which requires solving a forward and an inverse problem. Therefore we used the „Fieldtrip" free toolbox to implement a tool for EHG source localization. We solve the inverse forward problem using the boundary element method (BEM) method, and the inverse problem using the minimum norm estimate (MNE) method. We validate our method using simulated signals with different source locations, then apply this localization algorithm to real EHG for the source(s) localization of pregnancy and labor contractions.
- **Appendix**: we develop a suction electrode matrix for the animal experimentation protocol. This experimentation will be used to record uterine EHG from rat uterus to validate the physiological EHG model developed in our team and our methods. The benefit of using the rat uterus is that it contains two well organized layers of muscle fibers, structure that is not present in the human uterus: a longitudinal superficial layer and a deep circular layer of muscle fibers. So validation of the model and methods can be done easier because of the expected direction of propagation with the rat uterus, which is not possible with woman"s uterus.
- Discussion and general conclusions of this thesis are given with propositions for possible future work.

The results obtained in this thesis permitted us to write 3 published journal papers, 2 submitted journal papers, 5 international conference papers, and 1 national conference paper.

List of author's publications

Journal papers

Ahmad Diab, Mahmoud Hassan, Jérémy Terrien, Sofiane Boudaoud, Catherine Marque, and Brynjar Karlsson, "Improving Connectivity Measures Performance and Stability in Uterine EMG analysis," *IEEE Transactions on Biomedical Engineering*, 2014. (**Submitted**). *Publication related to chapter 3.*

Ahmad Diab, Mahmoud Hassan, Jérémy Laforet, Asgeir Alexandersson, Brynjar Karlsson, and Catherine Marque, "Analysis of Connectivity Strength and Direction of Simulated and

Real Multielectrode EHG Signals," *Medical & Biological Engineering & Computing*, 2014. (**Submitted**). *Publication related to chapter 3.*

Dima Alameddine, **Ahmad Diab**, Charles Muszynski, Brynjar Karlsson, Mohamad Khalil, and Catherine Marque, "Selection Algorithm for Parameters to Characterize Uterine EHG Signals for the Detection of Preterm Labor," *Signal Image and Video Processing*, 2014. *Publication related to chapter 2.*

Ahmad Diab, Mahmoud Hassan, Catherine Marque, and Brynjar Karlsson, "Performance analysis of four nonlinearity analysis methods using a model with variable complexity and application to uterine EMG signals," *Medical Engineering & Physics*, vol. 36, no. 6, pp. 761–767, Jun. 2014. *Publication related to chapter 2.*

Ahmad Diab, Mahmoud Hassan, Brynjar Karlsson, and Catherine Marque, "Effect of decimation on the classification rate of non-linear analysis methods applied to uterine EMG signals," *IRBM*, vol. 34, no.4-5, pp. 326–329, Oct. 2013. *Publication related to chapter 2.*

International conference papers

Ahmad Diab, Mahmoud Hassan, Jeremy Laforet, Brynjar Karlsson, and Catherine Marque, "EHG Source Localization Using Signals from a Uterus Electrophysiological Model," in *Proc. Virtual Physiological Human Conference 2014 (VPH)*, Trondheim, Norway, Sep. 2014. (**Accepted**). *Publication related to chapter 4.*

Catherine Marque, **Ahmad Diab**, Jérémy Laforêt, Mahmoud Hassan, and Brynjar Karlsson, "Dynamic behavior of uterine contractions: an approach based on source localization and multiscale modeling," in *Proc. six international conference on Knowledge and Systems Engineering (KSE)*, Hanoi, Vietnam, Oct. 2014. (**Accepted**). *Publication related to chapter 4.*

Ahmad Diab, Mahmoud Hassan, Sofiane Boudaoud, Catherine Marque, and Brynjar Karlsson, "Nonlinear estimation of coupling and directionality between signals: Application to uterine EMG propagation," in *Proc. IEEE Eng. Med. Biol. Soc. Conf. 2013*, Osaka, Japan, Jul. 2013, pp. 4366-4369. (**Poster presentation).** *Publication related to chapter 3.*

Ahmad Diab, Mahmoud Hassan, Jeremy Laforet, B. Karlsson, and C. Marque, "Estimation of Coupling and Directionality between Signals Applied to Physiological Uterine EMG Model and Real EHG Signals," in *Proc. XIII Mediterranean Conference on Medical and*

Biological Engineering and Computing 2013, Sevilla, Spain, Sep. 2013, pp. 718-721. (**Oral Presentation).** *Publication related to chapter 3.*

Ahmad Diab, Mahmoud Hassan, Catherine Marque, and B. Karlsson, "Comparison of methods for evaluating signal synchronization and direction: Application to uterine EMG signals," in *2nd International Conference on Advances in Biomedical Engineering (ICABME) 2013*, Tripoli, Lebanon, Sep. 2013, pp. 14-17.(**Oral presentation**). *Publication related to chapter 3.*

Ahmad Diab, Mahmoud Hassan, Catherine Marque, and Brynjar Karlsson, "Quantitative performance analysis of four methods of evaluating signal nonlinearity: Application to uterine EMG signals," in *Proc. IEEE Eng. Med. Biol. Soc. Conf. 2012*, San Diego, California, Aug. 2012, pp.1045-1048. (**Oral Presentation**). *Publication related to chapter 2.*

National conference paper

Ahmad Diab, Mahmoud Hassan, Brynjar Karlsson, and Catherine Marque, "Effect of decimation on the classification rate of nonlinear analysis methods applied to uterine EMG signals," in *Proc. Conférence de Recherche en Imagerie et Technologies pour la Santé (RITS)*, Bordeaux, France, 2013. (**Oral presentation**). *Publication related to chapter 2.*

References

[1] P. Johnson, "Suppression of preterm labour," *Drugs*, vol. 45, no. 5, pp. 684-692, May. 1993.

[2] H. Ruf, M. Conte, and J.P. Franquelbalme, "L"accouchement prématuré," in *Encycl. Med. Chir.*, 1988, Elsevier: Paris, pp. 12.

[3] J. M. Denney, J. F. Culhane, and R. L. Goldenberg, "Prevention of preterm birth," *Womens Health (Lond Engl),* vol. 4, pp. 625-38, Nov 2008.

[4] H. Leman, C. Marque, and J. Gondry, "Use of the electrohysterogram signal for characterization of contractions during pregnancy," *IEEE Trans. Biomed. Eng.,* vol. 46, pp. 1222-9, Oct 1999.

[5] J. Linhart, G. Olson, L. Goodrum, T. Rowe, G. Saade, and G. Hankins, "Pre-term labor at 32 to 34 weeks' gestation: effect of a policy of expectant management on length of gestation," *Am. J. Obstet. Gynecol.*, vol. 178, 1998.

[6] C. Marque, J. Duchêne, S. Leclercq, G. Panczer, and J. Chaumont, "Uterine EHG processing for obstetrical monitoring," *IEEE Trans. Biomed. Eng.*, vol. 33, no. 12, pp. 1182-7, Dec. 1986.

[7] S. Mansour, D. Devedeux, G. Germain, C. Marque, and J. Duchêne, "Uterine EMG spectral analysis and relationship to mechanical activity in pregnant monkeys," *Med. Biol. Eng. Comput.*, vol. 34, no. 2, pp. 115-21, Mar. 1996.

[8] M.P. Vinken, C. Rabotti, M. Mischi, and S.G. Oei, "Accuracy of frequency-related parameters of the electrohysterogram for predicting preterm delivery: a review of the literature," *Obstet. Gynecol. Surv.*, vol. 64, no. 8, pp. 529-41, Aug. 2009.

[9] R.E. Garfield, W.L. Maner, L.B. MacKay, D. Schlembach, and G.R. Saade, "Comparing uterine electromyography activity of antepartum patients versus term labor patients," *American Journal of Obstetrics and Gynecology*, vol. 193, no. 1, pp. 23-29, Jul. 2005.

[10] M. Hassan, J. Terrien, B. Karlsson, and C. Marque, "Comparison between approximate entropy, correntropy and time reversibility: Application to uterine electromyogram signals," *Medical engineering & physics (MEP)*, vol. 33, no. 8, pp. 980-986, oct. 2011.

[11] D. Devedeux, C. Marque, S. Mansour, G. Germain, and J. Duchêne, "Uterine electromyography: a critical review," *Am. J. Obstet. Gynecol.*, vol. 169, no. 6, pp. 1636-53, Dec. 1993.

[12] J. Gondry, C. Marque, J. Duchêne, and D. Cabrol, "Electrohysterography during pregnancy: preliminary report," *Biomed. Instrum. Technol.*, vol. 27, no.4, pp. 318-24, 1993.

[13] I. Verdenik, M. Pajntar, and B. Leskosek, "Uterine electrical activity as predictor of preterm birth in women with preterm contractions," Eur. J. Obstet. Gynecol. Reprod. Biol., vol. 95, no. 2, pp. 149-53, Apr. 2001.

[14] C. Sureau, "Etude de l'activité électrique de l'utérus au cours du travail," *Gynecol. Obstet.*, vol. 555, pp. 153-175, Apr-May. 1956.

[15] G. Fele-Žorž, G. Kavšek, Ž. Novak-Antolič, and F. Jager, "A comparison of various linear and non-linear signal processing techniques to separate uterine EMG records of term and pre-term delivery groups," *Med. Biol. Eng. Comput.*, vol. 46, no. 9, pp. 911-22, Sep. 2008.

[16] M.P.G.C. Vinken, C. Rabotti, M. Mischi, J.O.E.H. van Laar, and S.G. Oei, "Nifedipine-induced changes in the electrohysterogram of preterm contractions: feasibility in clinical practice," *Obstetrics and gynecology international*, vol. 2010, no. 2010, pp. 8, Apr. 2010.

[17] M. Khalil, and J. Duchêne, "Detection and classification of multiple events in piecewise stationary signals: Comparison between autoregressive and multiscale approaches," *Signal Processing*, vo. 75, no. 3, pp. 239-251, Jun. 1999.

[18] M. Hassan, J. Terrien, B. Karlsson, and C. Marque, "Interactions between Uterine EMG at Different Sites Investigated Using Wavelet Analysis: Comparison of Pregnancy and Labor Contractions," *EURASIP J. on Adv. in Sign. Process.*, vol. 2010, no. 17, pp. 9, Feb. 2010.

[19] J. Duchêne, C. Marque, and S. Planque, "Uterine EMG signal: Propagation analysis," in *12th Annual International Conference of the IEEE Engineering in Medicine and Biology Society (IEEE-EMBC)*, Philadelphia, Pennsylvania, USA, Nov. 1990, pp. 831-832.

[20] M. Hassan, J. Terrien, C. Muszynski, A. Alexandersson, C. Marque, and B. Karlsson, "Better pregnancy monitoring using nonlinear propagation analysis of external uterine electromyography," *IEEE Trans. Biomed. Eng.*, vol. 60, no. 4, pp. 1160-1166, Apr. 2013.

[21] C. Rabotti, M. Mischi, J.O.E.H van Laar, G.S Oei, and J.W.M Bergmans, "Inter-electrode delay estimators for electrohysterographic propagation analysis," *Physiol. Meas.*, vol. 30, no.8, pp. 745-61, Jun. 2009.

[22] M. Lucovnik, W. L. Maner, L. R. Chambliss, R. Blumrick, J. Balducci, Z. Novak-Antolic, and R. E. Garfield, "Noninvasive uterine electromyography for prediction of preterm delivery," Am J Obstet Gynecol, vol. 204, pp. 228 -238, 2011.

[23] E. Mikkelsen, P. Johansen, A. Fuglsang-Frederiksen, and N. Uldbjerg, "Electrohysterography of labor contractions: propagation velocity and direction," Acta obstetricia et gynecologica Scandinavica, vol. 92, no. 9, pp. 1070-1078, 2013.

[24] L. Lange, A. Vaeggemose, P. Kidmose, E. Mikkelsen, N. Uldbjerg, and P. Johansen, "Velocity and Directionality of the Electrohysterographic Signal Propagation," PLoS ONE, vol. 9, no. 1, pp. e86775, 2014.

[25] T.Y. Euliano, D. Marossero, M.T. Nguyen, N.R. Euliano, J. Principe, and R.K. Edwards, "Spatiotemporal electrohysterography patterns in normal and arrested labor," Am. J. Obstet. Gynecol., vol. 200, no. 1, pp. 54.e1–54.e7, 2009.

[26] H. de Lau, C. Rabotti, R. Bijloo, M.J. Rooijakkers, M. Mischi, and S.G. Oei, "Automated conduction velocity analysis in the electrohysterogram for prediction of imminent delivery: a preliminary study," Computational and Mathematical Methods in Medicine, vol. 2013, 7 pages, 2013.

[27] C. Rabotti, M. Mischi, G.S. Oei, and J.W.M. Bergmans, "Noninvasive Estimation of the Electrohysterographic Action-Potential Conduction Velocity," IEEE Trans. on Biomedical Engineering, vol. 57, no. 9, pp. 2178-2187, 2010.

Chapter 1: The uterus, preterm labor and measuring EHG.

1.1 Introduction

The ultimate goal of the work presented in this thesis is the detection of labor and the prediction of preterm labor, by analyzing the propagation of the uterine electrical activity (electrohysterogam, EHG) through the uterus, during labor and pregnancy. The uterus is a not well-understood organ. It is deceptively simple in structure but its behavior, when it goes from pregnancy towards labor, indicates that there are numbers of interconnected control systems involved in its functioning (electric, hormonal, mechanical). The physiological phenomena underlying labor are however still not completely understood.

Uterine contractility can be thought of as being dependent on two aspects, cells excitability and propagation of electrical activity to a part of, or the whole, uterus. Analyzing these two aspects as well as the localization of source(s) of uterine activity can bring useful information for the prediction of preterm labor. A lot of studies have been done on using excitability characteristic, in order to detect preterm labor [1-6], whereas, until recently, less effort has focused on characterizing the propagation of electrical activity. Furthermore, no work has been done concerning the localization of uterine electrical source(s).

In this chapter, we first give background on the physiology of the uterus, then on the factors that contribute to the generation of uterine contraction and to its propagation. We present then some of the basic characteristics of the EHG, and the methods that have previously been used for the detection of preterm labor threat. Finally we describe how EHG is recorded and the experimental protocol used to acquire the human EHG used throughout this thesis.

1.2 Uterine anatomy and physiology: an overview

1.2.1 Anatomy of the uterus

The non-pregnant uterus is pear-shaped, 7.5 cm in length, 4 to 5 cm in width at its upper portion, and 2 to 3 cm in thickness, and made up of the fundus, body and cervix (**Figure 1.1**). The uterine (Fallopian) tubes enter each superolateral angle, termed the cornu, above which lies the fundus. The uterine body narrows to a waist (the isthmus), which continues as the

cervix. The cervix is gripped around its middle by the vagina, and this attachment defines a supravaginal and a vaginal part of the cervix [7].

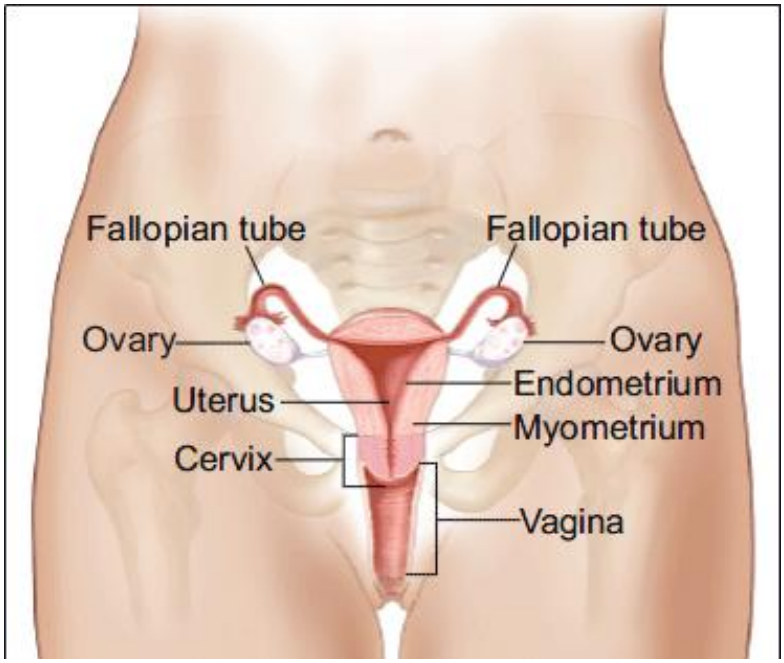

Figure 1.1: Subdivision and layers of the uterus [8].

The uterus is made up of three layers of tissue. The outer serosa layer, the middle muscular layer called myometrium which makes up the bulky uterine wall, composed of 3 layers of smooth muscle, and the innermost, composed of specialized mucous membrane, endometrium. The endometrium contains abundant blood supply. It is composed of two layers. These are stratum functionalis that shed during every menstruation. If pregnancy occurs it continues to be site of attachment and nourishment for morrula (fertilized zygote). The second layer of endometrium is stratum basale that attaches to myometrium [9]. The myometrium is the middle and thickest layer of the uterus. It is composed of longitudinal and circular layers of smooth muscle. During pregnancy, the myometrium increases both by hypertrophy of the existing cells and by multiplication of the cell number. When parturition takes place, coordinated contractions of the smooth muscle cells in the myometrium occur to expel the fetus out of the uterus. The serosa or peritoneum is the outermost layer of the uterus. It is a multilayered membrane that lines the abdominal cavity and supports and covers the organs.

The smooth cells progressively increase in size during the last stage of gestation with a maximum length of 300 μm and a maximum width of 10 μm [10]. Contractions of smooth muscle cells happen due to the interaction of myosin and actin filaments.

The uterine smooth muscle fibers are arranged in overlapping tissue-like bands, the exact arrangement of which is a highly debated topic [11]. All myocytes (uterine muscle cells) are gathered in packages or "bundles" (Ø 300 + / - 100 microns) with junctions between them. Packets are contiguous within a bundle or fasciculus. The bundles are arranged parallel to the surface of the uterus, transversely at the fundus and obliquely downward. Communicating bridges, named Gap Junctions, connect adjacent bundles. A diagram of this structural organization is shown **Figure 1.2**.

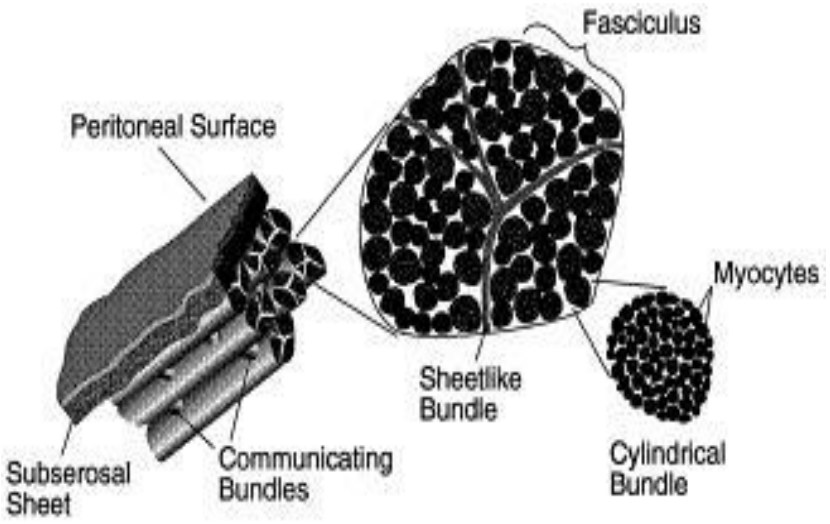

Figure 1.2: Three-dimensional structure of the woman uterus [12].

1.2.2 Uterine activity

The mechanical activity of the non-gravid uterus is cyclic and depends on the hormonal menstrual cycle. It includes an activity phase spread throughout the whole uterus, which permits the expulsion of blood and debris endometrial. The beginning of the cycle is characterized by contractions spread to the entire uterus directed towards the cervix and by frequency equal to 1-3/min. The mid-cycle, ovulatory period, is characterized by strong and regular contractions directed to the fundus of the uterus, with a frequency equal to 10/min, and which is thought to promote the progress of sperm. Then a quiescent phase occurs. It corresponds to the development of the endometrium that is required for any eventual implantation. The contractions are local, low-intensity directed towards the bottom and of frequency equal to 265/min [13].

The gravid uterus also contains a phase of relative quiescence during most of the pregnancy stage, followed by a period of activity leading to childbirth. In women, two types of uterine activities coexist:

- Contractions of very low amplitude, with frequency of 1/min and very local influence, named Low Amplitude High Frequency (LAHF, Onde Alvarez - OA- in French).
- Contractions of higher amplitude and lower frequency (one every 3 or 4 hours, at the beginning of their emergence around 18 weeks of gestation). These contractions called Braxton Hicks contractions become more frequent and stronger when approaching the term (1 per hour at 30th week) and have a wider field of influence than that of LAHF [14-15].

The most significant change noticed in early labor concerns the spread of activity. From partially propagated in late pregnancy, labor contractions become strong, rhythmic and spread to the entire uterus in a short time. The insertion of intrauterine catheters (= internal tocography) allows the recording and the definition of a set of parameters describing uterine contractions (UC) (**Figure 1.3**). These parameters are:

- The basic tone.
- The amplitude of UC.
- The frequency of UC.
- The duration of UC.

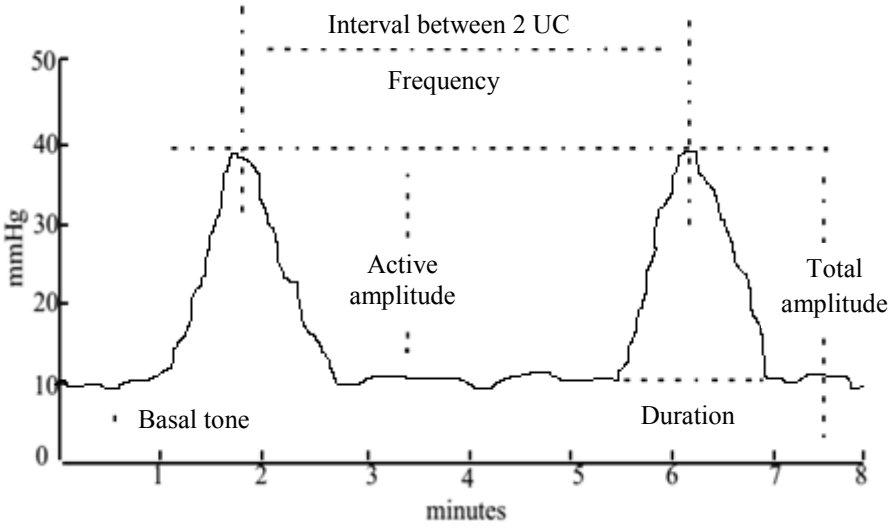

Figure 1.3: A diagram illustrating the different parameters of the uterine contraction (UC), edited from [16].

During normal labor, the uterine activity quantified by these different parameters will gradually increase. The basic tone varies from 5 to 13 mm Hg [17]. The total amplitude of the UC, which takes into account the basic tone, varies from 30 to 65 mmHg. In practice, the basal tone is not taken into account and therefore it is the active amplitude (or real intensity)

of UC which is usually considered [17]. The average interval between 2 UC (period) gives the frequency of UC in 10 minutes. It is initially 1 to 3 UC / 10 min and reached normally 4 or 5 UC / 10 min at the end of labor. Meanwhile, the average duration of the UC goes from 60 sec to 85 sec [18].

1.2.3 Cellular and ionic bases of myometrial contraction

In the uterine smooth muscle as in other smooth muscle, calcium seems to be the decisive and essential element of the intracellular mechanisms underlying the contractile activity. The key enzyme is the myosin light chains kinase (MLCK) which, activated by the complex Ca^{2+}-calmoduline (Ca^{2+}-CaM), phosphorylates the myosin light chain LC20 (**Figure 1.4**). It is in this phosphorylated form that myosin can interact with actin and cause contraction. The fall in the concentration of intracellular calcium $[Ca^{2+}]i$ leads to relaxation: the dephosphorylated myosin, by the action of a specific phosphating, then detaches from the actin. Furthermore, phosphorylation of MLCK causes a decrease in its ability to activate myosin and thereby to produce the contraction. This activation pattern (related to depolarization followed by repolarization) is well established in vitro but does not always seem to be strictly followed in vivo. In addition, the relative importance of different control channels varies according to whether it is a spontaneous contractile activity or that caused by extracellular signals. Some animal studies suggest the existence of other regulatory pathways involving protein kinase C (PKC) and the fine filament proteins, the caldesmon and calponin, whose role is far from being elucidated in the uterus [19-20].

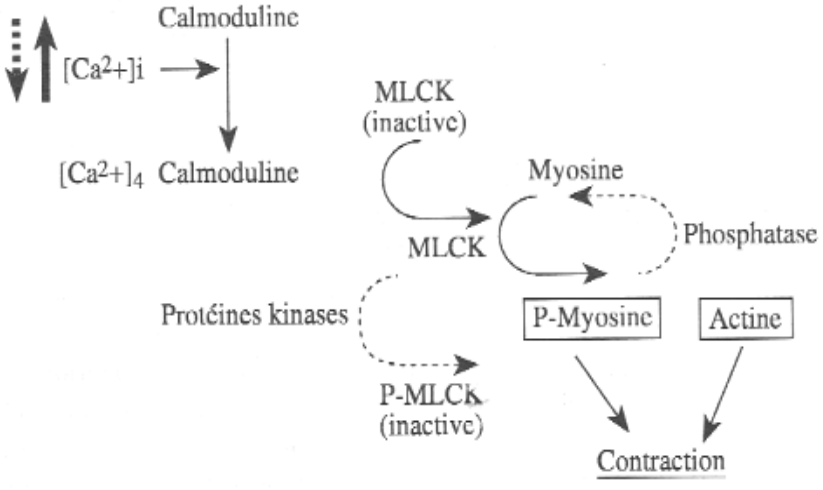

Figure 1.4: Biochemical mechanism of contraction (_____) and relaxation (- - - -) of the uterine muscle. MLCK: Kinase of myosin light chains [20].

Different structures and mechanisms are responsible for the increase in the concentration of free Ca, $[Ca^{2+}]i$, from about 10^{-7} to 10^{-6} M, which is essential for the activation of MLCK. Calcium channel conductance can be activated by a change in transmembrane potential (VOC-Voltage operated channels), of type L ("long lasting") and T ("transient"), by fixing a specific ligand (ROC, Receptor-operated channels) or by mechanical constraint. The available $[Ca^{2+}]i$ can also come from intracellular sites which have an increasing capacity for storing Ca^{2+} as gestation progresses.

1.2.4 Propagation of the uterine activity

The cause of uterine contractility is mainly myogenic. The muscle is solely responsible for its contraction, although intrinsic (mechano-receptor ...) and extrinsic control (sympathetic and parasympathetic systems) is present. Close to the time of delivery, the uterus initiates and coordinates the firing of individual myometrial cells to produce organized contractions causing the expulsion of the fetus from the mother‟s body. The contractile activity of the uterus results from the excitation and propagation of electrical activity.

Myometrial cells are coupled together electrically by gap junctions composed of connexin proteins [21]. This grouping of connexins provides channels of low electrical resistance between cells, and thereby furnishes pathways for the efficient conduction of action potentials. Throughout most of pregnancy, and in all species studied, these cell-to-cell channels or contacts are low, with poor coupling and decreased electrical conductance, a condition favoring quiescence of the muscle and the maintenance of pregnancy. At term, however, the cell junctions increase and form an electrical syncytium required for coordination of myometrial cells for effective contractions. The presence of the contacts seems to be controlled by changing estrogen and progesterone levels in the uterus [21]. The Gap Junction bridges are responsible for conducting the rapid communication of the action potential between different bundles [12].

Another mechanism for controlling the uterine activity is through calcium waves [22]. However, it is necessary to distinguish two types of wave: the intracellular calcium wave and the intercellular calcium wave. The intracellular calcium wave is consistent with rapid changes in intracellular calcium concentration [Ca2 +] in a single cell. This wave is capable of crossing the cell membrane and becomes an intercellular calcium wave. The intercellular calcium wave propagates slowly (~ 4 microns / sec) and to a relatively low maximum distance (~300 microns) corresponding to the size of a bundle [22-23].

Like cardiac cells, uterine myometrial cells can generate either their own impulses -pacemaker cells- or can be excited by the action potentials propagated from the other neighboring cells -pacefollower cells. But unlike cardiac cells, each myometrial cell can alternately act as a pacemaker or a pacefollower. In other words, there is no evidence of the existence of a fixed anatomic pacemaker area on the uterine muscle [11, 24]. The spontaneous oscillations in the membrane potential of the autonomously active pacemaker cells lead to the generation of an action potential burst when the threshold of firing is reached. The electrical activity arising from these pacemaker cells excites the neighboring cells, because they are coupled by electronic connections called gap junctions. It is believed that the action potential burst can originate from any uterine cell, thus the pacemaker site can shift from one contraction to another [11, 24].

Many hypotheses on the pacemaker cells have been issued including their number, position ... It seems that there is a one or more preferential pacemaker activities loci near the fundus, as found by Caldeyro-Barcia et al. [25]. This activity is then propagated in all directions, but ultimately from the fundus to the cervix.

1.3 Uterine electromyography

Uterine electrical activity is the result of the depolarization and repolarization of thousands of myometrial smooth muscle cells [10-11, 24]. The immediate succession of depolarization and repolarization phases of a myometrial cell induces a burst of action potentials. It has been shown that each contraction is associated to a burst of action potentials. The uterine electromyogram arises from the generation and transmission of these bursts of action potentials in the uterine muscle. By spreading through gap junctions, from one myometrial cell to another, this activation results in an increased and organized electrical activity, particularly in the last trimester of pregnancy and during labor [26]. This increased, organized uterine electrical activity precedes the uterine mechanical contraction and is associated to cervical shortening and dilatation, a phenomenon known as the uterocervical reflex [11, 27-29]. The frequency of the action potential within a burst, the duration of the burst and the total number of simultaneously active cells are directly related to the frequency, duration and amplitude of a contraction.

Early studies of the uterine electromyographic signal were performed by internal electromyography. They allowed the detailed description of the EMG signal, during

contraction, as an electrical activity whose frequency is mostly between 0.1 and 1Hz and that has an amplitude between 100 μV and 1.8 mV [30]. Simultaneous recording of internal and external EMG activity on the same woman showed a very good correlation between the two signals [11, 31]. This demonstrated that the surface EMG signal is representative of the electrical activity of the uterine muscle. These results have been confirmed in an analysis of the EMG signal of the pregnant macaque [4]. Using these results, the external uterine EMG has become a standard non-invasive method for the study of uterus electrical activity.

The electrohysterogram (EHG), that is the uterine EMG recorded, by using surface electrodes, is characterized by a low frequency activity (0.1 to 0.3 Hz) with a superimposed activity of higher frequency (FW, fast Wave: 0.3 to 2 Hz). The low frequency signal is considered as the result of mechanical disturbances induced by the deformation of the abdomen under the effect of contractions [32]. At the opposite, FW (parted then in two components FWL - Fast Wave Low- and FWH - Fast Wave High) is related to uterine contractions. A comparison study between contractions during pregnancy and labor showed that, for both type of contractions, the EHG energy is predominantly in the 0.2 - 3 Hz frequency band [2]. It has also been shown that there is nevertheless a difference in frequency distribution between these two types of contraction (pregnancy and labor). A shift towards higher frequencies is observed as term progresses [2].

Propagation of the uterine electrical activity

Electromyography studies performed by Garfield et al. show that there is infrequent and unsynchronized low uterine electrical activity throughout most of the pregnancy [33-34]. This is also demonstrated in the recording of human uterine electrical events (EHG) acquired from the abdominal surface during pregnancy [11]. There is little uterine electrical activity, consisting of infrequent and low amplitude EMG bursts, throughout most of pregnancy. When bursts occur prior to the onset of labor, they often correspond to periods of perceived contractility by the patient. During term and during preterm labor, bursts of EMG activity are frequent, of large amplitude, and are correlated with the large changes in intrauterine pressure and pain sensation.

The increase in gap junction number, and the resulting facilitated electrical transmission, provide better coupling between the cells resulting in synchronization and coordination of the contractile events of the whole uterus.

Thus the efficiency of contractions leading to labor depends on the burst activity synchronized over a large area of the uterus [35]. Therefore it is important to determine the extent of propagation throughout the multi-cellular uterine muscle bundle. Since the propagation of these uterine contractions can be in both longitudinal and transverse direction, due to the complex uterine structure, we need to determine the propagation characteristics over the entire maternal abdomen while performing surface recordings. We believe that information regarding the spatial-temporal activation of the uterus may be predictive of onset of labor leading to the delivery of the fetus. Thus, a complete spatial-temporal mapping of uterine activity throughout pregnancy is a key parameter that will improve the understanding of the uterine contraction mechanism.

1.4 Premature labor

According to the definition of the World Health Organization (WHO), preterm delivery is a delivery at a gestational age of less than 37 completed weeks or less than 259 days of amenorrhea. Every birth occurring after 22 weeks of amenorrhea and before 37 weeks is defined as a premature birth. A birth occurring before 22 weeks of amenorrhea is considered as an abortion by WHO.

Preterm labor is a topical issue because out of 750,000 births in France, 44,000 are premature [36]. Preterm labor is still the most common obstetrical complication during pregnancy, with 20% of all pregnant women at high risk of preterm labor. In the United States, more than half a million babies -that's 1 of 8- are born premature each year. At 1500 $ a day for neonatal intensive care, this constitutes expenditure well over 4 billion $ each year. Also, preterm birth accounts for 85% of infant mortality and 50% of infant neurologic disorders [37].

Preterm birth is a pathology that can lead to serious consequences for the child and has also a socio- economic cost. The main risks to children are:

- Respiratory distress (often associated with hyaline membrane disease)
- Infection
- Neurological Diseases
- Hypothermia
- Necrotizing enterocolitis

Over the last 20 years, advances in neonatal care for children of less than 1500 grams have increased significantly their survival rate. One of the major problems facing the obstetrical world through the development of an effective treatment, is that the causes of premature labor are not known in 40 % of cases [38]. However, some factors appear to play an important role in the prevention of preterm labor.

Socio-economic factors, microbial infections, uterine anomalies, premature rupture of membranes and various pathologies of pregnancy are factors involved in the risk of preterm labor.

The preterm birth rate has changed little over the past 30 years. Only France [39], Finland and Norway [40] observed a decrease between the late 60s and 80s. In France, the prematurity rate has stabilized between 1990 and 1995; it was 5.4% in 1995 [41]. Live births before 37 weeks increased steadily from 5.4% in 1995 to 6.6% in 2010 [42]. It reached 7 % in Canada and more than 10% in the United States [43] at the same time.

1.4.1 Detection of labor and prediction of premature labor

Optimal detection of labor implies finding markers indicating that the labor will occur, but also predicting whether it will actually result in a premature birth (premature labor), to avoid unnecessary treatment of significant number of patients. Moreover, these markers must be observed as early as possible, so clinicians will have time for intervention. For example, when the decision is to keep the fetus "in utero", it seems easier to prevent the onset of labor than to stop it. Similarly, when a premature rupture of membranes occurs, a delay is valuable so that the administration of corticosteroids can have effect on fetal lung maturation.
There are several methods presently used for the detection of preterm delivery among them:

- *Measurement of biochemical markers*:
    - Fetal Fibronectin (FFN) [44].
    - α-fetoprotein [45].
    - Placental peptides [46].

They have been proposed as methods for monitoring patients that have a risk for premature labor. Some results show that FFN can be used for the prediction of premature labor [47] although with poor likelihood ratios.

- *Clinical diagnosis*: This technique includes cervical dilation and effacement, vaginal bleeding, or ruptured membranes [48].

- *Maximal uterine contractions*: This technique measures the maximal number of contraction events seen in any 10-min period, measure done by a clinician based on tocodynamometer (TOCO) [49]. Tocodynamometers (TOCO) are external devices aiming to measure the force generated by the slight movement of the uterus caused by uterine contractions measured on the mother‟s abdomen. They give an indirect indication of uterine contraction. Their non-invasiveness allows the devices to be used for all pregnancies without risk to the fetus or to the mother. They are used in nearly all births in a medicalized setting. Nevertheless, TOCO monitoring is uncomfortable, inaccurate and depends on the subjective interpretation of the examiner. Intrauterine pressure (IUP) catheters provide the best information concerning uterine contractions, allowing the exact quantification of the mechanical effect of contractions. But the clinical usefulness of this technique is limited by its invasiveness, since it requires prior rupture of membranes in order to insert the pressure device into the uterus. This can increase the risk of infection or accidental induction of labor [50].

- *Abdominal and transvaginal ultrasound*: No clear success was achieved by using this technique to detect premature labor [51]. However, this technique gives prediction later after the onset of preterm labor symptoms. Furthermore, the measurement of the cervical length by ultrasonography is largely influenced by the varying amounts of urine in the bladder [47].

- *Detection of the circadian rhythm of uterine activity* [52].

Most of these methods of evaluation and monitoring of premature labor suffers from a problem of sensitivity and objectivity. Current treatment methods are however most effective when the detection of labor is made early. They are not usually applied unless the threat of labor is certain.

Other directions have been more recently investigated in order to define a reliable marker of preterm labor threat:

- *Magnetomyography (MMG)*: This technique measures noninvasively the magnetic fields associated with the uterine action potentials. Eswaran et al did the first MMG recordings of spontaneous uterine activity by using 151 magnetic sensor array [53].

- *Uterine electromyography or Electrohysterogram (EHG)*: Uterine EMG is the result of electrical activity originating from the depolarization-repolarization of billions of smooth muscle myometrial cells. It has been proved that synchronous myometrial and abdominal activities occur, which are temporally correlated with the mechanical activity of the uterus

during pregnancy and labor, whatever the species, including humans [11]. Numerous studies have shown that EHG can be appraised accurately and reliably from non-invasive trans-abdominal surface measurement [11, 50].

The study of uterine contractility by electromyography (EMG) has been ongoing for many years. One of the first studies was in 1931 [54]. Early studies focused on the temporal and frequency analysis of the signal. The electrohysterography signal (EHG) appeared to be a potential vector indicating the risk of preterm delivery. Indeed, there is a good correlation between the occurrence of a burst of electrical activity on the signal and the increase in intrauterine pressure [55].

Predicting preterm labor with this signal, however, has been the subject of many years of research and has not yet been fully achieved. These studies have evidenced the needs for the development of specific EHG processing methods, to extract characteristic contractility parameters, as well as a large amount of data to demonstrate their potential diagnosis efficacy.

1.4.2 Parameters extracted from EHG for preterm labor prediction

The excitability, propagation of uterine activity and position of uterine activity source(s), all influence the EHG characteristics mainly through its two frequency components, traditionally referred to as FWL (Fast Wave Low) and FWH (Fast Wave High). The propagation of the uterus electrical activity is supposed to be related to FWL, whereas the excitability of the uterus is supposed to be related to FWH [11]. Thus labor detection or preterm prediction has been attempted by extracting parameters from these two components of the signal. The EHG signal has been studied mainly on specific parts of the recordings, the bursts of electrical activity, that correspond to the mechanical contractions of uterus [56]. The main efforts in this direction using excitability parameters as well as propagation parameters are the following:

- *Excitability parameters*:

The first attempt to measure uterine electrical activity was done by Bode on 1931 [54]. Then many researchers tries to record uterine EMG invasively or not during labor [57-59]. Different parameters have then been extracted to characterize the electrical bursts of activity.

Temporal parameters:

- Sureau et al. analyze the evolution of amplitude in different physio-pathologic situations, but this parameter is influenced by many factors [32, 60].

- Gondry et al. follow of uterine activity during pregnancy *"longitudinal study"* using EHG temporal characteristic [61].
- Root mean square (RMS) value was used to detect the risk for preterm delivery [62].

Spectral parameters:

- When authors began the investigation the uterine EMG frequency content, they were limited at the begin to the *slow wave band* [59, 63]. But they doubted that the slow wave had any physiological meaning.
- Therefore most authors then studied only the electrohysterogram in the frequency band corresponding to FWH. They soon found a synchronization between the abdominal and myometrial electromyogram activities [28, 30, 64].
- The amplitude distribution as well as *the power density spectrum median and modus spectrum* of uterine EHG activity bursts were calculated and analyzed [2, 65].
- Marque et al. follow the EHG spectral content in function of contraction efficiency during labor [2].
- It was proved that, during pregnancy, uterine activity is minimal and characterized by electromyographic bursts infrequent, of low amplitude and low frequency content [61]. This activity becomes frequent, of large amplitude and higher frequency content during term and preterm labor [2], [27].
- It was observed by Marque et al. that the relative energy in the low frequency band to total frequency band (L/T) decrease whereas the relative energy in the high frequency band to total frequency band (H/T) increases, creating thus a shift to higher frequencies as delivery approaches [2].
- Close to delivery, the administration of nifedipine, make a shift of modus frequency of EHG power spectral density to lower frequencies when it is expected to rise [66].
- It was shown by Fele-Žorž et al. that the value of median frequency increases with the approaching of labor, which may be associated with term delivery [67].
- The duration, the mean value and/or standard deviation and the modus frequency of PSD, and the number of bursts per unit time extracted from EHG bursts were also evaluated. The artificial neural networks classified correctly the majority of term and preterm laboring and non-laboring bursts using these extracted parameters [68].

Time-frequency parameters:

- Leman et al. [69-70] used wavelet decomposition to denoise the EHG.
- Recently, wavelet transform approaches were used for the prediction of preterm labor risk [71].
- Wavelet analysis was used also for the detection and classification of EHG signals [72-73].
- Marque et al. guide a study for denoising, characterization and classification of EHG signals using time frequency parameter in order to build a portable device for home pregnancy monitoring [74].
- Duchêne et al. track the instantaneous frequency of the EMG burst recorded internally on monkey uterus and confirmed the relationship between surface electromyogram and internal electrical activity at the uterine muscle level [75].

Nonlinear parameters:

- Oczeretko et al. showed that the uterine activity of non-pregnant uterus presents nonlinear features [76]. Nonlinear time series analysis techniques were applied to uterine EMG signals since they can give information about the nonlinear features of EHG signals, which arise from the underlying uterus physiological processes [77].
- Some researchers claimed to show that the sample entropy method is a promising method in preterm and term labors classification [67]. They showed also that we can evaluate the progress of the labor using sample entropy method [78].
- Maner et al. showed that the bursts of patients who will deliver spontaneously within 24 h and those who will not can successfully be separated by this wavelet decomposition generated fractal dimension [79].
- Sabry-Rizk et al. examined the nonlinear dynamics of the uterus EMG signals on normal and abnormal labor contractions in the first stage of the labor. An attractor structure has been calculated on abdominal EMG signals at various relaxation and contraction periods. The observed black inertness of attractors was called nucleus. Precisely, by studying its fractal behavior it was shown that the size of the nucleus increases with cervical dilatation until it takes over the entire phase-space. The weak labor contractions, typical for failure in progress in the first stage of labor, showed predominantly periodic structures with or without small-size nuclei [80].
- Recently, time reversibility appear as a useful method for the detection of uterine EMG nonlinearity characteristic and pregnancy/labor classification [6].

- But all the nonlinear methods do not have the same performance, as it was shown with maximal Lyapunov exponent and correlation dimension, that did not manage to differentiate between labor and non-labor classes [67].

- *Propagation parameters*:

All the excitability parameters cited above were computed with a monovariate approach (one burst processed at a time, extracted from a single EHG signal). They, more or less, permited a differentiation between pregnancy and labor contractions, to provide information for preterm labor (PTL) diagnosis. As uterine contraction efficiency is related to both excitability and propagation, the computation of propagation parameters with the excitability one might improve this classification. Only few studies have been done to characterize the propagation of EHG signal. These studies can be summarized as following:

Linear and nonlinear correlation:

- Marque et al. have observed more correlation in low frequencies than high frequencies using the linear correlation coefficient which support the hypothesis that the propagation is related to FWL [81].

- Duchêne et al. were interrested in stuying uterine EMG propagation using autocorrelation, cepstrum and deconvolution function [82].

- The linear inter-correlation remains the main method that has been used for EHG propagation analysis [82-83].

- The inter-correlation function was used also by Mansour et al. to analyze the propagation of the internal uterine EMG on four internal electrodes, sutured on the uterus of a monkey during labor [4]. The signals were first filtered into FWL and FWH frequency bands. Then the inter-correlation function was calculated for each wave between the two pairs of electrodes. The results coincide with the hypothesis that the correlation is always higher for FWL than for FWH.

- Most of the researchers said that the synchronization of uterine electrical activity is the most important factor that leads to an efficient labor. To analyze the synchronization, uterine EMG activity can be recorded from the abdominal surface using multi-electrode measuring systems. Jiang et al. simultaneously measured uterine EMG activity using 16 channels [84]. They obtained 297 contractions from twenty patients

in labor. The energy on the frequency range between 0.2 and 0.45 Hz (FWL) and between 0.8 and 3 Hz (FWH) was calculated. In this study, analysis was restricted to the relative energy (H/L) of uterine EMG signals. The energy was computed for each channel individually, and divided by the minimum of the 16 channels. Then they imaged the synchronization of uterine contractions by means of uterine EMG topography. This method of representing the synchronization uses the relative amplitudes of uterine EMG signals in relation to the surface of uterus.

- It was proposed that the prediction of labor may be increased by the observation of synchronization together with the classical time – frequency analysis [85].

- Recently, it has been shown that the nonlinear correlation between EHG signals increases from pregnancy to labor [86]. However, in this study, authors have analyzed the connectivity on the whole uterine bursts (no pre-segmentation).

- The segmentation of monkey uterine EHG signals using bivariate and univariate piecewise stationary pre-segmentation algorithm was done successfully by Terrien et al. [87-88] and a comparison between univariate and bivariate segmentation algorithm was done. They investigate in this study the effect of taking only the higher frequency component of signal on the behavior of the nonlinear correlation within the EHG burst.

- The investigation of the effect of filtering human uterine EHG signals within its different frequency component (low and high component) was done also by Terrien et al. [89]. They prove that filtering the signals within FWL which is supposed to be related to propagation of EHG signals, increases the pregnancy/labor classification rate using nonlinear correlation coefficient method and makes the difference between both group more significant.

Identification of uterine activity origine, its movement and velocity:

- Planes et al. begin the quantification of propagation velocity using linear correlation [90].

- Using 240 extracellular electrodes placed around the whole uterus, Lammers et al. [91] measure the electrical activity of the term pregnant guinea pig uterus. Using this recording, they calculate the velocity of longitudinal and circumferential conduction.

Thus, they study the two-dimensional spread and the propagation of signals. They found that the velocity of spikes propagation is about 7 cm/s in the longitudinal direction, where the muscle bundles lie parallel to the plane of propagation, and about 3 cm/s in the circular direction, where muscle is organized at right angles.

- Some authors tried to identify the center of uterine activity by using eight channel measuring system and calculating continuously the "frequencies of movement patterns" from normalized and filtered signals. Euliano et. al. [92] followed the direction of propagation and movement of the center of activity (the origin of the contraction). This study reports an interesting pattern in women who delivered successfully: the direction of the center of uterine activity was predominantly to the fundal. This means that the relaxation of uterus begins from the lower uterine segment toward the upper portion of the uterus in women who deliver vaginally [92].

- Cadeyro-Barcia et al. also claimed by clinical studies that the uterus begins to contract in the upper fundal region and then this contraction is conducted toward cervix [93].

- Lammers et al. [91] conduct a study on the guinea pig uterus that shows that there are two possibilities for the origin of electrical activity, either the ovarian or cervical end of the uterus, and that the velocity was not affected by the propagation in either direction (i.e., toward the ovary or toward the cervix). However, the authors assumed that activity was initiated mostly in the ovarian end (corresponding to fundus in humans).

- Duchene et al. also show the existence of a constant chronogram during labor by studying the correlation of EHG envelopes recorded at several sites in the uterus of delivering macaques [82].

- The inter-electrode delay was estimated for surface multichannel EHG recordings in order to analyze the uterine activity propagation [94]. Authors focused on localizing pacemaker zones. Localization on the upper part was been observed on 65% of case.

- Most of the previous study performed on EHG did not study the directionality between signals. Whereas, few other studies evidenced a propagation that spreads in all directions, with a dominant direction down towards the cervix [95-96].

Source localization:

All the previous mentioned study that try to identify the uterine activity origin, are based on uterine EMG processing applied in the temporal, frequency and/or time-frequency domains, in order to measure coupling, synchronization, velocity or relation among signals channel. However, a lot work focused on source(s) localization of brain and cardiac activities have been developped recently by solving the called "forward" and "inverse" problem using EEG and MEG signals [97-98]. Unfortunately, to our knowledge, no similar study had been done on EHG signal for the localization of uterine activity sources. This kind of information may be useful for the monitoring of pregancy and labor contractions.

Clearly more studies on the origin and directionality of the signals are needed, as well as investigation of the pacemaker activity. The aim of this work is therefore to test the power of different synchronization methods to detect the evolution of uterine synchronization, from pregnancy to labor, and to estimate the direction between uterine EMG channels during pregnancy and labor. As EHG contains nonlinear characteristics, we will compare linear and nonlinear methods for this synchronization study. We expect thus to improve the performance of synchronization analysis and provide relevant features for a clinical diagnosis of preterm labor. Furthermore, in this study we investigated the possibility to solve the EHG forward/inverse problem in order to localize uterine EMG source(s).

1.5 Current work context

It was recently evidenced that the electrode configuration and the measurement protocol have a strong effect on the detection of uterine signals, that consequently affects the extraction of EHG characteristics, such as propagation parameters [99].

1.5.1 Electrode configuration

Most researchers used two to four electrodes in the analysis of the uterine contractility. Traditionally it was supposed that the increase in contractility is mainly related to modifications of the frequency and/or amplitude characteristics, that can be computed from only one EHG burst (monovariate approach). However, for a precise investigation of the propagation of electrical activity through the whole uterus, an increase in the number of electrodes is necessary (bi- or multivariate approach) [100].

Myometrial electromyograms collected by surface electrodes represent the summation of underlying cellular activities. This spatial integration implies an increase in signal amplitude,

and is usually associated with a low pass filtering effect that has been extensively investigated and modeled in striated muscles [101]. Abdominal electromyograms exhibit the activities similar to internal electromyograms, except that they are low-pass filtered by the conductive properties of tissues lying between the uterus and the electrodes [31].

Abdominal electrodes can be located anywhere as long as they are above the corpus uteri. However, placement along the vertical median axis provides a better signal/noise ratio because of a closer contact and a more constant position of the uterus relative to the abdominal wall during contractions [11].

For electrode configuration, most authors choose to record both myometrial and abdominal electromyograms with bipolar electrodes. So far only Mansour et al. [102] have obtained noiseless myometrial electromyograms, with monopolar electrodes directly sutured on monkey uterus. However, for abdominal recordings it is imperative to use bipolar electrodes, because the signal/noise ratio is lower than for internal ones. Bipolar electrodes reflect the difference between the two signals present below the two electrodes. Common noise, such as maternal electrocardiogram, maternal movements, electrode movements, and power line interference are thus efficiently rejected.

The bipolar recording mode affects the electrohysterogram spectral content. With the usual model of action potential propagating with a constant speed along a striated muscle fiber, power spectral density of electromyograms has been shown to depend on the inter-electrode distance, on the propagation velocity, and on the frequency band of the action potential [103]. Bipolar recording induces a high-pass filtering effect, thus eliminating the very low frequencies; there is also an increase in the higher frequencies when the distance between electrodes is small when compared with the distance between the fiber and the recording electrode pair [101, 103]. Also bipolarization induces a bias to the direction of propagation of uterine EMG signals by forcing the direction to be horizontal or vertical when the bipolarization is done between vertical or horizontal electrode pairs respectively.

As a consequence, the monitoring of human uterine activity should only be performed with bipolar abdominal electrodes, even though the bipolar recording mode induces a high-pass filtering of the signals. Abdominal electrohysterograms contain information related to myometrial electromyograms, except that the abdominal signal is low-pass filtered because of tissue filtering. Otherwise, a complete temporal and spectral electromyogram characterization

requires monopolar myometrial EMG recordings, which is obviously not possible for clinical monitoring.

Recently, attempts have been made for filtering monopolar EHG signals to obtain a proper signal to noise ratio, suitable for signal processing. To this end, Hassan et al. [104] developed a powerful EHG filtering methods based on the combination of canonical component analysis (CCA) and empirical mode decomposition (EMD). He proved that this method, named CCA-EMD, increases the signals to noise ratio of the monopolar EHG signals. The obtained SNR is larger than with bipolar EHG and with monopolar EHG filtered by other methods, such as wavelets and independent component analysis (ICA).

As the bipolarization decreases the spatial resolution, and may also cause a bias for the correlation analysis, if common electrodes are used to generate adjacent bipolar leads, the use of monopolar EHG could be of great interest for the study of uterine synchronization.

1.5.2 Multichannel experimental EHG recording protocol

Multichannel EHG signals is usually obtained by using multiple electrodes placed on the mother‟s abdomen. A high spatial resolution is needed in order to obtain a precise maping of uterine EHG contractions. The total number of electrodes is however limited by the abdominal surface, specially when the electrodes should be put along or as near a possible to the median vertical axis, in order to get a better signal-noise ratio (SNR). The use of monopolar recordings (signals used independantly) improves spatial resolution and also prevents from the propagation direction bias induced by the bipolarization of signals (signals used pairwise).

In order to study the propagation of the uterine electrical activity in the view of predicting preterm labor, [83] we decided to map uterine electrical activity by placing electrodes in a four by four grid on the woman‟s abdomen. Indeed we believe that using a grid of 16 electrodes, instead of a smaller number, may help to better understand the underlying mechanism of uterine contractions as well as to improve the prediction values for preterm labor.

Placing a large number of electrodes for measurements is time consuming and is difficult to perform, especially in a labor room setting. For this reason a project was launched in Iceland in 2009 to design a placement system that decreases placement time, reduces the complexity of the electrode positioning method, by defining a „standard‟ position for recording. The new

design retained involves a guide with holes, guiding the placement, as well as adhesion of the electrodes by means of a double-coated adhesive sheet. A simple frame ensures correct positioning of the guide onto the adhesive sheet, while positioning the electrodes. With about 2 cm inter-electrode distance, the 16 electrodes (8mm in diameter) are arranged in a 4x4 matrix. This system permitted us to standardize the signals acquisition during this French-Icelandic EHG propagation analysis project. A typical example of the matrix placement is illustrated in **Figure 1.5**.

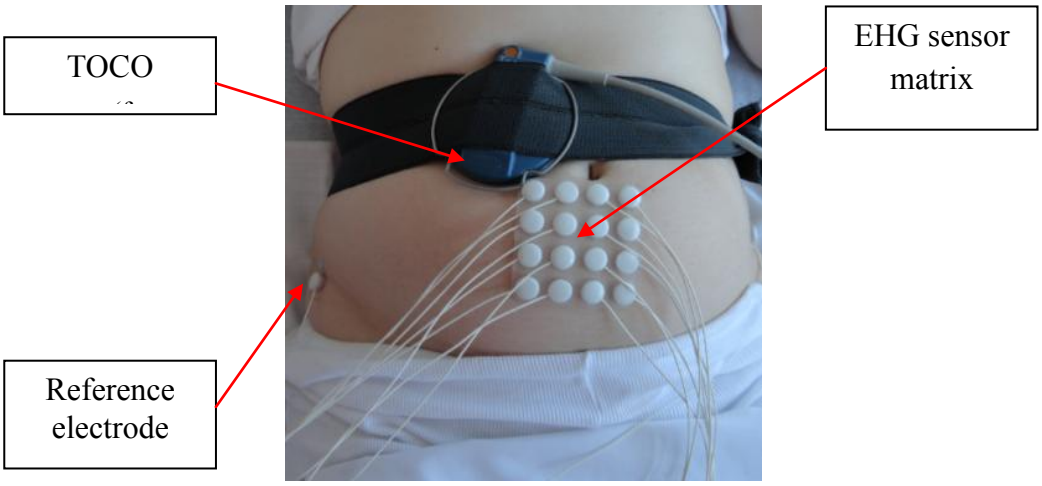

Figure 1.5: Typical example of the 4x4 electrodes matrix and TOCO sensor positioned on the woman‟s abdomen.

The measurements were first performed by using a 16-channel multi-purpose physiological signal recorder, most commonly used for investigating sleep disorders (Embla A10). We later used another multi-purpose physiological signal recorder (Porti 32, TMSi) with 32 possible channels. We used Reusable Ag/AgCl electrodes (8mm diameter). The measurements used in this work were first performed at the Landspitali University hospital in Iceland, following a protocol approved by the relevant ethical committee (VSN 02-0006-V2), and then at the Center of Amiens for Obstetrics and Gynecology in France, following a protocol approved by the regional ethical committee (ID-RCB 2011-A00500-41) of Amiens Hospital. The subjects were healthy women either in the first stages of labor having uneventful singleton pregnancies (Labor population), or healthy women having normal (Landspitali University hospital) or risk (CGO Amiens) pregnancies at varying gestational age (Pregnancy population). After obtaining mother‟s informed consent, her skin was carefully prepared using an abrasive paste and alcoholic solution. After that, the sixteen electrodes were placed on the abdominal wall according to **Figure 1.5**. The third electrode column was always put on the uterine median

vertical axis and the 10-11th electrode pair on the middle of the uterus (half way between the fundus and the symphysis). Two reference electrodes were placed on each of the woman‟s hip as shown in **Figure 1.5**.

The signal sampling rate was 200 Hz. The recording device has an anti-aliasing filter with a high cut-off frequency of 100 Hz. The tocodynamometer paper trace was digitalized in order to facilitate the segmentation of the uterine contractions.

1.5.3 Thesis roadmap

Monopolar EHG signals are very noisy and have low Signal to Noise Ratio (SNR). Indeed, they are often corrupted by electronic and electromagnetic noises, as well as by movement artifacts, skeletal EMG and electrocardiogram from both the mother and the fetus, preventing their direct use for propagation analysis. This is why, until now, most people studied only bipolar EHG.

Due to these observation and to the evolution of our team work, this thesis has been divided in two parts:

- The first step was to gather into one single dataset all the bipolar signals recorded by our colleagues using the protocol described above. We first processed bipolar signals, in order to get a correct SNR: vertical bipolar signals (BP1,... BP12) were computed as shown in **Figure 1.6**. These signals were used when analyzing the nonlinear characteristics of the EHG signal (chapter 2) since for this study (univariate analysis), we were neither interested in spatial resolution nor in propagation direction. I processed signals recorded on 23 women in Iceland: 11 recorded during pregnancy (33-39 weeks of gestation) and 12 during labor (39-42 weeks of gestation); and on 27 women in France: 25 recorded during pregnancy (33-39 weeks of gestation) and 2 during labor (39-42 weeks of gestation). After segmentation we obtained from this whole database 115 labor EHG bursts and 174 pregnancy EHG bursts related to different contractions, for each of the 12 bipolar channels.

- For the bivariate analysis, propagation analysis (synchronization, direction), and for source localization analysis, the CCA-EMD method was already well established in our team for denoising the monopolar EHG. As the spatial resolution is very important for propagation analysis, we there used monopolar signals. Another set was recorded in Iceland by using the same equipements and by the same operator. We thus used monopolar signals recorded only in Iceland, in order to get a very homogeneous poulation, made only from normal pregnacy

and normal labor contractions. We obtained signals from 18 women: 13 recorded during pregnancy (31-41 weeks of gestation) and 5 during labor (39-41 weeks of gestation), among them 6 women were recorded longitudinaly at different pregnancy terms. The recording duration was approximately 1 hour for each subject.

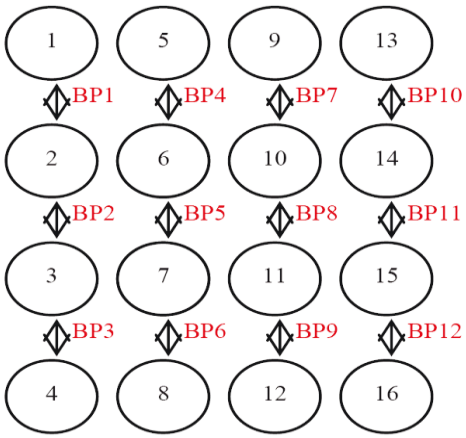

Figure 1.6: Electrodes combination (Bipolar and monopolar) on the women's abdominal wall.

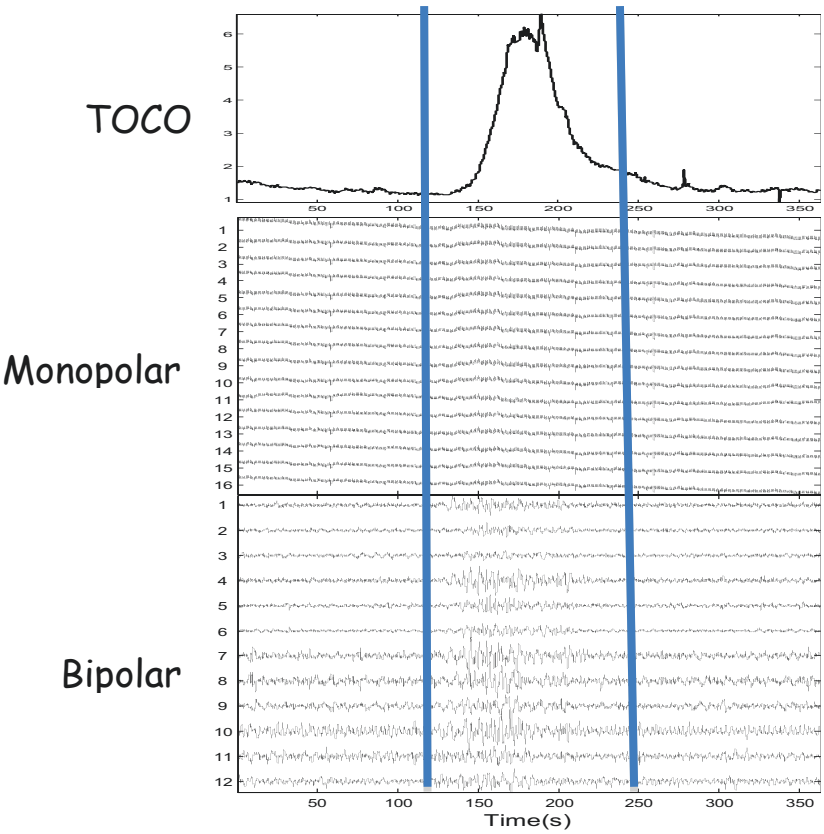

Figure 1.7: Digitized TOCO trace (Top), original monopolar signals (middle), corresponding bipolar signals (bottom). The thick blue lines define the beginning and the end of the burst according to TOCO.

These raw signals were then segmented, with the help of the scanned and digitized paper TOCO traces. For verification purpose, we also computed the bipolar signals from monopolar leads, to check the correctness of the segmentation. Indeed, in the raw monopolar signals the uterine bursts are corrupted by strong noise and artifacts. We could hardly identify and segment the uterine bursts by using this signal, even with the help of the TOCO trace. Using the bipolar signals permitted us to identify and then segment properly the uterine bursts **Figure 1.7**.

The monopolar segmented bursts were then filtered by using the CCA-EMD method. At the end we got 92 pregnancy and 84 labor filtered monopolar bursts related to different contractions, for each of the 16 monopolar channels.

1.6 Discussion and conclusion

We can conclude from the overview presented above, that the uterus is a complex organ. Understanding how this organ works might help us to detect the onset of labor as well as to predict PTL. There are many way of measuring EHG signals, the most used is the abdominal EHG due to its non-invasiveness. The processing of uterine EMG signals can give us information about the functioning of the uterus. We expect this information to permit us to monitor pregnancy and detect labor.

EHG has long been a promising vector of investigation for the detection of preterm labor. However the classical methods used in the past have not given rise to clinically used application. Recent efforts using non-linear signal processing and some preliminary work on uterine activity propagation have given promising results. Thus this thesis focuses on the analysis of excitability (linear, nonlinear) parameters, propagation (synchronization, direction) parameters and source(s) localization of the EHG during pregnancy and labor, in order to move forward to the final aim of this project, deriving objective means for the early detection of preterm delivery, based on the monitoring of the three physiological phenomenon: cell excitability, uterine synchronization and source(s) loci.

References

[1] R.E. Garfield, W.L. Maner, L.B. MacKay, D. Schlembach, and G.R. Saade, “Comparing uterine electromyography activity of antepartum patients versus term labor patients,” *American Journal of Obstetrics and Gynecology*, vol. 193, no. 1, pp. 23-29, Jul. 2005.

[2] C. Marque, J. Duchêne, S. Leclercq, G. Panczer, and J. Chaumont, "Uterine EHG processing for obstetrical monitoring," *IEEE Trans. Biomed. Eng.*, vol. 33, no. 12, pp. 1182-7, Dec. 1986.

[3] M.P. Vinken, C. Rabotti, M. Mischi, and S.G. Oei, "Accuracy of frequency-related parameters of the electrohysterogram for predicting preterm delivery: a review of the literature," *Obstet. Gynecol. Surv.*, vol. 64, no. 8, pp. 529-41, Aug. 2009.

[4] S. Mansour, D. Devedeux, G. Germain, C. Marque, and J. Duchêne, "Uterine EMG spectral analysis and relationship to mechanical activity in pregnant monkeys," *Med. Biol. Eng. Comput.*, vol. 34, no. 2, pp. 115-21, Mar. 1996.

[5] J. Terrien, C. Marque, and B. Karlsson, "Spectral characterization of human EHG frequency components based on the extraction and reconstruction of the ridges in the scalogram," in *29th Annual International Conference of the IEEE Engineering in Medicine and Biology Society(IEEE-EMBC)*, Lyon, France, Aug. 2007, pp. 1872-1875.

[6] M. Hassan, J. Terrien, B. Karlsson, and C. Marque, "Comparison between approximate entropy, correntropy and time reversibility: Application to uterine electromyogram signals," *Medical engineering & physics (MEP)*, vol. 33, no. 8, pp. 980-986, oct. 2011.

[7] H. Ellis, "Anatomy of the uterus," *Anaesthesia & Intensive Care Medicine*, vol. 6, no. 3, pp. 74-75, Mar. 2005.

[8] Available from: http://www.cancer.gov/cancertopics/pdq/treatment/ovarian-germ-cell/patient.

[9] D. Shier, J. Butler, and R. Lewis, "Hole's Human anatomy and physiology," *New York: McGraw-Hill*, 11th ed., F. Schreiber, Ed., 2001.

[10] A.I. Csapo, "Smooth muscle as a contractile unit," *Phys. Rev. Suppl.*, vol. 5, pp. 7-33, Jul. 1962.

[11] D. Devedeux, C. Marque, S. Mansour, G. Germain, and J. Duchêne, "Uterine electromyography: a critical review," *Am. J. Obstet. Gynecol.*, vol. 169, no. 6, pp. 1636-53, Dec. 1993.

[12] R.C. Young, and R.O. Hession, "Three-dimensional structure of smooth muscle in termpregnant human uterus," *Obstet. Gynecol.*, vol. 93, no.1, pp. 94-99, Jan. 1999.

[13] K. Chalubinski, J. Deutinger, and G. Bernaschek, "Vaginosonography for recording of cyclerelated myometrial contractions," *Fertility and sterility*, vol. 59, no. 1, pp. 225, Jan. 1993.

[14] R. Merger, J. Levy, and J. Melchior, Précis d'obstétrique, 5th ed., *Paris: Masson Ed.*, 1979.

[15] C. Wood, "Myometrial and tubal physiology," *Blackwell, Ed. Oxford: England*, 1972, pp. 324-375.

[16] F-J. Mercier, H.Bouaziz, D. Benhamou, "«Hypertonie uterine» : conduite a tenir," in *proc. MAPAR conf,* 1997, pp. 99-116.

[17] R. Merger, J. Lévy, and J. Melchior, "Accouchement normal," in *Précis d'Obstétrique*, Paris: Masson Ed., 1985, pp. 115-136.

[18] B. Maria, I. Matheron, and F. Stampf, "Première période du travail," in *Obstétrique, Médecine Sciences Flammarion*, C.D. Papiernik Ed., Pons JC., ed., 1995, pp. 1067-1116.

[19] S. Wray, “Uterine contraction and physiological mechanisms of modulation,” *American Journal of Physiology-Cell Physiology*, vol. 264, no. 1, pp. C1-C18, Jan. 1993.

[20] R.A. Word, J.T. Stull, M.L. Casey, and K.E. Kamm, “Contractile elements and myosin light chain phosphorylation in myometrial tissue from nonpregnant and pregnant women,” *Journal of Clinical Investigation*, vol. 92, no. 1, pp. 29-37, Jul. 1993.

[21] R. Garfield, and C. Yallampalli, “Structure and function of uterine muscle,” in *The uterus, Cambridge reviews in human reproduction*, Cambridge: UK, T. Chard, ed., 1994, pp. 54-93.

[22] R.C. Young, “A computer model of uterine contractions based on action potential propagation and intercellular calcium waves,” *Obstet. Gynecol.*, vol. 89, no. 4, pp. 604-608, Apr. 1997.

[23] R.C. Young, “Tissue-level signaling and control of uterine contractility: the action potential calcium wave hypothesis,” *J. Soc. Gyneco. Investig.*, vol. 7, no. 3, pp. 146-52, May-Jun. 2000.

[24] J.M. Marshall, “Regulation of activity in uterine smooth muscle,” *Physiol. Rev.*, vol. 5, pp. 213-27, Jul. 1962.

[25] R. Caldeyro-barcia, and J.J. Poseiro, “Physiology of the uterine contraction,” *Clin. Obstet. Gynecol.*, vol. 3, no. 2, pp. 386-408, 1960.

[26] Sims, S., E.E. Daniel, and R. Garfield, *Improved electrical coupling in uterine smooth muscle is associated with increased numbers of gap junctions at parturition.* The Journal of general physiology, 1982. **80**(3): p. 353-375.

[27] C. Buhimschi, M.B. Boyle, and R.E. Garfield, “Electrical activity of the human uterus during pregnancy as recorded from the abdominal surface,” *Obstet. Gynecol.*, vol. 90, no. 1, pp. 102-11, Jul. 1997.

[28] G.M.J.A. Wolfs, and M.V. Leeuwen, “Electromyographic Observations on the Human Uterus during Labour,” *Acta Obstet. Gynecal. Scand. Suppl.*, vol. 58, no. 90, pp. 1-62, 1979.

[29] A. Shafik, “Electrohysterogram: study of the electromechanical activity of the uterus in humans,” *Eur. J. Obstet. Gynecol. Reprod. Biol.*, vol. 73, no. 1, pp. 85-9, May. 1997.

[30] P. Lopes, G. Germain, G. Breart, S. Reitano, R. Le Houezec, and C. Sureau, “Electromyographical study of uterine activity in the human during labour induced by prostaglandin F2 alpha,” *Gynecol. and obstet. investigation*, vol. 17, no. 2, pp. 96-105, 1984.

[31] G. Wolfs, and H. Rottinghuis, “Electrical and mechanical activity of the human uterus during labour,” *Archiv für Gynäkologie*, vol. 208, no. 4, pp. 373-385, Jan. 1970.

[32] C. Sureau, “Etude de l’activité électrique de l’utérus au cours du travail,” *Gynecol. Obstet.*, vol. 555, pp. 153-175, Apr-May. 1956.

[33] R. Garfield, M. Blennerhassett, and S. Miller, “Control of myometrial contractility: role and regulation of gap junctions,” *Oxford reviews of reproductive biology*, vol. 10, pp. 436-90, 1988.

[34] R.E. Garfield, S. Sims, and E.E. Daniel, “Gap junctions: their presence and necessity in myometrium during parturition,” *Science*, vol. 198, no. 4320, pp. 958-60, Dec. 1977.

[35] H. Eswaran, H. Preissl, P. Murphy, J.D. Wilson, and C.L. Lowery, "Spatial-temporal analysis of uterine smooth muscle activity recorded during pregnancy," in *27th Annual International Conference of the IEEE Engineering in Medicine and Biology Society (IEE-EMBC)*, Shanghai, China, Jan. 2006, pp. 6665-6667.

[36] P. Johnson, "Suppression of preterm labour," *Drugs*, vol. 45, no. 5, pp. 684-692, May. 1993.

[37] M. Baggish, R. Valle, and H. Guedj, "Hysteroscopy: Visual Perspectives of Uterine Anatomy, Physiology & Pathology," *3rd Ed.*, Lippincott Williams & Wilkins, Philadelphia: USA, 2007.

[38] H. Ruf, M. Conte, and J.P. Franquelbalme, "L"accouchement prématuré," in *Encycl. Med. Chir.*, 1988, Elsevier: Paris, pp. 12.

[39] G. Bréart, B. Blondel, P. Tuppin, H. Grandjean, and M. Kaminski, "Did preterm deliveries continue to decrease in France in the 1980s?," *Pediatric and Perinatal Epidemiology*, vol. 9, no. 3, pp. 296-306, Jul. 1995.

[40] P. Olsén, E. Läärä, P. Rantakallio, M.-R. Järvelin, A. Sarpola, and A.-L. Hartikainen, "Epidemiology of preterm delivery in two birth cohorts with an interval of 20 years," *American Journal of Epidemiology*, vol. 142, no. 11, pp. 1184-1193, Aug. 1995.

[41] B. Blondel, G. Bréart, Ch. du Mazaubrun, and G. Badeyan, "Santé publique la situation périnatale en France," *J. Gynecol. Obstet. Biol. Reprod.*, vol. 26, no. 8, pp. 770-780, Dec. 1997.

[42] B. Blondel, N. Lelong, M. Kermarrec, and F. Goffinet, "La santé périnatale en France métropolitaine de 1995 à 2010. Résultats des enquêtes nationales périnatales," *La Revue Sage Femme*, vol. 11, no. 3, pp. 128-143, Jun. 2012.

[43] M.I. Heaman, A.E. Sprague, and P.J. Stewart, "Reducing the preterm birth rate: A population health strategy," *J. of Obstet., Gynecol., & Neonat. Nursing*, vol. 30, no. 1, pp. 20-29, Jan. 2001.

[44] J.C. Morrison, J.R. Allbert, B.N. McLaughlin, N.S. Whitworth, W.E. Roberts, and R.W. Martin, "Oncofetal fibronectin in patients with false labor as a predictor of preterm delivery," *American journal of obstetrics and gynecology*," vol. 168, no. 2, pp. 538-542, Feb. 1993.

[45] M.A. Williams, D.E. Hickok, R.W. Zingheim, R. Mittendorf, J. Kimelman, and B.S. Mahony, "Low birth weight and preterm delivery in relation to early-gestation vaginal bleeding and elevated maternal serum alpha-fetoprotein," *Obstetrics & Gynecology*, vol. 80, no. 5, pp. 745-749, Nov. 1992.

[46] M. McLean, A. Bisits, J. Davies, R. Woods, P. Lowry, and R. Smith, "A placental clock controlling the length of human pregnancy," *Nature medicine*, vol. 1, no. 5, pp. 460-463, May. 1995.

[47] J.D. Iams, "Prediction and early detection of preterm labor," *Obstet. Gynecol.*, vol. 101, no. 2, pp. 402-12, Feb. 2003.

[48] R.K. Creasy, "Preterm birth prevention: where are we?," *American journal of obstetrics and gynecology*, vol. 168, no. 4, pp. 1223-1230, Apr. 1993.

[49] D.C. Dyson, K.H. Danbe, J.A. Bamber, Y.M. Crites, D.R. Field, J.A. Maier, L.A. Newman, D.A. Ray, D.L. Walton, and M.A. Armstrong, "Monitoring women at risk for preterm labor," *New England J. Med.*, vol. 338, no. 1, pp. 15-9, Jan. 1998.

[50] D. Schlembach, W.L. Maner, R.E. Garfield, and H. Maul, "Monitoring the progress of pregnancy and labor using electromyography," Eur. J. Obstet. Gynecol. Reprod. Biol., vol. 144, no. 1, pp. S33-9, May. 2009.

[51] R. Romero, R. Gomez, and W. Sepulveda, "The uterine cervix, ultrasound and prematurity," *Ultrasound. Obstet. Gynecol.*, vol. 2, no. 6, pp. 385-8, Nov. 1992.

[52] A.M. Germain, G.J. Valenzuela, M. Ivankovic, C.A. Ducsay, C. Gabella, and M. Serón-Ferré, "Relationship of circadian rhythms of uterine activity with term and preterm delivery," Am. J. Obstet. Gynecol., vol. 168, no. 4, pp. 1271-7, Apr. 1993.

[53] H. Eswaran, H. Preissl, J.D. Wilson, P. Murphy, S.E. Robinson, and C.L. Lowery, "First magnetomyographic recordings of uterine activity with spatial-temporal information with a 151-channel sensor array," *Am. J. Obstet. Gynecol.*, vol. 187, no. 1, pp. 145-51, Jul. 2002.

[54] O. Bode, "Das elektrohysterogramm," *Arch. Gyndk*, vol. 28, no. 1, pp. 123-128, 1931.

[55] A. Verhoeff, "Myometrial Contractility and Gap Junctions: An Experimental Study in Chronically Instrumented Ewes," Erasmus University Rotterdam, pp. 1-87, Nov. 1985.

[56] H. Maul, W.L. Maner, G.R. Saade, and R.E. Garfield, "The physiology of uterine contractions," *Clinics in perinatology*, vol. 30, no. 4, pp. 665-676, Dec. 2003.

[57] L. Dill, and R. Maiden, "The electrical potentials of the human uterus in labor," *American journal of obstetrics and gynecology*, vol. 52, no. 5, pp. 735-745, Nov. 1946.

[58] C.M. Steer, and G. Hertsch, "Electrical activity of the human uterus in labor; the electrohysterograph," *American journal of obstetrics and gynecology*, vol. 59, no.1, pp. 25-40, Jan. 1950.

[59] E.H. HON, and C.D. DAVIS, "Cutaneous and uterine electrical potentials in labor-an experiment," *Obstetrics & Gynecology*, vol. 12, no. 1, pp. 47-53, Jul. 1958.

[60] C. Sureau, J. Chavinié, and M. Cannon, "L"electrophysiologie uterine," *Bull Fed Soc Gynecol Obstet*, vol. 17, pp. 79-140, 1965.

[61] J. Gondry, C. Marque, J. Duchêne, and D. Cabrol, "Electrohysterography during pregnancy: preliminary report," *Biomed. Instrum. Technol.*, vol. 27, no.4, pp. 318-24, 1993.

[62] I. Verdenik, M. Pajntar, and B. Leskosek, "Uterine electrical activity as predictor of preterm birth in women with preterm contractions," Eur. J. Obstet. Gynecol. Reprod. Biol., vol. 95, no. 2, pp. 149-53, Apr. 2001.

[63] S. Larks, N. Assali, D. Morton, and W. Selle, "Electrical activity of the human uterus in labor," *Journal of Applied Physiology*, vol. 10, no. 3, pp. 479-483, May. 1957.

[64] H.W. Hsu, J.P. Figueroa, M.B. Honnebier, R. Wentworth, P.W. Nathanielsz, “Power spectrum analysis of myometrial electromyogram and intrauterine pressure changes in the pregnant rhesus monkey in late gestation,” *Am. J. Obstet. Gynecol.*, vol. 161, no. 2, pp. 467-73, Aug. 1989.

[65] N. Val, B. Dubuisson, and F. Goubel, “Aide au diagnostic de l‟accouchement par l‟électromyogramme abdominal: sélection de caractères,” in *Reconnaissance de formes, intelligence artificielle*, vol. 3, pp. 42-50, 1979.

[66] M.P.G.C. Vinken, C. Rabotti, M. Mischi, J.O.E.H. van Laar, and S.G. Oei, “Nifedipine-induced changes in the electrohysterogram of preterm contractions: feasibility in clinical practice,” *Obstetrics and gynecology international*, vol. 2010, no. 2010, pp. 8, Apr. 2010.

[67] G. Fele-Žorž, G. Kavšek, Ž. Novak-Antolič, and F. Jager, “A comparison of various linear and non-linear signal processing techniques to separate uterine EMG records of term and pre-term delivery groups,” *Med. Biol. Eng. Comput.*, vol. 46, no. 9, pp. 911-22, Sep. 2008.

[68] M. Diab, C. Marque, and M. Khalil, “An unsupervised classification method of uterine electromyography signals: classification for detection of preterm deliveries,” *Journal of Obstetrics and Gynaecology Research*, vol. 35, no. 1, pp. 9-19, Feb. 2009.

[69] H. Leman, C. Marque, and J. Gondry, “Use of the electrohysterogram signal for characterization of contractions during pregnancy,” *IEEE Trans. Biomed. Eng.,* vol. 46, pp. 1222-9, Oct 1999.

[70] P. Carre, H. Leman, C. Fernandez, and C. Marque, “Denoising of the uterine EHG by an undecimated wavelet transform,” *IEEE Trans. Biomed. Eng.*, vol. 45, no. 9, pp. 1104-13, Sep. 1998.

[71] M. Hassan, J. Terrien, B. Karlsson, and C. Marque, “Interactions between Uterine EMG at Different Sites Investigated Using Wavelet Analysis: Comparison of Pregnancy and Labor Contractions,” *EURASIP J. on Adv. in Sign. Process.*, vol. 2010, no. 17, pp. 9, Feb. 2010.

[72] M. Khalil, and J. Duchêne, “Detection and classification of multiple events in piecewise stationary signals: Comparison between autoregressive and multiscale approaches,” *Signal Processing*, vo. 75, no. 3, pp. 239-251, Jun. 1999.

[73] M. Khalil, and J. Duchêne, “Uterine EMG analysis: a dynamic approach for change detection and classification,” *IEEE Trans. Biomed. Eng.*, vol. 47, no. 6, pp. 748-56, Jun. 2000.

[74] C. Marque, H. Leman, M.L. Voisine, J. Gondry, and P. Naepels, “Processing of uterine electromyogram for contraction characterization during pregnancy: Traitement de l'electromyogramme uterin pour la caracterisation des contractions pendant la grossesse,” *RBM-News*, vol. 21, no. 9, pp. 200-211, Dec. 1999.

[75] J. Duchêne, D. Devedeux, S. Mansour, and C. Marque, “Analyzing Uterine EMG: Tracking Instantaneous Burst Frequency,” *IEEE Eng. Med. Biol. Mag.*, vol. 14, no. 2, pp. 125-131, Mar-Apr. 1995.

[76] E. Oczeretko, A. Kitlas, J. Swiatecka, M. Borowska, and T. Laudanski, "Nonlinear dynamics in uterine contractions analysis," in *Fractals in Biology and Medicine*, Birkhäuser Basel, Springer, 2005, pp. 215-222.

[77] I.A. Rezek, and S.J. Roberts, "Stochastic complexity measures for physiological signal analysis," *IEEE Trans. on Biomed. Eng.*, vol. 45, no. 9, pp. 1186-1191, Sep. 1998.

[78] J. Vrhovec, "Evaluating the progress of the labour with sample entropy calculated from the uterine EMG activity," *Elektrotehniski vestnik-Electrotechnical Review*, vol. 76, no. 4, pp. 165-170, Jan. 2009.

[79] W.L. Maner, L.B. MacKay, G.R. Saade, and R.E. Garfield, "Characterization of abdominally acquired uterine electrical signals in humans, using a non-linear analytic method," *Med. Biol. Eng. Comput.*, vol. 44, no. 1-2, pp. 117-23, Mar. 2006.

[80] M. Sabry-Rizk, W. Zgallai, E.R. Carson, P. Hardiman, A. MacLean, and K.T.V. Grattan, "Nonlinear dynamic tools for characterizing abdominal electromyographic signals before and during labour," *Trans. of the instit. of Measu. and Cont.*, vol. 22, no. 3, pp. 243-270, Aug. 2000.

[81] C. Marque, "Analyse de la dynamique des contractions uterines par électromyographie abdominale," *Ph.D. dissertation*, Dept. Génie biomédical, Université de Technologie de Compiègne, Compiègne, France, 1987.

[82] J. Duchêne, C. Marque, and S. Planque, "Uterine EMG signal: Propagation analysis," in *12th Annual International Conference of the IEEE Engineering in Medicine and Biology Society (IEEE-EMBC)*, Philadelphia, Pennsylvania, USA, Nov. 1990, pp. 831-832.

[83] B. Karlsson, J. Terrien, V. Gudmundsson, T. Steingrimsdottir, and C. Marque, "Abdominal EHG on a 4 by 4 grid: mapping and presenting the propagation of uterine contractions," in *Proc. 11th Mediterranean Conference on Medical and Biological Engineering and Computing (MEDICON)*, Ljubljana, Slovenia, 2007, pp. 139-143.

[84] W. Jiang, G. Li, and L. Lin, "Uterine electromyogram topography to represent synchronization of uterine contractions," *International Journal of Gynecology & Obstetrics*, vol. 97, no. 2, pp. 120-124, May. 2007.

[85] J. Terrien, C. Marque, J. Gondry, T. Steingrimsdottir, and B. Karlsson, "Uterine electromyogram database and processing function interface: An open standard analysis platform for electrohysterogram signals," Comput. in bio. & med., vol. 40, no. 2, pp. 223-230, Feb. 2010.

[86] M. Hassan, J. Terrien, C. Muszynski, A. Alexandersson, C. Marque, and B. Karlsson, "Better pregnancy monitoring using nonlinear propagation analysis of external uterine electromyography," *IEEE Trans. Biomed. Eng.*, vol. 60, no. 4, pp. 1160-1166, Apr. 2013.

[87] J. Terrien, M. Hassan, C. Marque, and B. Karlsson, "Use of piecewise stationary segmentation as a pre-treatment for synchronization measures," in *Proc. IEEE Eng. Med. Biol. Soc. Conf.* 2008, Vancouver, BC, Aug. 2008, pp. 2661-2664.

[88] J. Terrien, G. Germain, C. Marque, and B. Karlsson, "Bivariate piecewise stationary segmentation; improved pre-treatment for synchronization measures used on non-stationary biological signals," *Medical engineering & physics*, vol. 35, no. 8, pp. 1188-96, Aug. 2013.

[89] J. Terrien, T. Steingrimsdottir, C. Marque, and B. Karlsson "Synchronization between EMG at Different Uterine Locations Investigated Using Time-Frequency Ridge Reconstruction: Comparison of Pregnancy and Labor Contractions," *EURASIP J. Adv. Signal Process.*, vol. 2010, pp. 1-10, Jun. 2010.

[90] J. G. Planes, J. P. Morucci, H. Grandjean, and R. Favretto, "External recording and processing of fast electrical activity of the uterus in human parturition," Med Biol Eng Comput, vol. 22, pp. 585-91, Nov 1984.

[91] W.J. Lammers, H. Mirghani, B. Stephen, S. Dhanasekaran, A. Wahab, M.A.H. Al Sultan, and F. Abazer, "Patterns of electrical propagation in the intact pregnant guinea pig uterus," *Am. J. Physiol. Regul. Integr. Comp. Physiol.*, vol. 294, no. 3, pp. R919-28, Mar. 2008.

[92] T.Y. Euliano, D. Marossero, M.T. Nguyen, N.R. Euliano, J. Principe, and R.K. Edwards, "Spatiotemporal electrohysterography patterns in normal and arrested labor," *Am. J. Obstet. Gynecol.*, vol. 200, no. 1, pp. 54.e1–54.e7, Jan. 2009.

[93] C. Alvarez, and S. Reynolds, "A better understanding of uterine contractility through simultaneous recording with an internal and a seven channel external method," *Surgery, gynecology & obstetrics*, vol. 91, no. 6, pp. 641-650, Dec. 1950.

[94] C. Rabotti, M. Mischi, J.O.E.H van Laar, G.S Oei, and J.W.M Bergmans, "Inter-electrode delay estimators for electrohysterographic propagation analysis," *Physiol. Meas.*, vol. 30, no.8, pp. 745-61, Jun. 2009.

[95] E. Mikkelsen, P. Johansen, A. Fuglsang-Frederiksen, and N. Uldbjerg, "Electrohysterography of labor contractions: propagation velocity and direction," *Acta obstetricia et gynecologica Scandinavica*, vol. 92, no. 9, pp. 1070-1078, Sept. 2013.

[96] A. Diab, M. Hassan, S. Boudaoud, C. Marque, and B. Karlsson, "Nonlinear estimation of coupling and directionality between signals: Application to uterine EMG propagation," in *Proc. IEEE Eng. Med. Biol. Soc. Conf.* 2013, Osaka, Japan, Jul. 2013, pp. 4366-4369.

[97] J.D. López, V. Litvak, J.J. Espinosa, K. Friston, and G.R. Barnes, "Algorithmic procedures for Bayesian MEG/EEG source reconstruction in SPM," *NeuroImage*, vol. 48, pp. 476-487, Jan. 2014.

[98] J. Mattout, C. Phillips, W.D. Penny, M.D. Rugg, and K.J. Friston, "MEG source localization under multiple constraints: An extended Bayesian framework," *NeuroImage*, vol. 30, no. 3, pp. 753-767, Apr. 2006.

[99] J. Alberola-Rubio, G. Prats-Boluda, Y. Ye-Lina, J. Valerob, A. Peralesb, and J. Garcia-Casado, "Comparison of non-invasive electrohysterographic recording techniques for monitoring uterine dynamics," *Medical engineering & physics*, vol. 35, no. 12, pp. 1736-1743, Dec. 2013.

[100] J. Terrien, C. Marque, G. Germain, and B. Karlsson, "Sources of bias in synchronization measures and how to minimize their effects on the estimation of synchronicity: application to the uterine electromyogram," in *Rec. Adv. in Biom. Eng.*, Ganesh R Naik Ed., 2009, pp. 73-100.

[101] J.-N. Helal, and P. Bouissou, "The spatial integration effect of surface electrode detecting myoelectric signal," *IEEE Trans. on Biomed. Eng.*, vol. 39, no. 11, pp. 1161-1167, Nov. 1992.

[102] S. Mansour, J. Duchêne, G. Germain, and C. Marque, "Uterine EMG: Experimental and mathematical determination of the relationship between internal and external recordings," in *13th Annual International Conference of the IEEE Engineering in Medicine and Biology Society (IEEE-EMBC)*, Orlando, FL, USA, Oct/Nov. 1991, pp. 485-486.

[103] L. Lindström, and I. Petersen, "Power spectrum analysis of EMG signals and its applications," *Prog. Clin. Neurophysiol.*, vol. 10, pp. 1-51, 1983.

[104] M. Hassan, S. Boudaoud, J. Terrien, B. Karlsson, and C. Marque, "Combination of Canonical Correlation Analysis and Empirical Mode Decomposition applied to denoise the labor electrohysterogram," *IEEE Trans. Biomed. Eng.*, vol. 85, no. 9, pp. 2441-2447, Sep. 2011.

Chapter 2: Excitability analysis using nonlinear methods

2.1 Introduction

One of the most common ways to obtain information on neurophysiologic systems is to study the features of the signal(s) using time series analysis techniques. They traditionally rely on linear methods in both time and frequency domains [1], such as peak frequency of signals PSD [2], and burst energy [3]. Unfortunately, these methods cannot give information about purely nonlinear features of the signal.

Due to the intrinsic nonlinearity of most biological systems, these nonlinear features may be present in physiological data and even be a characteristic of major interest. Indeed, the nonlinear analysis may give information about the underlying physiological processes, many of which have complex behavior. Monovariate nonlinear time series analysis methods were first applied to neurophysiological data about two decades ago [4]. Recently, much attention has been paid to the use of nonlinear analysis techniques for the characterization of biological signals [5]. They have been widely applied to EEG signals since these signals are highly nonlinear and nonstationary. Among those applications we can cite: study of the anesthetic drug effect during anesthesia by using Approximate entropy [6], measure of the depth of anesthesia using Detrended fluctuation analysis [7], and sleep stages study [8], study of the effect of antipsychotics on EEG complexity in drug-naive schizophrenia using multiscale entropy [9]. Nonlinear analysis were also used in cardiovascular dynamic analysis [10], study of cardiovascular ageing [11], prediction of paroxysmal atrial fibrillation [12], and fetal heart rate analysis [13]. MEG was also a field for nonlinear analysis application such as for the analysis of Alzheimer disease [14]. Complexity of striated muscle EMG signals was also measured by using entropy based methods (Fuzzy Entropy, Approximate Entropy, Sample entropy) [15]. Several measures have thus been proposed to detect nonlinear characteristics in time series. The performances of these methods are often compared with their results on surrogate data, which provides a rigorous framework for detecting nonlinearity. Multiple surrogates and their z-score are used to statistically test the presence or absence of non-linearity in time series. The z-score itself has sometimes been used as a measure of nonlinearity [5, 16].

The uterus is a not well-understood organ. It is deceptively simple in structure but its behavior, as observed by electromyography (electrohysterogram, EHG), when it moves from pregnancy towards labor, indicates that there are numbers of interconnected control systems involved in its functioning (electric, hormonal, mechanical). Nonlinear characteristics have been observed in the EHG and some success has been achieved by using these characteristics to obtain information that is potentially clinically useful [5, 16-17]. Recently, several applications of nonlinear analysis methods have been done on EHG signals. We can cite here the use of Sample Entropy [18], Lempel-Ziv complexity [19] and Approximate entropy [20]. In most of these studies the authors have reported some practical disadvantages of the methods, like the huge calculation time due to using surrogates analysis, or promising but inconclusive results due to the small databases available.

However, whatever the studied signal, the sensitivity of nonlinear methods to the actual nonlinearity level, and to some usual preprocessing steps (decimation, filtering), as well as their robustness to noise has rarely been evaluated in the past. While surrogates are important tools to rigorously detect nonlinearity, their usefulness for evaluating the level of existing nonlinearity is not clear, and their usefulness is limited by their complexity and highly time consuming computation.

This chapter presents a work that extends previous work done in our team, which deals with the comparison between Approximate Entropy, Correntropy and Time reversibility [16]. In the present work, we compare new methods and also use a much larger database of real signals than during the previous work. In addition, we propose in this work to complete this comparison by the investigation of the method‟s sensitivity to the varying complexity of signals and then to their SNR. We also studied the effect of two usual preprocessing steps, decimation (or down sampling) and filtering, on the performances of the methods. Papers that investigate the effect of preprocessing are rare in the EHG literature. We found one example of this systematic analysis for Sample entropy [21] only. None of these topics has previously been considered in our team.

Four nonlinear methods from three nonlinear families: Statistic family (Time reversibility [22]), Predictability family (Sample Entropy [23], Delay Vector Variance [24]) and Chaos theory family (Lyapunov Exponents [25]) were tested in this work. Sensitivity of these methods to the complexity degree (*CD*) of signal as well as robustness analysis were made on a Henon model synthetic signals where *CD* can be controlled. The sensitivity to *CD* was first

studied by using the direct value provided by the method. It was then studied by using surrogates and *z*-score, as this measure permits to evaluate the nonlinearity. We try in this study to evidence which methods are the most sensitive to the change of signal complexity. A second objective was to determine whether the use of surrogates give better overall results than the direct application of the methods. This is also of major practical importance for clinical application, as the generation of surrogates is computationally very time consuming. The methods were compared using the MSE (Mean Square Error) of the Monte Carlo instances of the signal. Finally, these non-linear methods are applied to real EHG signals, and used to discriminate pregnancy and labor contractions. The methods‟ discriminating power is compared to that of three well known linear characteristics based on the frequency content of the signal: Mean Power Frequency (MPF), Peak Frequency (PF) and Median Frequency (MF). We also tested, on real EHG signals, the sensitivity of these methods to decimation and filtering, by comparing the effect of these two preprocessing techniques (with and without down sampling and filtering) on method performances, for the discrimination between pregnancy and labor contractions.

2.2 Materials and methods

2.2.1 Data

2.2.1.1 Synthetic signals

In this work, we used the Henon nonlinear dynamic model because the complexity degree of this model can be easily controlled. The Henon map is a well-known two-dimensional discrete-time system given by

$$Y_{t+1} = c - Y_t^2 + CD * X_t,$$

$$X_{t+1} = Y_t,$$

where Y_t and X_t represent dynamical variables, CD is the complexity degree and c is the dissipation parameter. In this work, we use $c = 1$ as in [26] and $CD \in [0, 1]$ to change the model complexity [27] (**Figure 2.1**). The number of generated points is fixed to 1000.

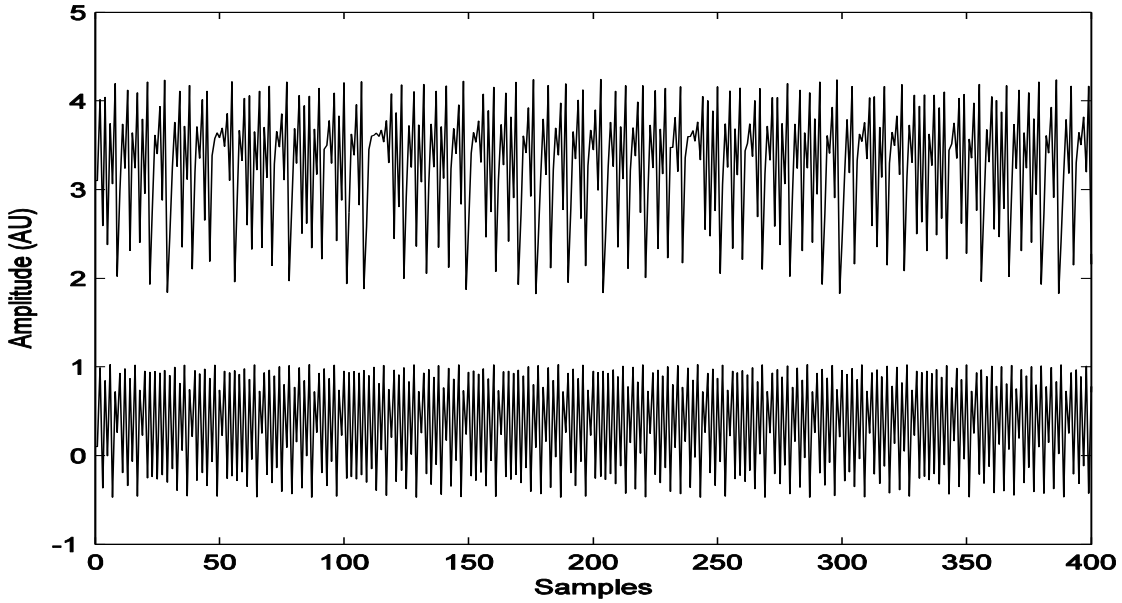

Figure 2.1: Simulated signal generated by using the Henon model with different complexity degrees (*CD*). Top: *CD* = 0.1, Bottom: *CD* = 0.9.

For the robustness analysis, we add white Gaussian noise to the synthetic signal, first with a fixed 5db SNR, with *CD* varying between 0 and 1, then with variable levels 1db, 2db, 5db, 10db, 100db, with *CD* fixed to 0.8. For each *CD* value we use, 30 Monte Carlo instances.

2.2.1.2 Real signals

In this chapter we use signals recorded with the experimental protocol described in Chapter 1. As the methods tested here are "monovariate", we thus used only one channel (bipolar vertical7: Vb7) from the 4*4 electrode matrix located on the women's abdomen. This channel is located on the median vertical axis of the uterus (see [28] for details), midway between the symphysis and the uterine fundus, which is the reference electrode position in our team. The signals were recorded on women in France and in Iceland. In Iceland we recorded signals on 22 women: 11 recorded during normal pregnancies (33-39 weeks of gestation) and 11 during term labors (39-42 weeks of gestation). In France we recorded signals on 27 women: 25 recorded during risk pregnancies (33-39 weeks of gestation) and 2 during term labors (39-42 weeks of gestation). The EHG signals were segmented manually to extract the bursts related to uterine activity (**Figure 2.2**). After segmentation we obtained 115 labor bursts and 174 pregnancy bursts. The analysis below was applied to the segmented uterine bursts.

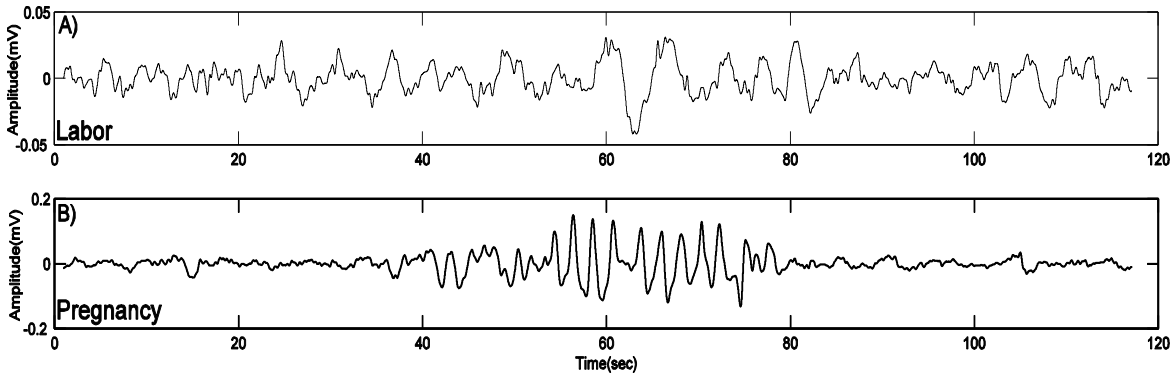

Figure 2.2: Example of segmented real EHG bursts. (A) Labor burst, (B) Pregnancy burst.

2.2.2 Nonlinear analysis methods

2.2.2.1 Time reversibility

A time series is said to be reversible only if its probabilistic properties are invariant with respect to time reversal. Time irreversibility, method issued from the Statistic family, can be taken as a strong signature of nonlinearity [22]. In this study we used the simplest way, described in [29] to compute the Time reversibility of a signal S_n:

$$Tr(\tau) = (\frac{1}{N-\tau}) \sum_{n=\tau+1}^{N} (S_n - S_{n-\tau})^3$$

where N is the signal length and τ is the time delay.

2.2.2.2 Chaos theory family

a) Phase space

The first step of a chaotic analysis involves reconstructing the phase space from a single time series. Phase space is an abstract mathematical space in which is viewed the system dynamic. It is constructed by using a time delay and an embedding dimension. The choice of the appropriate time delay τ and embedding dimension *m,* is important for the success of reconstructing the attractor from finite data [30].The reconstructed trajectory, *X*, can be expressed as a matrix where each row is a phase-space vector [31]. That is,

$$X = [X_1 X_2 ... X_M]^T \ ,$$

where *Xi* is the state of the system at discrete time *i*. For an N-point time series $\{x_1, x_2,...,x_N\}$, each *Xi* is given by:

$$X_i = [x_i, x_{i+\tau}, ..., x_{i+(m-1)\tau}] \ ,$$

where τ is the time lag or reconstruction delay, and m is the embedding dimension. Thus, X is an $M \times m$ matrix, and the constants m, M, τ, and N are related by:

$$M = N - (m - 1)\tau$$

As previously stated, the good reconstruction of the phase space depends on the two parameters, τ and m. We thus chose an optimal value for each one of these parameters. For the time delay, τ, we use the first local minimum of the average mutual information between the set of measurements $X(i)$ and $X(i + \tau)$. Mutual information measures the general dependence of two variables [32].

We estimated the minimum embedding dimension, m, by using an algorithm proposed by Kennel et al. [33]. The algorithm is based on the idea that, when passing from dimension m to dimension $m+1$, one can differentiates points on the orbit that are true neighbors from those that are false ones. A false neighbor is a point in the data set that is identified as a neighbor solely because the attractor is viewed in a too small embedding space. When the embedding dimension is large enough, all neighbors of every attractor point in the multivariate phase space will be true neighbors [30].

b) Lyapunov exponents

Lyapunov exponent (LE) is inspired from the Chaos theory. It is a quantitative indicator of system dynamics, which characterizes the average convergence or divergence rate between adjacent tracks in phase space [25]. We used the way described in [34] to compute LE:

$$\lambda = \lim_{t \to \infty} \lim_{\|\Delta_{y_0}\| \to 0} \left(\frac{1}{t} \right) \log \left(\|\Delta_{y_t}\| / \|\Delta_{y_0}\| \right),$$

Where $\| \Delta_{y_0} \|$ and $\| \Delta_{y_t} \|$ represent the Euclidean distances between two states of the system, respectively to an arbitrary time t_0 and a later time t.

2.2.2.3 Predictability family

a) Sample entropy

Sample Entropy (*SampEn*) is chosen from the Predictability family. It is the negative natural logarithm of the conditional probability that a dataset of length N, having repeated itself for m samples within a tolerance r, will also repeat itself for $m+1$ samples. Thus, a lower value of *SampEn* indicates more regularity in the time series [23]. We used the way described in [18] to compute *SampEn* :

For a time series of N points, $x_1, x_2, \ldots, x_N$, we define subsequences, also called template vectors, of length m, given by: $y_i(m) = (x_i, x_{i+1}, \ldots, x_{i+m-1})$ where $i = 1, 2, \ldots, N-m+1$.

Then the following quantity is defined: $B_i^m(r)$ as $(N-m-1)^{-1}$ times the number of vectors X_j^m within r of X_i^m, where j ranges from 1 to $N-m$, and $j \neq i$, to exclude self-matches, and then define:

$$B^m(r) = \frac{1}{N-m} \sum_{i=1}^{N-m} B_i^m(r)$$

Similarly, we define $A_i^m(r)$ as $(N-m-1)^{-1}$ times the number of vectors X_j^{m+1} within r of X_i^{m+1}, where j ranges from 1 to $N-m$, where $j \neq i$, and set

$$A^m(r) = \frac{1}{N-m} \sum_{i=1}^{N-m} A_i^m(r)$$

The parameter $SampEn(m,r)$ is then defined as $lim_{N\to\infty}\{-ln[A^m(r)/B^m(r)]\}$, which can be estimated by the statistic:

$$SampEn(m,r,N) = -\ln[A^m(r)/B^m(r)]$$

where N is the length of the time series, m is the length of sequences to be compared, and r is the tolerance for accepting matches.

b) Delay vector variance

The delay vector variance (DVV) method belongs to the Predictability method family. It is used for detecting the presence of determinism and nonlinearity in a time series and is based upon the examination of local predictability of a signal [24]. We use the measure of unpredictability σ^{*2} described in [35]:

Time series can be represented conveniently in the phase space by using time delay embedding. When time delay is embedded into a time series, it can be represented by a set of delay vectors (DVs) of a given dimension. If m is the dimension of the delay vectors then it can be expressed as $X(k) = [x_{(k-m\tau)} \ldots x_{(k-\tau)}]$, where τ is the time lag. For every DV $X(k)$, there is a corresponding target, namely the next sample x_k. A set $\beta_k(m, d)$ is generated by grouping those DVs that are within a certain Euclidean distance d to DV $X(k)$. This Euclidean distance will be varied in a standardized manner with respect to the distribution of pair-wise distances

between DVs. For a given embedding dimension m, a measure of unpredictability σ^{*2} (target variance) is computed over all sets of β_k.

The mean μ_d and the standard deviation σ_d are computed over all pair-wise Euclidean distances between DVs given by $\|x(i) - x(j)\| (i \neq j)$. The sets β_k *(m, d)* are generated such that $\beta_k = \{x(i) \backslash \|x(k) - x(j)\| \leq d\}$ i.e., sets which consist of all DVs that lie closer to *X(k)* than a certain distance *d*, taken from the interval [μ_d-n_d*σ_d; μ_d+n_d*σ_d] where n_d is a parameter controlling the span over which to perform DVV analysis.

For every set β_k*(m, d)* the variance of the corresponding targets σ_k^2*(m, d)* is computed. The average over the *N* sets β_k*(m, d)* is divided by the variance of the time series signal σ_x^2 , giving thus the inverse measure of predictability, namely target variance σ^{*2}.

$$\sigma^{*2} = \frac{(1/N)\sum_{k=1}^{N} \sigma_k^2}{\sigma_x^2}$$

2.2.3 Surrogates

To compare method ability to detect non-linearity in a signal, their results are often compared with the ones obtained on surrogate data. To obtain the surrogate data one has to shuffle the original signal so that the surrogate presents linear properties but keeps the other characteristics of the signal. This provides a rigorous framework for detecting nonlinearity, by using a statistical test to compare the results obtained from the original signals and from the surrogates. The application of a method on multiple surrogates, coupled with a statistical test on their z-score, permits to test the presence or absence of non-linearity in a time series. As the z-score itself is normalized with respect to the standard deviation of the results on the surrogates, it has sometimes been used as a measure of nonlinearity in its own right. In this work we use both the direct result of the analyzed methods and the ones obtained when coupled with the z-score, in order to compare which one is the best for our purposes. We present below the details of the surrogates and z-score computation used in this work.

2.2.3.1 Surrogates

Three main algorithms exist for generating surrogate data: Fourier Transformed (FT), Fourier Shuffled (FS) and Iterative Amplitude Adjusted Fourier Transformed (IAAFT). We introduce below the IAAFT algorithm as it preserves more accurately the power spectrum than the FS surrogate. Furthermore, the IAAFT algorithm (**Figure 2.3**) completely preserves the histogram of the original time series [36].

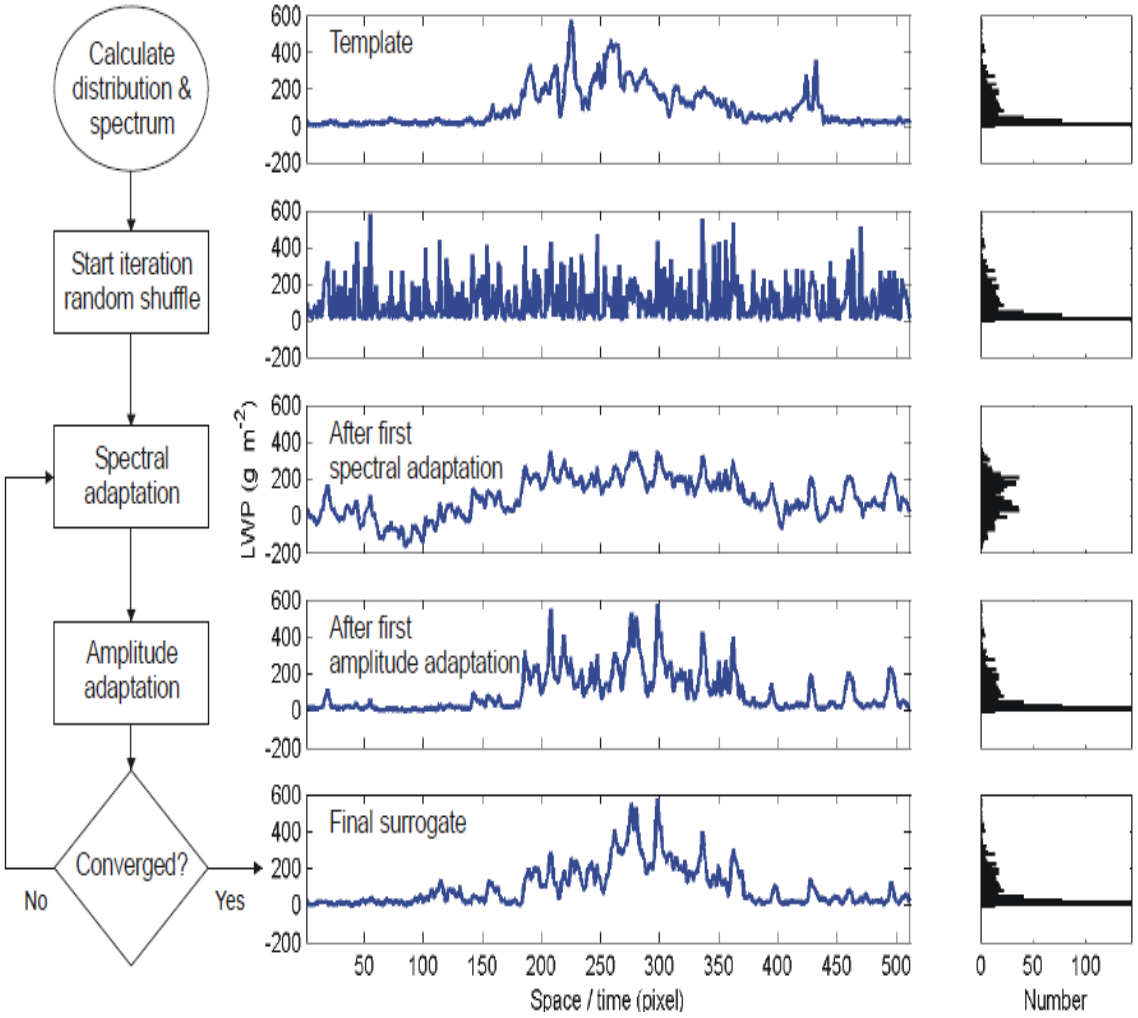

Figure 2.3: The IAAFT algorithm. Left: block diagram of the algorithm; middle: original (upper), intermediate and surrogate (lower) time series; right: time series histograms [37].

The IAAFT algorithm consist of the following steps:

1. Estimate the power spectrum of the original time series by the Fourier Transform.
2. Make a FS surrogate data of the original time series by shuffling the original data and keeping the same rank order as the FT surrogate data (inverse Fourier Transform of the spectrum estimated in the previous step) after a phase randomization. Although the FS surrogate completely preserves the empirical histogram, it cannot completely preserve the power spectrum as the FT surrogate.
3. Apply Fourier Transform to the FS surrogate. Here, the power spectrum is replaced by the one of the original time series, estimated at the first step, but the phase of the FS surrogate spectrum is preserved.

4. Apply inverse Fourier Transform to the data obtained at the third step. Although the generated time series has the same power spectrum as the original time series, its empirical histogram is different from the original one.
5. In order to preserve the histogram of the original data, the original time series is re-ordered to have the same rank order than the generated time series obtained at the fourth step. The re-ordered original time series is an IAAFT surrogate.
6. If the discrepancy of the power spectrum between the original and the IAAFT surrogate obtained in the previous step is not small enough, repeat the above steps by replacing the FS surrogate by the IAAFT surrogate in the third step. Large numbers of repetitions of these steps preserve more accurately the power spectrum of the original data than the only FS surrogate does [36].

2.2.3.2 Null hypothesis

The most commonly used null hypothesis considers that a given time series is generated by a Gaussian linear stochastic process and collected through a nonlinear measurement static function. Thus, well-designed surrogates must have the same linear properties as the original signal (frequency content, autocorrelation and amplitude distribution…). However, any underlying nonlinear dynamic structure within the original data is altered in the surrogates by phase randomization [16]. The surrogate-generated data are compared to the original data by a discriminant nonlinear measure. If the value of the measure for the original time series lies within the distribution of surrogate values, with a level of confidence, the null hypothesis is accepted and the original series is considered as linear. If the measurement gives quite different values for the original series and the surrogates, the null hypothesis is rejected and the original series is considered as non-linear.

2.2.3.3 Statistical test for nonlinearity (z-score)

If we want the power of the statistical test to be α, we have to design at least a number of $(1/\alpha\text{-}1)$ sets of surrogate data. We have to generate a set of M surrogate data for every synthetic or real EHG signal, in order to test the null hypothesis. The null hypothesis is rejected at the 0.05 significance level, if the discriminating statistic (value of method) q_0, from an applied nonlinear method on the original data set, is statistically different from statistics $q_1,\ldots,q_M$ of the M surrogates [38].

To compare the original and surrogate series, discriminative statistics are calculated for both series. The statistics of significance z-score is

$$Z_{score} = \frac{|q_0 - \langle q_s(i)\rangle|}{\sigma_q(i)}$$

where q_0 stands for the statistic on the original time series, $\langle q_s(i)\rangle$ stands for the mean and $\sigma_q(i)$ for the standard deviation of the statistic on the surrogate time series, for $i=1,2,...,M$. For α=0.05, the critical value of z-score is 1.96. Therefore, the null hypothesis is rejected when z-score >1.96, with a 0.05 significance level and the original signal is thus considered as nonlinear [38].

2.2.4 Mean square error

Methods are compared by using the Mean Square Error (MSE), which is the estimate of the square of the standard deviation (σ^2) calculated, for the example of Time reversibility, in the following way:

$$MSE(CD) = \frac{1}{n}\sum_{i=1}^{n}\left(Tr^{(CD)} - Tr_i{}^{(CD)}\right)^2$$

where n is the number of Monte Carlo instances of signal generated by the model, $Tr^{(CD)}$ is the mean of Time reversibility over the n Monte Carlo trials on a complexity degree *CD*. We compute the MSE for each value of complexity degree *CD*.

2.3 Results

2.3.1 Results for synthetic signals

2.3.1.1 Evolution with CD

In this section we study the evolution of the values generated by the four methods (Time reversibility -*TR*-, Lyapunov exponent -*LE*-, Sample Entropy –*SampEn*-, delay vector variance -*DVV*) while varying the complexity degree (*CD*) of the Henon synthetic model, in four cases: 1) direct application of the method with no added noise, 2) direct application of the method with added noise, 3) using surrogates with no added noise and 4) using surrogates with added noise. The added noise is a white Gaussian noise with a fixed SNR of 5 db (SNR close to the SNR of real signals) and due to the limitation of EHG bandwidth, while the *CD* of the Henon model varies between 0 and 1. Our first objective is to test the sensitivity of methods to varying *CD* of the signal, with and without noise. Our second objective is to test if the use of surrogates improves the method sensitivity to complexity or not. Thus if we can find a method that yields good sensitivity without using surrogates, then we can reduce the

calculation time as the use of surrogates is computationally very expensive. We compared the methods by using two criteria, the method‟s sensitivity to the change of *CD* (slope of the curve "value of the method" vs. "*CD*") and the MSE of the method for different values of *CD*.

Figure 2.4-A1 presents the mean value given by each method, for the first case (direct method with no noise), as a function of *CD,* computed from the 30 Monte Carlo instances of the signal generated by the Henon model. **Figure 2.4-A2** presents the MSE of the methods for each complexity degree for the same case. We see in **Figure 2.4-A1** that in this direct case without noise, the four methods evolve well but with different sensitivity (slopes). Time reversibility and Lyapunov Exponent are more sensitive than the other two methods. But regarding the MSE, **Figure 2.4-A2,** we find that Time reversibility gives a much lower MSE than the Lyapunov Exponent.

For testing the effect of noise on the sensitivity (case 2) and the accuracy of the methods, we add noise (SNR=5db) to the signal generated by the Henon model. **Figure 2.4-B1** presents the effect of noise on the methods. We notice no significant evolution for Lyapunov Exponent and Sample Entropy. The sensitivity of Time reversibility and DVV decreases with the addition of noise. However, the sensitivity of Time reversibility remains the highest of the 4 methods. In the other hand we find in **Figure 2.4-B2** that DVV and Sample Entropy give the lowest MSE. But as Sample Entropy does not demonstrate any sensitivity to the variation of *CD*, this method is of no value in the case of noisy signal. Time reversibility gives an intermediate MSE and the highest sensitivity when compared to the other methods applied to noisy signals.

We then applied the methods to the synthetic signals with surrogates by using the z-score as the measure, in order to investigate if the use of surrogates improves the results or not. **Figure 2.4-C1** presents the z-score for each method versus *CD* with no added noise (case 3). We can notice that all the methods reflect the non-linearity of the signal generated by the Henon model, as theirs z-score are always above 1.96. In terms of sensitivity to *CD* variation, Sample Entropy is the best, but with the highest MSE (**Figure 2.4-C2**). Time reversibility presents an acceptable evolution for lower *CD*. But beyond *CD* = 0.4 an unexpected decrease occurs in the curve and the Tr value remains constant after *CD*=0.7. This method gives however the lowest MSE (**Figure 2.4-C2**). The DVV method presents an intermediate slope, contrary to the Lyapunov Exponent that presents no evolution with *CD*. Both DVV and Lyapunov exponent gives low MSE in this case.

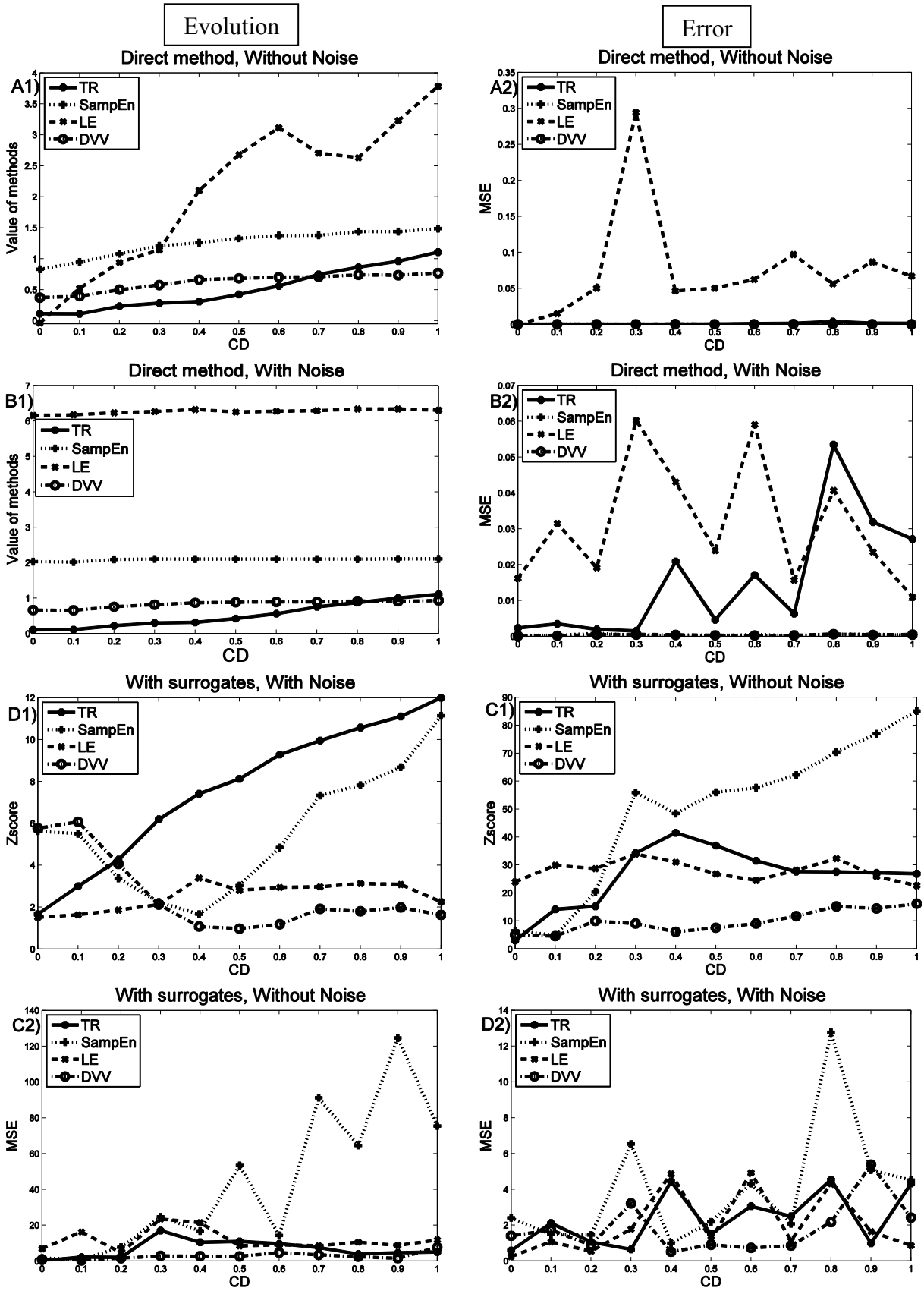

Figure 2.4: Results obtained for Henon model by using Monte-carlo simulations. Left: Evolution of the methods with variable complexity in different cases. Right: MSE of the methods with variable complexity degree in different cases. (A) Case 1: direct method with no added noise, (B) Case 2: direct method with added noise, (C) Case 3: with surrogate use and no added noise, (D) Case 4: with surrogate use and added noise.

The methods were then applied to the signals by using again surrogates and z-score, but now with added noise (SNR=5db) (case 4). All the methods still reveal the nonlinearity of the model. Indeed z-score is above 1.96 for all the methods, except for DVV where it gives a z-score value lower then 1.96 for *CD* between 0.4 and 0.6. We can clearly notice an increase in the sensitivity of Time reversibility **Figure 2.4-D1** when compared to the case in **Figure 2.4-C1**. Sample Entropy has a good evolution beyond *CD* = 0.4 but, on the other hand, it presents a rapid increase in MSE (**Figure 2.4-D2**). The Lyapunov Exponent and DVV do not evolve as a function of *CD* (**Figure 2.4-D1**) and they give similar MSE than Time reversibility (**Figure 2.4-D2**).

2.3.1.2 Evolution with SNR

We also investigated the effect of noise on the MSE of these methods. Our objective was to study the robustness of our methods by measuring the MSE of the methods with different signal to noise ratio (SNR). From this study we could gain useful information concerning the efficiency of the methods when dealing with real signals, which are usually known to be very noisy. **Figure 2.5** presents the MSE of the application of the methods (y axis) with different SNR (x axis) for synthetic signals generated by the Henon model in two cases, direct application (**Figure 2.5-A**) and by using surrogates (**Figure 2.5-B**). The complexity degree *CD* is set equal to 0.8 for the Henon model, as for this *CD*, we are sure that the model has a chaotic behavior and is not entered in a periodic cycle. In the direct case, an expected result is obtained for all methods (**Figure 2.5-A**). The MSE decreases (more or less) when SNR increases. In the case of the application of surrogates (**Figure 2.5-B**), a very surprising result is obtained: the MSE of all the methods increases with increasing SNR.

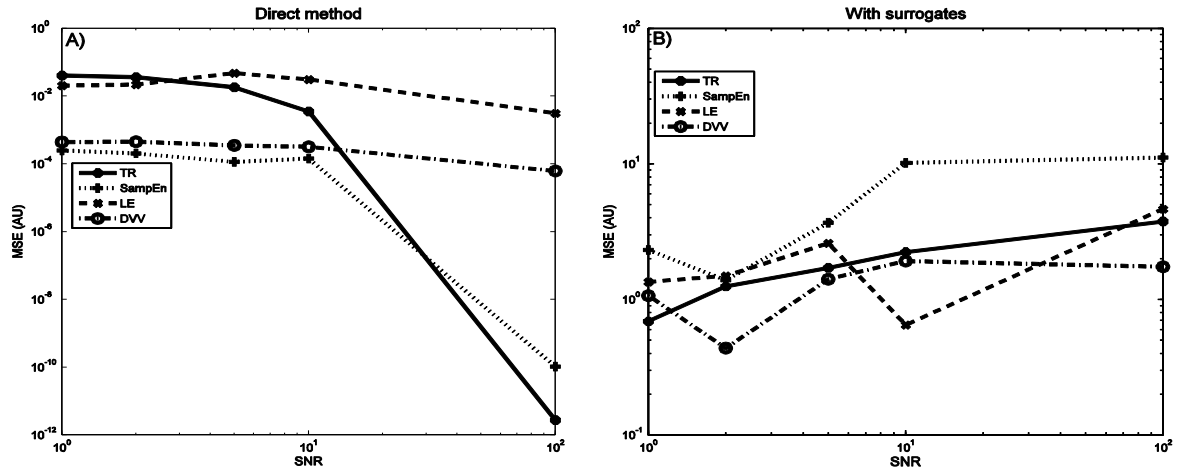

Figure 2.5: A Logarithmic plot of Mean Square Error of the four methods as a function of Signal to Noise Ratio using Monte-carlo simulation for synthetic signals generated with Henon model. (A) Direct method, (B) With surrogate use: SNR=[1,2,5,10,100].

2.3.2 Results for real signals

2.3.2.1 Labor prediction performance using linear and nonlinear methods

The different nonlinear methods were applied to real uterine EMG signals (EHG), first with a direct application of the method, and then with use of surrogates. For comparison purpose, we computed, from these real signals, three linear frequency based parameters classically used for the analysis of the EHG. The values were then used to classify the contraction signals according to two classes: Pregnancy or labor contractions. We used Receiver Operating Characteristic (ROC) curves in order to test the discriminating power of each parameter (non linear or frequency based). A ROC curve is a graphical tool that permits the evaluation of a binary, i.e. two classes classifier. A ROC curve is the curve corresponding to TPR (True Positive Rate or Sensitivity) vs. FPR (False Positive Rate or 1-Specificity) obtained for different classification parameter thresholds. ROC curves are classically compared by means of their Area Under the Curve (AUC), which is estimated by the trapezoidal integration method.

Our first objective was to compare the performances of linear and nonlinear methods and to verify that the nonlinear methods reveal the evolution of EHG characteristics better than the linear ones. Our second objective was to test if the use of surrogates improves the classification of EHG bursts into Pregnancy or Labor classes. The characteristics of all the ROC curves using and not using surrogates are presented in **Table 2.1**. The ROC curves obtained with the different methods using and not using surrogates are presented in **Figure 2.6-A** and **Figure 2.6-B** respectively. In case of direct application, the performances in correct classification, Pregnancy or Labor, varies markedly from AUC=0.478 for Sample Entropy to AUC=0.842 for Time reversibility. From these results, it is clear that nonlinear methods improve the classification of Pregnancy and Labor signals. Indeed, the highest AUC (0.842), sensitivity (0.86) and specificity (0.72) are obtained for Time reversibility, whatever the nonlinear or linear methods used. The Mean Power Frequency and Lyapunov Exponent methods also give an acceptable performance (**Figure 2.6-A**) with AUC=0.778 and AUC=0.758 respectively. When using surrogates, all the ROC curves presents approximately the same appearance with the highest AUC=0.650 obtained for Sample Entropy. In this case, we notice that the performance of Sample entropy increases while that of DVV remains approximately the same. On the other hand, the performance of Time reversibility and Lyapunov Exponent decreases with the use of surrogates. All the AUC obtained with these

non-linear methods are, in this case, similar to the ones obtained with linear frequency parameters.

We can thus conclude from this first study, that nonlinear methods improve the classification between pregnancy and labor contractions when compared to linear methods. Furthermore, even if the use of surrogates improves the performance of some methods, it does not globally improve the classification results.

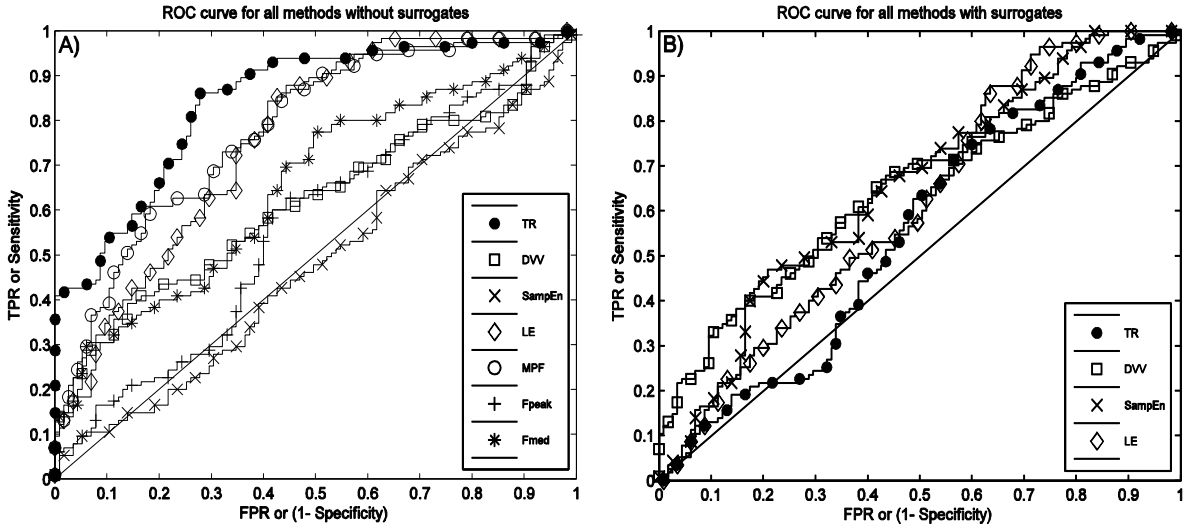

Figure 2.6: Example of ROC curves obtained for the prediction of labor with the different linear and nonlinear methods. (A) Direct method, (B) With use of surrogates.

2.3.2.2 Effects of decimation on labor prediction performance

Table 2.1 (Direct method / with Surrogates)

ROC curves obtained for labor prediction

Parameter	AUC		Specificity		Sensitivity	
	Dir.	Sur.	Dir.	Sur.	Dir.	Sur.
Time reversibility	**0.842**	0.560	**0.721**	0.513	**0.860**	0.626
Sample Entropy	0.478	**0.650**	0.382	**0.593**	0.643	0.643
Lyapunov Exponent	0.758	0.614	0.643	0.591	0.756	0.530
Delay Vector Variance	0.615	0.642	0.582	0.573	0.600	**0.669**
	AUC		Specificity		Sensitivity	
Mean Power Frequency	**0.778**		**0.678**		**0.730**	
Peak Frequency	0.561		0.582		0.600	
Median Frequency	0.654		0.556		0.704	

In this section, we study the sensitivity of non-linear-methods to one of the pre-processing steps of interest, down sampling. Our signals were recorded with a sampling frequency of 200 Hz. The useful content of EHG is known to range between 0.2 and 3 Hz [39]. A high sampling frequency makes the calculations more intensive, but on the other hand, a low sampling frequency may negatively affect the results of some processing methods. To properly evidence this possible effect, we applied the nonlinear methods on the same signals, first with the original sampling frequency (200 Hz), then after decimation (20 Hz). We chose a factor 10 for the decimation based on the signal bandwidth mentioned above. A 20 Hz sampling frequency is sufficient to respect the Shannon theory while keeping a correct time resolution.

We thus investigated the effect of down sampling on the performances of the nonlinear parameters for pregnancy/labor classification. Our objective is to see if down sampling has a significant impact on the results, and, in this case, if it increases or decreases the classification performance. If the down sampling impact is positive or negligible, we will gain in computational time without affecting the classification efficiency.

As previously, to evaluate the performance of the studied parameters for pregnancy/labor classification, we used ROC curves.

Figure 2.7-A presents the ROC curves for the 4 non-linear methods when applied to the original signals (sampling rate=200 Hz), and **Figure 2.7-B** present them when methods were applied to the decimated signals (sampling rate=20 Hz). The area under the curve (AUC) for the ROC curves is presented in **Table 2.2**.

It is clear from **Figure 2.7** that Tr and LE are relatively insensitive to down sampling, as their AUC in the two cases are similar (**Table 2.2**). DVV is more affected than Tr and LE. Its already low discrimination power becomes even worse. The performance of SampEn increases drastically after down sampling as its AUC goes from 0.478 to 0.672 (**Table 2.2**). Furthermore, after down sampling, the computation time for the four methods decreases from 8.27 hours to 18 minutes, on a computer running with Intel 4 processors and 8 Gb RAM motherboard (**Table 2.2**).

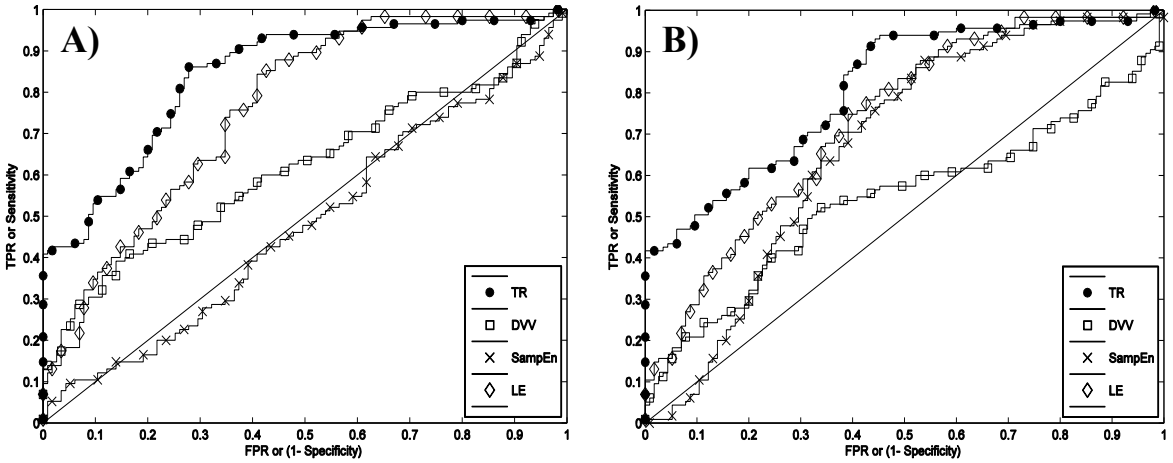

Figure 2.7: ROC curves for labor/pregnancy classification for all methods without (A) and with down sampling (B).

Table 2.2: Comparison of methods performance for labor/pregnancy classification, with and without down sampling.

Classification parameter	ROC curve AUC	
	Fs=200 Hz	**Fs=20 Hz**
TR	0.842	0.809
DVV	0.615	0.541
SampEn	0.478	0.672
LE	0.758	0.731
Computational Time	8,27 h	18 min

2.3.2.3 Effect of filtering on labor prediction performance

In this section, we study the sensitivity of non-liner-methods to the second preprocessing step of interest, which is filtering. Indeed, the uterine EMG content ranges from 0 to 3Hz [39]. The selection of digital filters, classically used to remove noise from signals before the processing, may influence the results. We chose to apply to our signals four Butterworth digital filters which have a smooth frequency response and are computationally non-intensive [34]. We used three band-pass filters:

- [0.1Hz - 0.3Hz]: To test the susceptibility of the methods tested to frequency content in the lower frequencies (FWL).
- [0.3Hz - 1Hz]: To exclude most components of motion, respiration, and cardiac signal [40].

- [0.3Hz - 3Hz]: To test the susceptibility of the methods tested to frequency content in the higher frequencies [34] (FWH).

The different methods were applied to real uterine EMG signals, once without filtering and then after filtering of the signals with the three filters [0.1Hz - 0.3Hz], [0.3Hz - 1Hz], [0.3Hz - 3Hz]. So by using filters with different pass band, we test which studied methods are sensitive to the choice of the filtering bandwidth, and also, which methods will possibly benefit from this preprocessing.

The results, for the discrimination of Pregnancy and Labor contractions, are presented using ROC curves **Figure 2.8**(a-b-c-d). Each figure presents one method applied without filtering and with the 3 defined filters. The characteristics of the obtained ROC curves are presented **Table 2.3**.

It is clear from the results **Figure 2.8**(a) that all the ROC curves (3 filters and without filtering) of Time reversibility are similar. The AUCs are also similar whatever the filtering or with no filter (**Table 2.3**). Tr is not sensitive to the signal bandwidth.

Delay Vector variance method"s classification power, **Figure 2.8**(b), increases a little bit when the signals are filtered in the [0.1Hz - 0.3Hz] bandwidth, decreases a little bit in the [0.3 Hz - 1Hz] bandwidth and remains approximately the same in the [0.3 Hz - 3Hz] bandwidth, when compared to no filtering (**Table 2.3**). DVV seems thus insensitive to filtering.

Sample Entropy method **Figure 2.8**(c), is highly sensitive to filtering in the [0.1Hz - 0.3Hz] bandwidth (FWL). Indeed, we can notice a very clear improvement of classification performance when the signal is filtered into this bandwidth: AUC rises from 0.481, with no filtering, to 0.780, for filtering in the [0.1-0.3Hz] bandwidth (**Table 2.3**). The increase in Sample Entropy classification performance (AUC) is much lower when filtering in the 2 other bandwidths.

Filtering into the three bandwidths does not bring any improvement of the classification performance for Lyapunov Exponents, **Figure 2.8**(d). Indeed, its AUC even decreases slightly with the [0.1-0.3Hz] filter and remains approximately the same with the [0.3-3Hz] and [0.3-1Hz] bandwidth filters (**Table 2.3**).

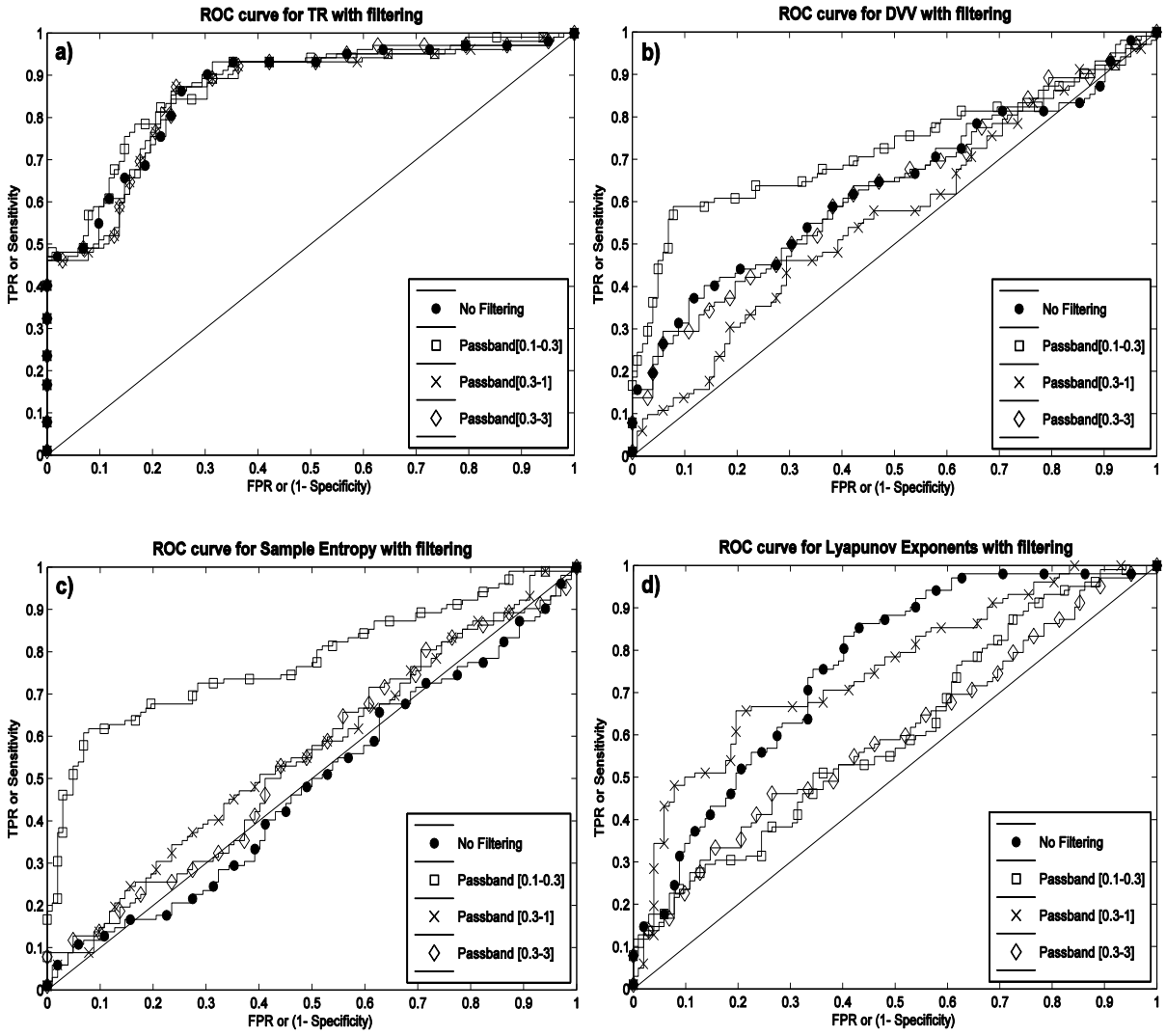

Figure 2.8: ROC curves obtained for: Time reversibility (a), Delay Vector Variance (b), Sample Entropy (c) and Lyapunov Exponents (d), without or with filtering (3 defined filters).

Table 2.3 :Comparison of methods performance for labor/pregnancy classification without and with (3 used filters) filtering.

Classification parameter	**AUC**			
	No filtering	***Passband [0.1Hz-0.3Hz]***	***Passband [0.3Hz-1Hz]***	***Passband [0.3Hz-3Hz]***
TR	0.862	0.874	0.855	0.860
DVV	0.632	0.725	0.564	0.628
SampEn	0.481	0.780	0.558	0.542
LE	0.757	0.603	0.753	0.596

2.4 Discussion

In this chapter, a comparison between four nonlinear methods coming from three families: Statistic (Time reversibility), Predictability (Sample Entropy and Delay Vector Variance), Chaos theory (Lyapunov Exponents), has been performed on synthetic signals generated by the Henon nonlinear stationary model, in order to test their sensitivity to the change in signal complexity, in normal and noisy conditions, with or with no use of surrogates. While being far from the optimal model for uterine electrical activity, the Henon model is still one of the best one available to test the performances of nonlinearity methods. Until now, there is no physiological model available that can represent the underlying physiological mechanisms and complexity of the uterine contractility and of the resulting EHG.

We analyzed, quantitatively and as comprehensively as possible, these four very different nonlinear methods. All four methods were found to reflect correctly the increasing complexity of the signals in the simplest case (direct application of the method with no added noise), but with different sensitivities. In the case of added noise and direct application of the method, as expected, a decrease in the sensitivity of all methods occurred at very low Signal to Noise Ratio (SNR=5db). Indeed, none of the methods detected the varying complexity of the signal, except for Time reversibility, which gave a noticeable evolution even at this very low noise levels. The sensitivity of Sample Entropy increased by using surrogates and it gave the highest sensitivity of all the methods, in the case of use of surrogates with no added noise. Indeed Sample Entropy was previously proved to be sensitive to many aspects of the signal characteristics, including the sampling rate of the signal [21]. Unexpected results were obtained in the case of surrogates use and with added noise. The evolution of Time reversibility improved when compared to the previous case, and Sample Entropy still presented a good sensitivity. We noticed that in the case of surrogate use, Sample Entropy gave the highest sensitivity of the methods but also associated with the highest MSE. This makes it unreliable in this case.

To summarize our findings on synthetic signals, Time reversibility was found to be the least sensitive to noise, presented a better sensitivity to complexity evolution for higher noise level than the other methods, and was associated with a low MSE. Time reversibility gave the best results in most of the studied cases. But we can conclude from the study that there is no universal method to detect signal complexity. Indeed, none of the studied methods performed better than the other ones in all of the studied cases.

In this chapter we also presented results obtained by using nonlinear and linear methods for labor/pregnancy classification of real EHG bursts, as well as the results of the effect of decimation and filtering on this classification performance. Comparison of the four methods, with or without surrogate use, evidenced that nonlinear methods applied with no surrogate use are clearly better in classifying correctly pregnancy and labor contractions than the linear ones. We can see also that the use of surrogates improves the performance of some methods like Sample Entropy. These results confirm the results obtained during the study on synthetic signal, since the sensitivity of Sample Entropy increases if surrogates are used (which justifies a posteriori the use of the Henon model).

To sum up, the main findings of the study concerning the nonlinearity and complexity are the following: (i) Some of the studied methods are insensitive to varying signal complexity; (ii) The Sample Entropy method performances are dependent on the use of surrogates; (iii) Generally speaking, none of the studied methods performed better than the other ones in all studied situations and cases; (iv) Time reversibility method is very sensitive to the change in model complexity, giving average or good performances, associated with the lowest MSE in most situations.

The main findings concerning the effect of down sampling are: (i) The performance of LE and Tr, which were previously evidenced in this study as being the most powerful methods for labor/pregnancy classification, are slightly reduced by down sampling. AUC of Tr decreases from 0.842 to 0.809. But this may be an acceptable tradeoff with the computation time saved thus; (ii) The performances of the DVV method are more affected than those of Tr and LE; (iii) The performances of SampEn is, as expected, highly influenced by down sampling due to SampEn dependence on signal point numbers and sampling, as indicated in its name. They are remarkably increased by down sampling. Thus, to optimize the performances of this method, the sampling frequency needs to be carefully chosen. But its AUC stays lower than the one of Tr, Tr remaining thus the best method for pregnancy/labor classification.

Down sampling by a factor of 10 decreases the computational time by a factor of 27.5. This makes the clinical application of these methods much more realistic and will help us to attempt to use these methods (Tr for example) for the prediction of normal and preterm labor.

The main findings concerning the study of the effect of filtering are the following: (i) Time reversibility, which has been evidenced as the more powerful methods in the previous sections, is the less sensitive methods to all bandwidth filtering among all methods. Tr

remains the best methods whatever the filter. This is very positive since no filtering preprocessing step would be needed for Tr to get the best performance; (ii) DVV and Lyapunov exponents methods are a little bit more sensitive to filtering; (iii) Sample entropy method is very sensitive to the bandwidth [0.1-0.3Hz], considered as the low frequency band of EHG (FWL) which exclude the baseline noise and the high frequency component of EHG (FWH). Its AUC increases from 0.481 with no filtering to 0.780 after filtering with the bandwidth [0.1-0.3Hz]. This result seems logical as SampEn searches for similar patterns in the signal, it is very affected by the frequency content of the signal. SampEn will be able to find similar patterns more easily in low frequency signal than high frequency and noisy signal. When removing, with a low-pass filter, the high frequency/noisy component of the signal, we thus notice an improvement in performance for the low frequency component of EHG signal.

2.5 Conclusion and perspective

Several methods have been introduced to tackle the difficult problem of analyzing nonlinear characteristics of EHG signals. The results of this study lead us to the conclusion that the best method of the four tested ones, for our application on real EHG, is Time reversibility. Indeed Tr deals robustly with real, usually noisy, signals. It has a good sensitivity to complexity, one of the EHG characteristics that permit to classify uterine contraction efficiency better than linear frequency parameters. Time reversibility seems to be the less sensitive method to down sampling and filtering and stay the best method with and without both preprocessing techniques. Using surrogates and the z-score as a measure of nonlinearity does not seem to bring any improvement to the Time reversibility performance. Therefore we will not use them for further work on EHG complexity analysis by using Tr.

We can conclude also that down sampling does not cause a significant decrease in the classification rate of the studied methods. The classification results remain similar despite the fairly drastic down sampling that we performed in this limited preliminary study. The increase in the classification rate of SampEn confirms that this method is very sensitive to the sampling frequency of the signal. So the sample frequency as well as the frequency band of analysis, should be chosen very carefully to increase the performance of SampEn.

There are some weaknesses points in our study that we are aware of and that we aim to improve in further studies. The Time reversibility method is very dependent on the length of

signal and on the choice of time delay (τ). So we aim to find a way to optimize these parameters. Also we have not taken into account the effect of nonstationarity of the signals for the analysis of the method performances. We think that a time varying windowed study of the signal may reduce the influence of this characteristic. An application on a physiologic model that is closer to reality than the pure Henon synthetic model may help us to get a more reliable interpretation of the results. This kind of model is currently being developed in our group and will soon permit us to test the methods on a much more realistic physiological models [41].

In further work we also aim to use all of the available channels (VA1,...,VA12) instead of only one channel, as done in this work in order to test if we can even increase the classification rate, as evidenced in a preliminary work [42].

Future work will tackle also the question of the optimal sampling frequency for all these methods in general and for SampEn in particular. We will, for example, apply the methods on signal decimated by several factors (ranging for example from 20 to 5) in order to choose the optimal sampling frequency that gives the highest classification performance.

After the validation of the classification rate of our parameters by using ROC curve, we will attempt to use the most efficient parameters as input to a more advanced and sophisticated classifier such as Support Vector Machine (SVM), to predict normal or preterm labors.

The conclusion obtained from this chapter guide us for the next analysis (presented in the next chapter) dealing with the coupling and the synchronization between the 16 channels of EHG recording matrix. Since nonlinear methods have been evidenced to be better than linear ones in this previous monovariate EHG analysis, we will then study 2 nonlinear coupling and synchronization methods for this bivariate analysis, and also compare them with a linear method.

References:

[1] J.S. Bendat, and A.G. Piersol, “Random Data Analysis and Measurement Procedures,” *Measurement Science and Technology*, vol. 11, no. 12, pp. 1825, Dec. 2000.

[2] R.E. Garfield, W.L. Maner, L.B. MacKay, D. Schlembach, and G.R. Saade, “Comparing uterine electromyography activity of antepartum patients versus term labor patients,” *American Journal of Obstetrics and Gynecology*, vol 193, no. 1, pp. 23-29, Jul. 2005.

[3] H. Maul, W.L. Maner, G. Olson, G.R. Saade, and R.E. Garfield, “Non-invasive transabdominal uterine electromyography correlates with the strength of intrauterine pressure and is predictive of labor and delivery,” *J. Matern Fetal Neonatal Med*, vol. 15, no. 5, pp. 297-301, 2004.

[4] E. Pereda, R.Q. Quiroga, and J. Bhattacharya, “Nonlinear multivariate analysis of neurophysiological signals,” *Progress in Neurobiology*, vol. 77, no. 1-2, pp. 1-37, Sep-Oct. 2005.

[5] M. Hassan , J. Terrien, , A. Alexandersson, C. Marque, and B. Karlsson, “Nonlinearity of EHG signals used to distinguish active labor from normal pregnancy contractions,” in *32nd Annual International Conference of the IEEE Engineering in Medicine and Biology Society (IEE-EMBC)*, Buenos Aires, Argentina, Aug-Sep. 2010, pp. 2387-90.

[6] J. Bruhn, H. Röpcke, and A. Hoeft, “Approximate entropy as an electroencephalographic measure of anesthetic drug effect during desflurane anesthesia,” *Anesthesiology*, vol. 92, no. 3, pp. 715-726, Mar. 2000.

[7] M. Jospin, P. Caminal, E. Jensen, H. Litvan, M. Vallverdu, M.M.R.F Struys, H.E.M Vereecke, and D. Kaplan, “Detrended fluctuation analysis of EEG as a measure of depth of anesthesia,” *IEEE Trans. Biomed. Eng.*, vol. 54, no. 5, pp. 840-846, May. 2007.

[8] R. Acharya U., O. Fausta, N. Kannathala, T. Chuaa, and S. Laxminarayan , “Non-linear analysis of EEG signals at various sleep stages,” *Computer methods and programs in biomedicine*, vol. 80, no. 1, pp. 37-45, Oct. 2005.

[9] T. Takahashi, R.Y. Cho, T. Mizuno, M. Kikuchi, T. Murata, K. Takahashi, and Y. Wada, “Antipsychotics reverse abnormal EEG complexity in drug-naive schizophrenia: A multiscale entropy analysis,” *NeuroImage*, vol. 51, no. 1, pp. 173-182, May. 2010.

[10] D. Kaplan, M. Furman, S. Pincus, S. Ryan, L. Lipsitz, and A. Goldberger, “Aging and the complexity of cardiovascular dynamics,” *Biophysical Journal*, vol. 59, no. 4, pp. 945-949, Apr. 1991.

[11] Y. Shiogai, A. Stefanovska, and P.V.E. McClintock, “Nonlinear dynamics of cardiovascular ageing,” *Physics Reports*, vol. 488, no. 2-3, pp. 51-110, Mar. 2010.

[12] M. Mohebbi, and H. Ghassemian, “Prediction of paroxysmal atrial fibrillation based on non-linear analysis and spectrum and bispectrum features of the heart rate variability signal,” *Computer Methods and Programs in Biomedicine*, vol. 105, no. 1, pp. 40-49, Jan. 2012.

[13] M. G. Signorini, G. Magenes, S. Cerutti, and D. Arduini, “Linear and nonlinear parameters for the analysisof fetal heart rate signal from cardiotocographic recordings,” *IEEE Trans. Biomed. Eng.*, vol. 50, no. 3, pp. 365-374, Mar. 2003.

[14] C. Gómez, R. Horneroa, D. Abasolo, A. Fernandez, and M. Lopez, “Complexity analysis of the magnetoencephalogram background activity in Alzfheimer's disease patients,” *Medical engineering & physics*, vol. 28, no. 9, pp. 851-859, Nov. 2006.

[15] W. Chen, J. Zhuang, W. Yu, and Z. Wang, "Measuring complexity using FuzzyEn, ApEn, and SampEn," *Medical engineering & physics*, vol. 31, no. 1, pp. 61-68, Jan. 2009.

[16] M. Hassan, J. Terrien, B. Karlsson, and C. Marque, "Comparison between approximate entropy, correntropy and time reversibility: Application to uterine EMG signals," *Medical Engineering & Physics (MEP)*, vol. 33, no. 8, pp. 980-986, Oct. 2011.

[17] A. Diab, M. Hassan, C. Marque, and B. Karlsson, "Quantitative performance analysis of four methods of evaluating signal nonlinearity: Application on uterine EMG signals," in *34th Annual International Conference of the IEEE Engineering in Medicine and Biology Society (IEE-EMBC)*, San Diego, California, Aug-Sep. 2012, pp. 1045-48.

[18] D. Radomski, A. Grzanka, S. Graczyk, and A. Przelaskowski, "Assessment of Uterine Contractile Activity during a Pregnancy Based on a Nonlinear Analysis of the Uterine Electromyographic Signal," in *Information Tech. in Biomedicine*, ASC 47, Springer: Berlin Heidelberg, E. Pietka and J. Kawa, Eds., 2008, pp. 325–331.

[19] R. Nagarajan, "Quantifying physiological data with Lempel-Ziv complexity-certain issues. Biomedical Engineering," *IEEE Trans. Biomed. Eng.*, vol. 49, no. 11, pp. 1371-1373, Nov. 2002.

[20] S. Graczyk, J. Jezewski, K. Horoba, and J. Wrobel, "Analysis of abdominal electrical activity of uterus-approximate entropy approach," in *22nd Annual International Conference of the IEEE Engineering in Medicine and Biology Society (IEE-EMBC)*, Chicago, Illinois, Jul. 2000, pp. 1352-55.

[21] J. Vrhovec, "Evaluating the progress of the labour with sample entropy calculated from the uterine EMG activity," *Elektrotehniski vestnik-Electrotechnical Review*, vol. 76, no. 4, pp. 165-170, 2009.

[22] C. Diks, J.C. van Houwelingen, F. Takens, and J. DeGoede, "Reversibility as a criterion for discriminating time series," *Physics Letters A*, vol. 201, no. 2-3, pp. 221-228, May. 1995.

[23] J.S. Richman, and J.R. Moorman, "Physiological time-series analysis using approximate entropy and sample entropy," *American Journal of Physiology-Heart and Circulatory Physiology*, vol. 278, no. 6, pp. H2039-H2049, Jun. 2000.

[24] T. Gautama, D.P. Mandic, and M.M. Van Hulle, "The delay vector variance method for detecting determinism and nonlinearity in time series," *Physica D: Nonlinear Phenomena*, vol. 190, no. 3-4, pp. 167-176, Apr. 2004.

[25] A. Wolf, J.B. Swift, H.L. Swinney, and J.A. Vastano, "Determining Lyapunov exponents from a time series," *Physica D: Nonlinear Phenomena*, vol. 16, no. 3, pp. 285-317, Jul. 1985.

[26] S. M. Pincus, "Approximate Entropy as a Measure of System-Complexity," *Proceedings of the National Academy of Sciences of the United States of America*, vol. 88, no. 6, pp. 2297-2301, Mar. 1991.

[27] G.A. Casas, and P.C. Rech, "Multistability annihilation in the Hénon map through parameters modulation," *Communications in Nonlinear Science and Numerical Simulation*, vol. 17, no. 6, pp. 2570-2578, Jun. 2012.

[28] B. Karlsson, J. Terrien, V. Guðmundsson, T. Steingrímsdóttir, and C. Marque, "Abdominal EHG on a 4 by 4 grid: mapping and presenting the propagation of uterine contractions," in *11th Mediterranean Conference on Medical and Biological Engineering and Computing*, Ljubljana, Slovenia, Jun. 2007, pp. 139-143.

[29] T. Schreiber, and A. Schmitz, "Surrogate time series," *Phys. D*, vol. 142, no. 3-4, pp. 346-382, Aug. 2000.

[30] C.K. Lee, H.G. Jo, and S.K. Yoo, "Non-linear Analysis of Single Electroencephalography (EEG) for Sleep-Related Healthcare Applications," *Healthc Inform Res*, vol. 16, no. 1, pp. 46-51, Mar. 2010.

[31] M.T. Rosenstein, J.J. Collins, and C.J. De Luca, "A Practical Method for Calculating Largest Lyapunov Exponents from Small Data Sets," *Physica D-Nonlinear Phenomena*, vol. 65, no. 1-2, pp. 117-134, May. 1993.

[32] H.D.I. ABARBANEL, "Analysis of Observed Chaotic Data," in *Rev. Mod. Phys.*, New York, London: Springer, 1st Ed., 1996.

[33] M.B. Kennel, R. Brown, and H.D.I. Abarbanel, "Determining Embedding Dimension for Phase-Space Reconstruction Using a Geometrical Construction," *Physical Review A*, vol. 45, no. 6, pp. 3403-3411, Mar. 1992.

[34] G. Fele-Zorz, G. Kavsek, Z. Novak-Antolic, and F. Jager, "A comparison of various linear and non-linear signal processing techniques to separate uterine EMG records of term and pre-term delivery groups," *Med. Biol. Eng. Comput.*, vol. 46, no. 9, pp. 911-22, Sep. 2008.

[35] S. Kuntamalla, and R.G. L. Reddy "The Effect of Aging on Nonlinearity and Stochastic Nature of Heart Rate Variability Signal Computed using Delay Vector Variance Method," *International Journal of Computer Applications*, vol. 14, no. 5, pp. 40-44, Jan. 2011.

[36] T. Suzuki, T. Ikeguchi, and M. Suzuki, "Effects of data windows on the methods of surrogate data," *Phys Rev E Stat Nonlin Soft Matter Phys*, vol. 71, no. 5, pp. 056708, May. 2005.

[37] V. Venema, F. Ament, and C. Simmer, "A Stochastic Iterative Amplitude Adjusted Fourier Transform algorithm with improved accuracy," *Nonlinear Processes in Geophysics*, vol. 13, no. 3, pp. 321-328, Jul. 2006.

[38] S. Slađana, "Surrogate data test for nonlinearity of the rat cerebellar electrocorticogram in the model of brain injury," *Signal Processing*, vol. 90, no. 12, pp. 3015-3025, Dec. 2010.

[39] D. Devedeux, C. Marque, S. Mansour, G. Germain, and J. Duchêne, "Uterine electromyography: a critical review," *Am. J. Obstet. Gynecol.*, vol. 169, no. 6, pp. 1636-53, Dec. 1993.

[40] M. Lucovnik, R.J. Kuon, L.R. Chambliss, W.L. Maner, S.-Q. Shi, L. Shi, J. Balducci, and R.E. Garfield, "Use of uterine electromyography to diagnose term and preterm labor," *Acta. Obstet. Gynecol. Scand.*, vol. 90, no. 2, pp. 150-7, Feb. 2011.

[41] J. Laforet, C. Rabotti, J. Terrien, M. Mischi, and C. Marque, "Toward a Multiscale Model of the Uterine Electrical Activity," IEEE Trans. Biomed. Eng., vol. 58, no. 12, pp. 3487-3490, Dec. 2011.

[42] M. Hassan, J. Terrien, A. Alexandersson, C. Marque, and B. Karlsson, "Improving the classification rate of labor vs. normal pregnancy contractions by using EHG multichannel recordings," in *32nd Annual International Conference of the IEEE Engineering in Medicine and Biology Society (IEE-EMBC)*, Buenos Aires, Argentina, Aug-Sep. 2010, pp. 4642-4645.

Chapter 3: Coupling and directionality. A propagation analysis of EHG signals

Understanding the direction and quantity of information flowing in a complex system is a fundamental task in signal processing. In most coupled systems, such as neuronal areas in human body, the intrinsic and internal variants, and the interdependencies among their subsystems are not accessible. Therefore, in order to quantify the interdependencies among the uterine muscle, attempts have been made to measure the synchronization between their outputs represented as time series measured using electrode sensors. We introduce in this chapter methods used to study the relationships between such signals. We then test their sensitivity to some specific signal characteristics using synthetic and real data. We present also our approach to improving these method‟s performances. Globally this chapter is divided into two parts: in the first part we compare the coupling methods, whereas in the second one we test their sensitivity to some characteristic of signal (nonstationarity, frequency band) or signal recording (bipolar or monopolar recording).

3.1 Introduction

The usual problem in the analysis of multivariate data is whether signals are dependent or not [1]. This type of data exists in coupled systems in many branches of life sciences, particularly in bio-signals where synchronization has been noted in an increasing variety of signals such as EEG [2-3], ECG [4], and EHG [5-6]. The EHG signal contains nonlinear [7] and non stationary [8] characteristics. Therefore, the application of purely linear techniques such as cross-spectrum or cross-correlation analysis [9] may present strong limitations.

The uterus is deceptively simple in structure but its functioning is quite complex and poorly understood as it moves from pregnancy towards labor. There are numerous interconnected control systems involved in its functioning (electric, hormonal, mechanical) [6]. For that we present in this chapter an investigation of the EHG propagation characterization in order to differentiate between labor and pregnancy contractions as well as for the monitoring of pregnancy.

- Synchronization evolution with pregnancy:

How uterine synchronization evolves during pregnancy, and also if there is any difference in terms of coupling and direction coupling between labor and pregnancy, remains an open question. Furthermore, the most appropriate method to investigate the coupling and directionality of EHG is not clearly defined. The last point of interest is if any and then which synchronization analysis methods could contribute significantly to differentiating between pregnancy and labor contractions.

In the literature, most studies indicate that synchronization increases when labor approaches and that labor is associated with a greater coupling among uterine cells [10-11]. A small number of studies have been done, either of the mechanical or the electrical uterine activity, with the aim of localizing the uterine electrical activity origin. These studies can be summarized as following:

- Cadeyro-Barcia et al. claimed by clinical studies of the mechanical activity, that the uterus begins to contract in the upper fundal region and then this contraction is conducted toward cervix [12].

- Euliano et. al. [13] followed the direction of the propagation of the center of uterine electrical activity (origin of the contraction) and its movement. This study reports an interesting pattern in women who delivered successfully: the direction of the center of uterine activity was predominantly to the fundal.

- Lammers et al. [14] conduct a study that shows that there are two possibility for the origin of electrical activity, either the ovarian or cervical end of the uterus. However, the authors assumed that activity was initiated mostly in the ovarian end (corresponding to fundus in humans).

- The inter-electrode delay was estimated for surface multichannel EHG recordings in order to analyze the uterine activity propagation [15]. Authors focused on localizing pacemaker zones. Localization on the upper part was been observed on 65% of case.

- Few other studies evidenced a propagation that spreads in all directions, with a dominant direction down towards the cervix [16-17].

- Mikkelsen et al. shown, by studying the velocity and direction propagation of EHG during labor, that labor contractions propagate both in the downward (58%) and upward (42%) direction. They suggest also a multidirectional propagation pattern [18].

- Another study stated in a study on 35 contractions obtained from 6 women that 63% of the contractions originated in the upper part of the uterus and 37% originated in the lower part of the uterus [19].

Most of these studies were not aimed at studying the directionality between signals. They were more focalized on the measure of coupling and synchronization between EHG channels, by using linear and nonlinear methods, or on the measure of propagation velocity. They didn‟t either monitor the evolution along pregnancy of coupling and direction. In this chapter we performed, for pregnancy monitoring, a longitudinally (at successive terms of pregnancy) measure of directionality, in addition to the coupling between uterine EMG channels, using three nonlinear and linear methods.

To address these questions, the objective of this chapter is to provide evidence on the usefulness and appropriateness of linear and nonlinear directional and coupling analysis for, first, synthetic, then simulated and finally real uterine EMG signals.

Therefore, in the first part of this chapter, two nonlinear methods, nonlinear correlation coefficient h^2 [20] and general synchronization H [21], and one linear method, granger causality GC [22] are applied to a synthetic two dimensional nonlinear coupled Rössler model in two ways. First the coupling value of the model is varied and then, the coupling direction is changed, in order to compare the performance of the nonlinear methods versus the linear one in evaluating the value of coupling as well as to detect the direction of these synthetic signals. The method which yields the best result on the Rössler model is then tested and validated using a new uterine EMG physiological model [23]. This is the first time that this multiscale physiological model is used to evaluate candidate methods for EHG processing. The method is then applied to a dataset of real uterine EMG signals measured in pregnancy and in labor to study its possible evolution with weeks before labor (WBL). We also tested the difference between the coupling and the coupling direction map, at terms going from 3 WBL to labor, in order to understand what happens to the coupling and its direction when going from pregnancy to labor.

- <u>Methodological and preprocessing problems:</u>

Although noticeable advances have been made both in recording and processing EHG signals, a number of methodological questions remain open regarding the optimal way to process the data to evaluate connectivity between uterus locations. Therefore, the aim of the second part

of this chapter is to analyze the impact of four methodological factors or preprocessing, on the analysis of EHG signals:

- Connectivity detection method.

A lot of work has been done on EHG in order to investigate its propagation characteristics. These works have used various classical methods such as correlation [13, 24-25] and propagation velocity [26-27]. Recently we have shown that the nonlinear correlation between EHG signals increases from pregnancy to labor [10]. However, in this study we analyzed the connectivity on the whole uterine bursts (no pre-segmentation) and without taking into account the direction of propagation. Most previous studies did not study the directionality between EHG signals from different locations. However, a few studies have evidenced a propagation that spreads in all directions, with a dominant direction down towards the cervix [13, 17-18].

- Piecewise stationary segmentation (preprocessing).

The segmentation of EEG and monkey uterine EHG signals was shown to be useful by Terrien et al. [28-29], comparing bivariate and monovariate piecewise stationary pre-segmentation algorithm. The results evidenced the superiority of the bivariate technique. In the same work the effect of taking only the higher frequency component of signal (FWH) on the behavior of the nonlinear correlation within the EHG burst was studied. This showed that using the narrow band (filtered) signal, the synchronization increased in the EHG burst instead of decreasing using the full band (non filtered) signal.

- Frequency bands filtering (preprocessing).

The investigation of the effect of filtering the human uterine EHG signals into its different frequency components (low FWL and high FWH components) was also done by Terrien et al. [11]. They demonstrated that filtering the signals to focus on FWL increases the pregnancy/labor classification rate when using nonlinear correlation method. This observation supports the hypothesis that FWL is related to propagation of uterine activity and that it could reflect better the increased coordination of the uterus in labor.

To our knowledge, no one has applied the combination of these pretreatments (segmentation and filtering) in order to improve the differentiation between pregnancy and labor in human EHG using both connectivity and directionality analysis.

- EHG measurement type (bipolar/monopolar).

There are strong indication that the electrode configuration and the detailed measurement protocol has a strong effect on the detection of uterine signals which can severely affect the characterization of the propagation of uterine contractions by processing the EHG [30]. Detailed investigation of the effect of the type of recording (bipolar/monopolar) on EHG connectivity has not been performed before.
We thus raised the question of the effect of nonstationarity, frequency content, and the measurement type (bipolar/monopolar) of EHG on coupling and direction estimation between EHG signals in order to test which method of coupling would be the most appropriate in order to differentiate between pregnancy and labor contractions. In the second part of this chapter, we attempt to answer these questions have been done using the methods described below.

The same connectivity methods used in the first part of this chapter (nonlinear correlation coefficient h^2 [20], general synchronization H [21], and granger causality GC [22]), were also used in the second part of this chapter. They were first applied to a four-dimensional coupled non-linear non-stationary (NLNS) synthetic Rössler model. The methods were then applied to a dataset of real uterine EHG signals measured during pregnancy and labor to investigate the coupling and the direction maps generated by the three methods. The changes in these parameters when going from pregnancy to labor were analyzed. We investigated the effect associated with *bPSP* segmentation on the three connectivity methods. Then we tested the effect of using only the low frequency band (FWL) of real signals for the same analysis as above. We also compared the results of the connectivity methods using the real EHG recordings in bipolar and monopolar configurations.

3.2 Material and methods

3.2.1 Data

3.2.1.1 Synthetic signals

To evaluate our coupling and direction measures in the first part of this chapter, we applied them to a stationary two dimensional coupled Rössler nonlinear model defined as:

$$
\begin{aligned}
\frac{dx_1}{dt} &= -w_x x_2 - x_3 + \eta \\
\frac{dx_2}{dt} &= -w_x x_1 + a x_2 + \eta \\
\frac{dx_3}{dt} &= b + x_3 (x_1 - c) + \eta \\
\frac{dy_1}{dt} &= -w_y y_2 - y_3 + C(x_1 - y_1) + \eta \\
\frac{dy_2}{dt} &= w_y y_1 + a y_2 + \eta \\
\frac{dy_3}{dt} &= b + y_3 (y_1 - c) + \eta
\end{aligned}
\qquad (1)
$$

with a = 0.15, b = 0.2 and c = 10. The factor C, which varies from 0 (independence) to 1 (total coupling), permits us to control the coupling strength between the two oscillators. The two signals of length 5000 data points that we use to evaluate the coupling are x_1 and y_1. the frequencies of both oscillators were shifted using w_x = 0.95 and w_y = 1.05 which are the values used in [31]. The stochastic influence is given by a Gaussian distributed white noise η.

Then to study the effect of non-stationarity of times series on the used coupling and direction measures in the second part of this chapter, we use a four-dimensional coupled Rössler NLNS model. The model is modulated with a controlled sinusoid signal to introduce a non-stationarity into it [32]. The four dimensional nonlinear stationary Rössler system is defined as:

$$
\begin{pmatrix} \frac{dX_j}{dt} \\ \frac{dY_j}{dt} \\ \frac{dZ_j}{dt} \end{pmatrix} = \begin{pmatrix} -\Omega_j Y_j - Z_j + [\sum_i k_{ji}(X_i - X_j)] + \eta_j \\ \Omega_j X_j + a Y_j \\ b + (X_j - c) Z_j \end{pmatrix} \qquad (2)
$$

with *i,j=1,2,3,4* and the frequencies of the four oscillators were shifted using Ω_1=1.01, Ω_2=0.99, Ω_3= 0.97 and Ω_4= 1.03. The parameters of the oscillators were set to a= 0.15, b= 0.2, and c= 10 as in [33]. The stochastic influence is given by a Gaussian distributed white noise η_j. The interaction between oscillators i and j is modeled by means of a coupling between the X_i and X_j components which coupling strength is adjusted by the coupling parameters $k_{ji} \neq 0$. In our study, the coupling parameters have been set to k_{21}=0.1, k_{31}=0.5, k_{32}=0.3 and k_{42}= 1 (**Figure 3.1**). The remaining coupling strengths have been set to zero.

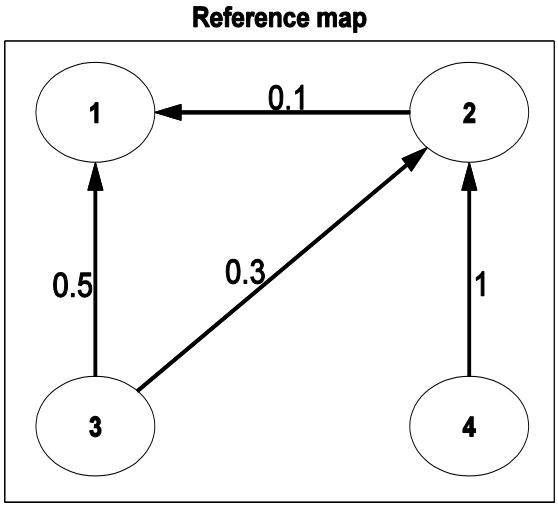

Figure 3.1: The map of direction using the reference coupling value.

The modulation of nonlinear stationary Rössler model to make it non-stationary is done by using the sinusoidal signal S(n):

$$S(n) = A\sin(2 * \pi * f_0 * n/fe), \qquad (3)$$

where A=1, f_0=0.1 Hz, n=0:4999 and fe=100 Hz. We modulate the output of each pilot system by this sinusoid to obtain a non-linear non-stationary (NLNS) Rössler model.

This system has been simulated by using an Euler method with an integration step of 0.05 and a sampling step of 0.1. We have generated 30 Monte Carlo instances of each signal with length of 5000 data points. The time-series analysis techniques have been applied to the X-components of the system.

3.2.1.2 Simulated signals from a uterus electrophysiological model

We used an electrophysiological model developed within a European project (http://www.erasysbio.net/index.php?index=268). This multiscale model describes the evolution of the uterine electrical activity, from its genesis at the cellular level, then to its propagation at the myometrium level, and up to its projection through the volume conductor tissues to the abdominal surface [23].

The electrical source is a volume current source density. For the volume conductor, we adopt the description developed in [34]. The volume conductor is considered as made of parallel interfaces separating the four different abdominal tissues, namely: the myometrium, where the source is located at a given depth, the abdominal muscle, fat, and skin. **Figure 3.2** presents a representation of the model including tissue layers and the electrodes.

The volume conductor effect depends on the tissue thicknesses, their conductivities, and the source depth. All the tissues are assumed to be isotropic with the exception of the abdominal muscle. For the tissue conductivities, the values reported in the literature are used for simulating a signal propagating along the direction parallel to the vertical line of the abdomen [35-36]. Finally, we assume the source to be close to the myometrium–abdominal muscle interface.

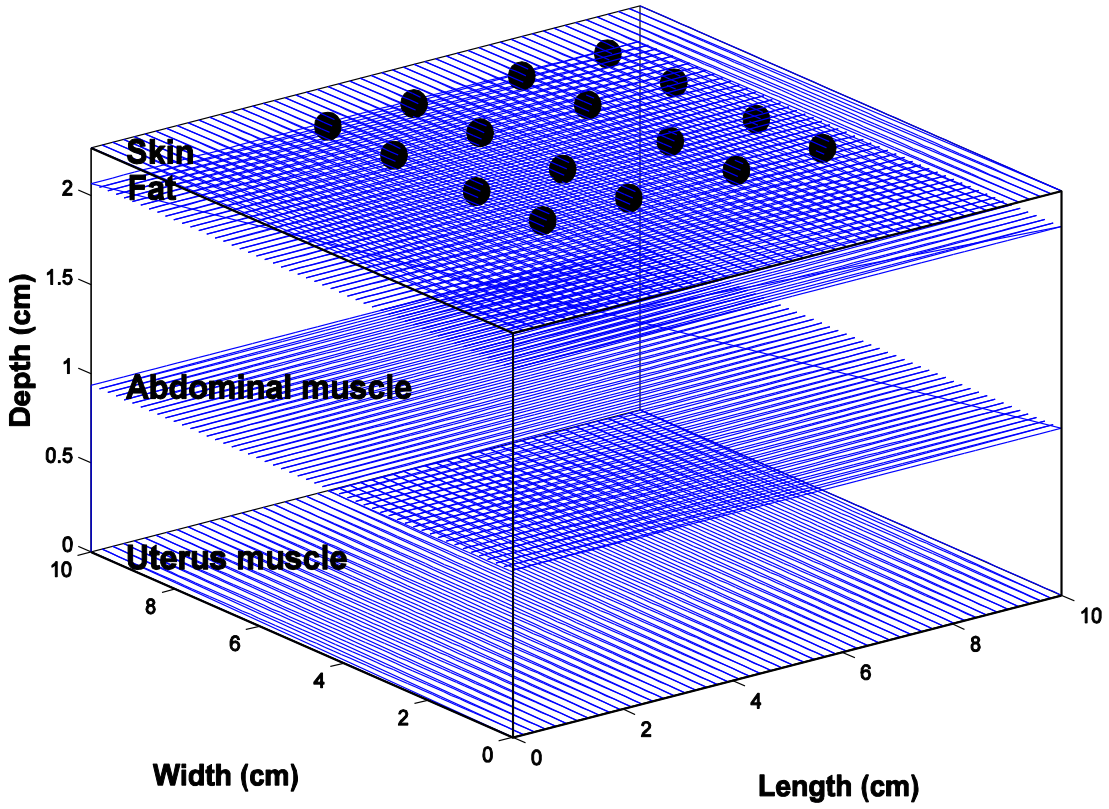

Figure 3.2: Physiological model representation with the four layers (uterine and abdominal muscle, fat and skin). The black circles represent the electrodes.

3.2.1.3 Real signals

Signals recorded by the experimental protocol described in chapter 1 and used in chapter 2 are used also in this chapter. Whereas the methods used here are "bivariate" in the sense that we used all the combinations between the 16 monopolar channels of the 4x4 recording matrix located on the women's abdomen (see [37] for details). The signals were recorded with a sampling frequency of 200 Hz during pregnancy and in labor at the Landspitali University Hospital in Iceland, following a protocol approved by the relevant ethical committee (VSN 02-0006-V2). The uterine EMG signals were segmented manually to extract uterine activity bursts, then filtered using a CCA-EMD method developed by our team [38]. After segmentation and filtering, we obtained 84 labor and 92 pregnancy bursts. We have grouped

the segmented contractions in 7 groups of weeks before labor (WBL). Details for each group are presented in **Table 3.1**. The analysis below was applied to these segmented uterine bursts.

Table 3.1: Details on Database Group (WBL)

WBL	7	6	5	4	3	2	1	Labor
Number of women	1	2	2	4	6	4	5	5
Number of contractions	1	17	3	13	22	15	21	84
Mean Term	34	33	35	36	37	37	39	39
h^2 standard deviation*10^{-17} in **Figure 3.6**	0	0.9	0.99	3.2	2.3	1.1	2.5	7.9

3.2.2 Methods

3.2.2.1 Nonlinear correlation coefficient (h^2)

The nonlinear correlation analysis is a nonparametric method used for evaluating the dependency of a random process (signal Y) on another process (signal X), independently of the type of relationship between the two processes.

The underlying idea is that if the value of X is considered as a function of the value of Y, the value of Y given X can be predicted according to a nonlinear regression curve. The variance of Y according to this regression curve is termed as the explained variance, since it is explained (or predicted) by the knowledge of X. The unexplained variance is estimated by subtracting the explained variance from the original one. The correlation ratio h^2 describes the reduction of variance of Y that can be obtained by predicting the Y values from those of X, according to the regression curve, as h^2 = (total variance − unexplained variance) / total variance.

In practice, to estimate the nonlinear correlation coefficient h^2, a scatter plot of Y versus X is studied. The values of X are subdivided into bins; for each bin we calculate the X value of the midpoint P_i and the average value of Y, Q_i, computed from the same bin interval. The regression curve is approximated by connecting the resulting points (P_i, Q_i) by straight line segments. The nonlinear correlation coefficient between demeaned signals X and Y is then calculated as follows (for more details see [39]):

$$h^2_{Y|X} = \frac{\sum_{k=1}^{N} Y(k)^2 - \sum_{k=1}^{N} \left(Y(k) - f(X_i)\right)^2}{\sum_{k=1}^{N} Y(k)^2} \qquad (4)$$

where N is the length of Y signal and $f(X_i)$ is the linear piecewise approximation of the nonlinear regression curve obtained using a continuous piecewise affine function. For

practical application, the number of bins (i) needs, however, to be defined. Our experience shows that this parameter is not crucial regarding the performances of the method. It has to be set anyway in accordance to the nonlinear function that might exist between the input time series. Here we choose i=15.

The estimator $h^2_{Y|X}$ ranges from 0 (Y is independent of X) to 1 (Y is fully determined by X). For a nonlinear relationship, $h^2_{x|y} \neq h^2_{y|x}$ and the difference $\Delta h^2 = h^2_{x|y} - h^2_{y|x}$ indicates the degree of asymmetry of the nonlinear coupling. This asymmetry, used to compute the direction of coupling, is not ensured by linear correlation coefficient. The delay at which the maximum value for h^2 is obtained is used as an estimate of the time delay between the signals. Therefore, we can also obtain the difference $\Delta\tau = \tau_{x|y} - \tau_{y|x}$. By combining the information on asymmetry and time delay in coupling, the following direction index has recently been proposed by Wendling et al. [40] to provide a robust measure of the direction of coupling:

$$D_{x|y} = \tfrac{1}{2}\left[\operatorname{sgn}\left(\Delta h^2\right) + \operatorname{sgn}\left(\Delta\tau\right)\right] \qquad (5)$$

If $D_{x|y} = +1$ (or -1) then $X \rightarrow Y$ (or $Y \rightarrow X$ respectively). $D_{x|y} = 0$ indicates a bidirectional (Y ↔ X) coupling between signals.

3.2.2.2 General synchronization (*H*)

From time series measured in two systems X and Y, we reconstruct delay vectors $x_n=(x_n, ..., x_{n-(m-1)\tau})$ and $y_n=(y_n, ..., y_{n-(m-1)\tau})$, where n=1,...,N; m is the embedding dimension and τ denotes the delay time. Let $r_{n,j}$ and $s_{n,j}$, j=1,..., k, denote the time indices of the k nearest neighbors of x_n and y_n, respectively. For each x_n, the squared mean Euclidean distance to its k neighbors is defined as:

$$R_n^{(k)}(X) = \frac{1}{k}\sum_{j=1}^{k}\left(x_n - x_{r_{n,j}}\right) \qquad (6)$$

The Y-conditioned squared mean Euclidean distance is:

$$R_n^{(k)}(X \mid Y) = \frac{1}{k}\sum_{j=1}^{k}\left(x_n - x_{s_{n,j}}\right)^2 \qquad (7)$$

Thus, a nonlinear interdependence measure can be defined accordingly [39]:

$$H^{(k)}(X|Y)=\frac{1}{N}\sum_{n=1}^{N}\log\frac{R_n(X)}{R_n^{(k)}(X|Y)} \tag{8}$$

where $R_n(X)$ is the average distance of a vector x_n to all the other vectors. This measure is close to zero if X and Y are independent, while it is positive if nearness in Y also implies nearness in X for equal time partners. The nonlinear interdependence is an asymmetric measure, in the sense that $H(X|Y) \neq H(Y|X)$ so $H(X|Y) > H(Y|X)$, if $X \rightarrow Y$.

The phase space depends on two parameters, the time delay τ and the embedding dimension m. We use the first local minimum of the average mutual information and the false nearest neighbor algorithm to estimate the time delay (τ), and the minimal embedding dimension (m) respectively. The estimated value of time delay and dimension were 10 and 6 respectively.

3.2.2.3 Granger causality (*GC*)

Granger argued that if X is influencing Y, then adding past values of the first variable to the regression of the second one will improve its prediction performance, which can be assessed by comparing the univariate and bivariate fitting of AR models to the signals [39]. The AR model order is approximated to the Schwarz's Bayesian Criterion (SBC). Thus, for the univariate case, one has:

$$\begin{aligned} x(n) &= \sum_{k=1}^{p} a_{xk}\, x(n-k) + u_x(n), \\ y(n) &= \sum_{k=1}^{p} b_{yk}\, y(n-k) + u_y(n) \end{aligned} \tag{9}$$

where a_{xk} and b_{yk} are the model parameters, p the model order, and u_x and u_y are the uncertainties or the residual noises associated with the model. Here, the prediction error, for a given signal, depends only on its past values.

On the other hand, for bivariate AR modeling,

$$\begin{aligned} x(n) &= \sum_{k=1}^{p} a_{xyk}\, x(n-k) + \sum_{k=1}^{p} b_{xyk}\, y(n-k) + u_{xy}(n), \\ y(n) &= \sum_{k=1}^{p} a_{yxk}\, x(n-k) + \sum_{k=1}^{p} b_{yxk}\, y(n-k) + u_{yx}(n) \end{aligned} \tag{10}$$

where the prediction error for each individual signal depends on the past values of both signals. The prediction performance of both models can be assessed by the variances of the prediction errors:

$V_{X/X\_} = Var(u_x)$ and $V_{Y/Y\_} = Var(u_y)$ for the univariate AR model.

$V_{X/X\_,Y\_} = Var(u_{xy})$ and $V_{Y/Y\_,X\_} = Var(u_y x)$ for the bivariate AR model.

Where $Var(.)$ indicates the variance operator, and $X|X\_$ and $X|X\_$, $Y\_$ indicate predicting X by its past values alone and by past values of X and Y, respectively.

If $V_{X/X\_,Y\_} < V_{X/X\_}$, then Y causes X in the sense of Granger causality. The Granger causality of Y to X can be quantified as:

$$G_{Y\to X} = \ln\left(\frac{V_{X/X\_}}{V_{X/X\_,Y\_}}\right) \qquad (11)$$

If $G_{Y\to X} > G_{X\to Y}$, then $Y \to X$ and vice versa.

3.2.3 Bivariate piecewise stationary signal pre-segmentation

Several algorithms exist that can be used to segment a piecewise stationary signal. One such algorithm was developed by Carré and Fernandez [41], used for univariate signal segmentation. This algorithm starts by the decomposition of a signal into successive dyadic partitions. The log-spectrum corresponding to each partition is computed and denoised by undecimated wavelet transform if appropriate. A binary tree of the spectral distance between two adjacent partitions is then formed. Then they search for the tree that minimizes the sum of the spectral distances by Coifman-Wickerhauser algorithm.

Terrien et al. [28] used this technique to segment a pair of signals as pretreatment for connectivity estimation. These methods have been used with success on monkey EHG signals [28]. The segmentation was however based on the changes observed in only one of the signals so transitions that may occur in the other signals are not taken into account.

To improve the method and to adapt it to the task of finding stationary parts of a pair of signals, Terrien et al. [29] proposed to use the cross spectrum of the two signals instead of the auto spectrum of only one channel, thus taking into account the statistical changes in both channels at the same time. This preprocessing step has been proven to be useful for coupling analysis. In the second part of this chapter, we adopt the approach developed by Terrien et al. [29] since our methods are applied to bivariate signals.

3.2.4 From the methods to the direction maps

To estimate the coupling between two channel *x* and *y*, each method takes both signals *x* and *y* as input. We took all the possible combinations of two channels among all the available channels. We thus obtain n^2 values of coupling for each method. These values were saved in a matrix *n* x *n* (*n* is the number of channels and is equal to 2, 4 or 16 in case of bi-dimensional, four dimensional synthetic signals or real signals respectively).

The above computation is done for each contraction (real EHG) and each Monte Carlo trial (synthetic signals). If we have *m* contractions or *m* Monte Carlo trials, we obtain *m* x (*n* x *n*) matrices of coupling values. Finally we compute the mean over the dimension *m* of the *m* x (*n* x *n*) matrices to obtain just one *n* x *n* matrix for the *m* contractions or the *m* Monte Carlo trials. These values in the final *n* x *n* matrix can be coded by color scale and represented in a color map matrix (see **Figure 3.5**, **Figure 3.7** and **Figure 3.11**). In **Figure 3.6** and **Figure 3.9**, we computed the mean of the final *n* x *n* matrix to obtain one value for each group.

We took from the final *n* x *n* coupling matrix, the value of coupling between *x* and *y*, and the value between *y* and *x*. These values are used for the estimation of direction as mentioned above in the methods description. Then we plot the map of direction as in **Figure 3.5**, **Figure 3.7**, **Figure 3.8** and **Figure 3.11**.

When we use methods with *bPSP*, we do the same thing as above, but with an additional step, the segmentation. We apply the methods to each segment of both signals (*x* and *y*), not to the whole signals, then we take the mean over all segments and we continue as above.

3.3 Results

As we said in the introduction, this chapter is divided into two parts. We present first, the results of the part that is dedicated to the comparison of methods using synthetic, simulated and real data (Part 1). Then we present the results of the part that is dedicated to test their sensitivity to some characteristics of the signal (nonstationarity, frequency band) or to signal recording (bipolar or monopolar recording), (Part 2).

3.3.1 Part 1: Comparison of methods

3.3.1.1 Results on synthetic signals

Here we test the sensitivity of the methods to two signal aspects: varying coupling levels and direction changes. To investigate the sensitivity of the methods to coupling changes we apply

the methods to a synthetic signal generated by the Rössler model described above (1), with coupling level going from 0 to 1 (**Figure 3.3**). For each coupling degree, we generate 30 instances of the signal and we apply the three methods to the signals. We then plot the mean of the 30 values with the standard deviation for each method, normalized by its maximum (**Figure 3.3**). This kind of sensitivity test cannot be done on the physiological model that we use it in the next step, because its unknown coupling between signals cannot be controlled.

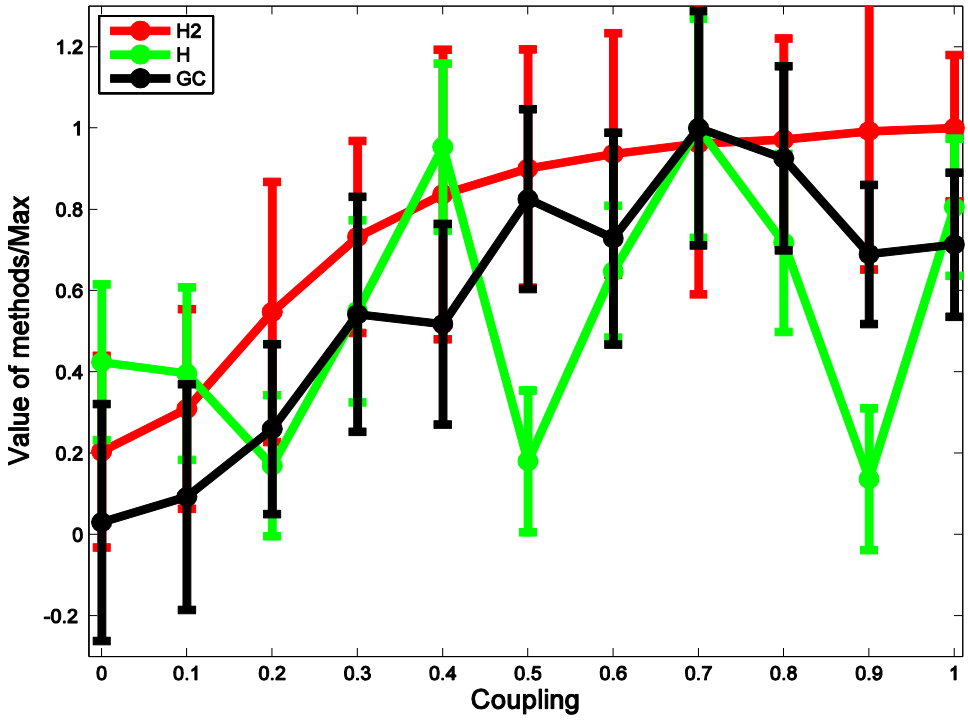

Figure 3.3: Evolution of connectivity estimated by the three methods and normalized by the maximum, for each method, as function of the coupling degree of the signals generated by Rössler model. The error bars represent the standard deviation of methods for each coupling level.

As we see in **Figure 3.3,** h^2 presents a very good evolution with coupling, increasing consistently with the increase in coupling degree. It has a small bias at C=0 since it give 0.2 for no coupling. *GC* presents an evolution from C=0 to 0.7. Then it decreases above 0.7, but it has the lowest bias for C=0. *H* does not present any clear evolution. It fluctuates between 0.1 and 1 when coupling increases and presents the highest bias. In terms of standard deviation, the 3 methods present approximately the same variability.

To investigate the sensitivity of the methods to changes in direction of coupling, we apply the same methods to synthetic signals generated by the same Rössler model, but with the coupling

degree fixed at 0.5 (**Figure 3.4**). The length of both generated signals is 6000 points. Initially, the direction is from signal x_1 to y_1 for the whole signal duration. To create a direction change, we cut the signals into three equal parts of 2000 points each. We keep the two extreme parts of both signals unchanged and we swap their middle parts. The direction is then from x_1 to y_1 for the first and the third parts, and from y_1 to x_1 for the middle part, as indicated in **Figure 3.4** (top) by the arrows and by the reference curve in **Figure 3.4** (bottom). We then compute the synchronization and the direction from x_1 to y_1 along the obtained signals. The results shown in **Figure 3.4** (middle) are the mean of 30 Monte-Carlo trials.

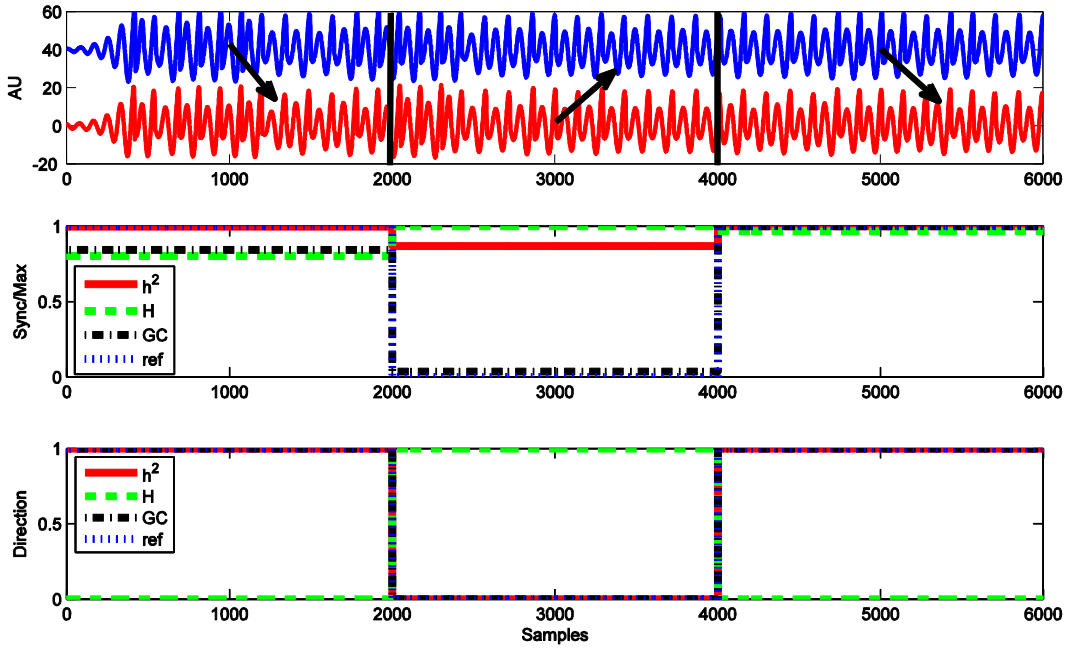

Figure 3.4: Sensitivity of methods to the change of direction between signals. Top: signal generated by Rössler model after the change of direction; Middle: synchronization estimation; Bottom: direction estimation. The blue curve is the reference curve.

We see in **Figure 3.4** (middle) the superiority of h^2 and GC over H, because the synchronization measure given by h^2 and GC in the middle part (2000-4000) is smaller than the ones obtained for the extreme parts, which coincide with the reference curve. This is the expected behavior since the coupling in the middle part is from y_1 to x_1 (due to the swap) and the measure of synchronization is computed from x_1 to y_1. However, H gives an opposite results which is erroneous and in contradiction with the underlying coupling. This erroneous behavior is clearer in the plot of direction in **Figure 3.4** (bottom), since 1 indicates a direction from x_1 to y_1 and 0 the opposite direction. It is clear that h^2 and GC give the right direction for

all signal parts while H gives the opposite of the true directions. This result is in agreement with the previous evolution study.

According to both study results (coupling and direction) we can confirm that h^2 is the best of the 3 methods as it permits to evidence both coupling evolution and direction for the Rössler synthetic model. We then move on testing h^2 on the physiological model.

3.3.1.2 Results on signals from electrophysiological model

Figure 3.5 presents the test of h^2 on simulated signals when applied to the physiological model data. The model creates a propagating wave of excitation from a given initial site. This results in a wave that has a known geometry. The model outputs a signal that would be observed at the abdominal surface with the same electrode configuration as the one used when measuring real signals (4x4 electrode grid).

We apply h^2 to the signal obtained with a planar propagation in the uterus from left to right under the electrode grid. We also apply h^2 on a signal generated with a radial propagation, with the origin close to the center of the electrode grid. After verification of their Gaussian distributions, a threshold of $m+2\sigma$ was applied to the results of the correlation matrix, where m is the mean of the correlation matrix and σ its standard deviation. The threshold was applied in order to remove insignificant coupling values among channels. The main purpose of this processing was to increase the figure readability.

As we can see in the direction map in the case of planar propagation, **Figure 3.5** (e), all the arrows reveal the planar propagation of the action potential (left to right) illustrated in **Figure 3.5** (a), but with a bi-directionality between most of the electrodes. The correlation among the channels is distributed around the diagonal in the h^2 matrix (**Figure 3.5** (c)).

In the case of radial propagation, the direction of arrows in **Figure 3.5** (f) is toward the center, which reveals the radial propagation, but with some shifting to the left and to the top due to the asymmetry of the center of the electrode grid with respect to the center of propagation. Here, the correlation among channels shown in **Figure 3.5** (d) is distributed to the whole matrix. The results show that the underlying directionality and coupling is reflected by the results obtained by computing h^2 on the 4x4 matrix as well as on the directionality map. The next step is to apply this technique to real signals expecting the observation of patterns in the EHG that would reflect the underlying propagation of uterine activity.

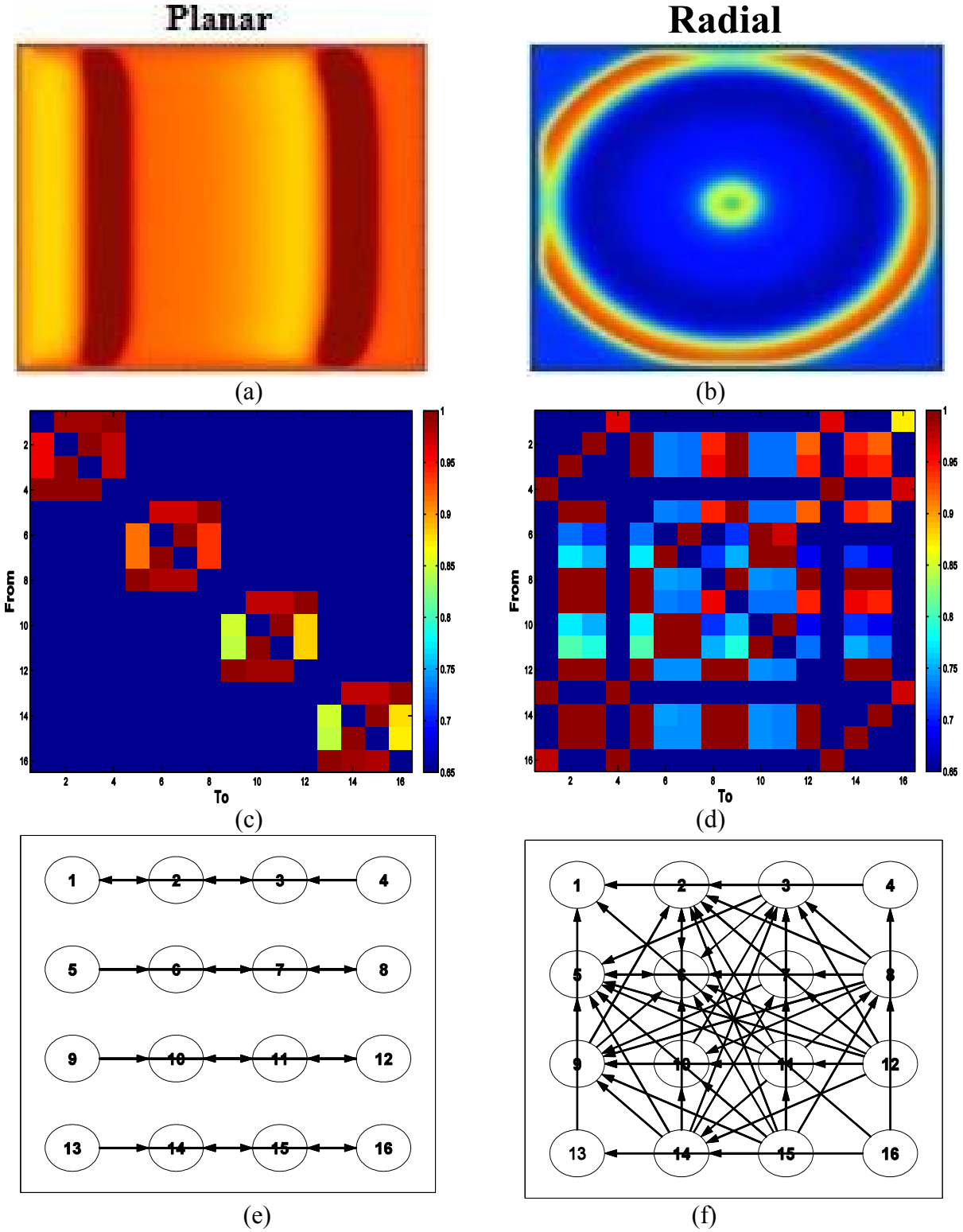

Figure 3.5: Results obtained with the physiological model of EHG propagation. Planar propagation wave of action potential (a), radial propagation wave of action potential (b). Quantity of information flow for planar propagation (c) and circular propagation (d). Direction of information flow for planar propagation (e) and circular propagation (f) between the 16 monopolar channels of uterine EMGs simulated by the physiological model when using the h^2 method.

3.3.1.3 Results on real signals

We investigate in this section the coupling evolution measured by h^2 (**Figure 3.6**) with respect to decreasing term before delivery (WBL). We also calculate the matrix of correlation using h^2 (**Figure 3.7** (a-c-e-g)), and the direction map (**Figure 3.7** (b-d-f-h)) between the 16 monopolar channels of real signals, recorded at 3 WBL, 2 WBL, 1 WBL and during labor, in order to visually monitor the changes in the correlation matrix and the direction map along term. We observe also the difference between EHG connectivity of pregnancy and labor contractions.

h^2 was applied to real uterine EMGs recorded on several women during different times of gestation. h^2 was applied to all the possible combinations of the 16 channels, for each contraction in each WBL. We plot in **Figure 3.6** the mean of the resultant coupling matrix over all the contractions for each WBL. A Kruskal-Wallis statistical test was applied to the results (**Table 3.2**). The most significant differences represented in bold in **Table 3.2** (p<0.01) between all gestational groups for h^2 are presented graphically in **Figure 3.6**.

It is clear from **Figure 3.6** that there is no monotonic evolution from 7 WBL to labor. The means of each WBL data are associated to extremely low standard deviations (red bars), which are also presented in **Table 3.1**. h^2 increases between 7 and 4 WBL, decreases between 2 WBL and labor, and exhibits a rupture at 3WBL.

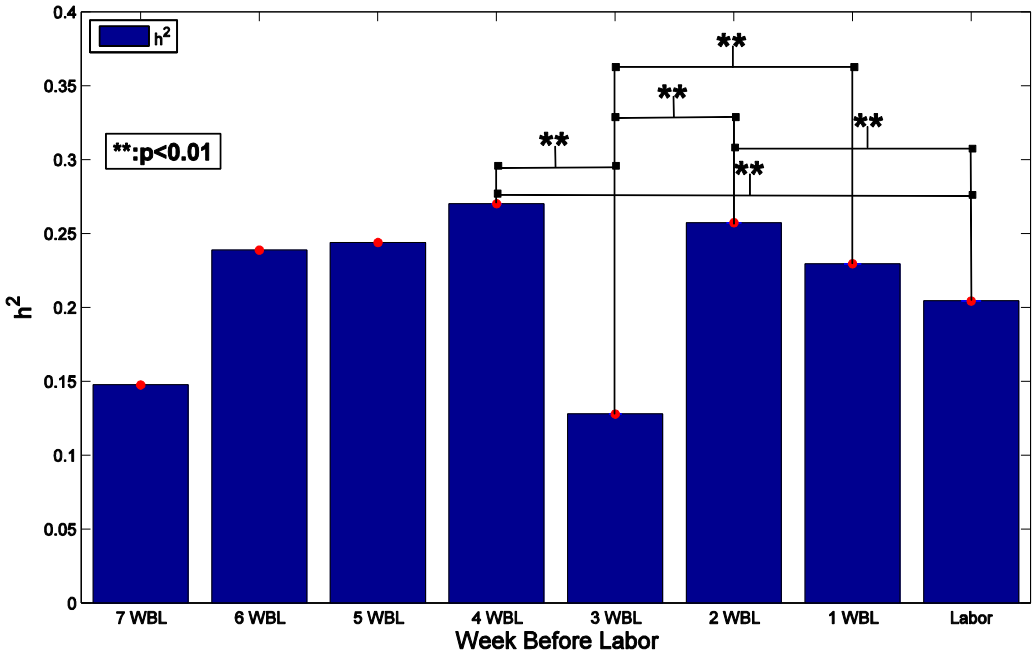

Figure 3.6: Evolution of connectivity estimated by h^2 as a function of weeks before labor (WBL), with its standard deviation (red).

It is also clear that we have a high significant difference ($p< 0.01$) between labor, 2 WBL, and 4 WBL. The same observation can be made between 3 WBL and 4 WBL, and 2 WBL and 1WBL. The *p*-value with 1% significance level are marked in bold in **Table 3.2**.

Table 3.2: *P*-VALUE Obtained by Kruskal-Wallis Test for h^2 Method

6	0.7724						
5	0.1797	0.7110					
4	0.1068	0.9833	0.5449				
3	0.5464	0.0126	0.0153	**2.30e-5**			
2	0.1585	0.9247	0.7670	0.3940	**2.96e-5**		
1	0.3316	0.8117	0.6996	0.0748	**0.0001**	0.2854	
0	0.7444	0.3986	0.1773	**0.0052**	0.0127	**0.0089**	0.043
WBL	7	6	5	4	3	2	1

To visually analyze the differences between 3 WBL, 2 WBL, 1 WBL and labor, we estimate the matrix of correlation and the map of direction between the 16 channels using h^2 (**Figure 3.7**). We select the aforementioned WBL because these are the successive groups that contain the highest number of contractions (22, 15, and 21 contractions) and women (6, 4,and 5 woman) for 3 WBL, 2 WBL, and 1 WBL respectively. The result is the average over all contractions at each term.

It is clear that the correlation in **Figure 3.7** (a-c-e) is random for 3 WBL, 2 WBL and 1 WBL respectively, whereas the correlation matrix for labor in **Figure 3.7** (g) is more regular, since the row and the column represented by channel 9 divide the matrix in four more or less active regions. We can notice, for each region, a high interaction and correlation between the channels.

In terms of direction, we see in **Figure 3.7** (b) that at 3 WBL, the arrows point in all directions (propagation to the entire matrix), but with no dominant direction. The node 6 which is in the upper part of the map receives the highest number of inward arrows. Then at 2 WBL, **Figure 3.7** (d), the multi-directionality is still present. But it is also obvious that the concentration of the inward arrows is shifted one row down to node 7. At 1 WBL, the concentration begins to be to the lowest row as we see for node 4 in **Figure 3.7** (f). During labor, **Figure 3.7** (h), the arrows point also in all directions but with a dominant direction toward the bottom (node 4, 7, 8, 12) of the matrix (toward the cervix).

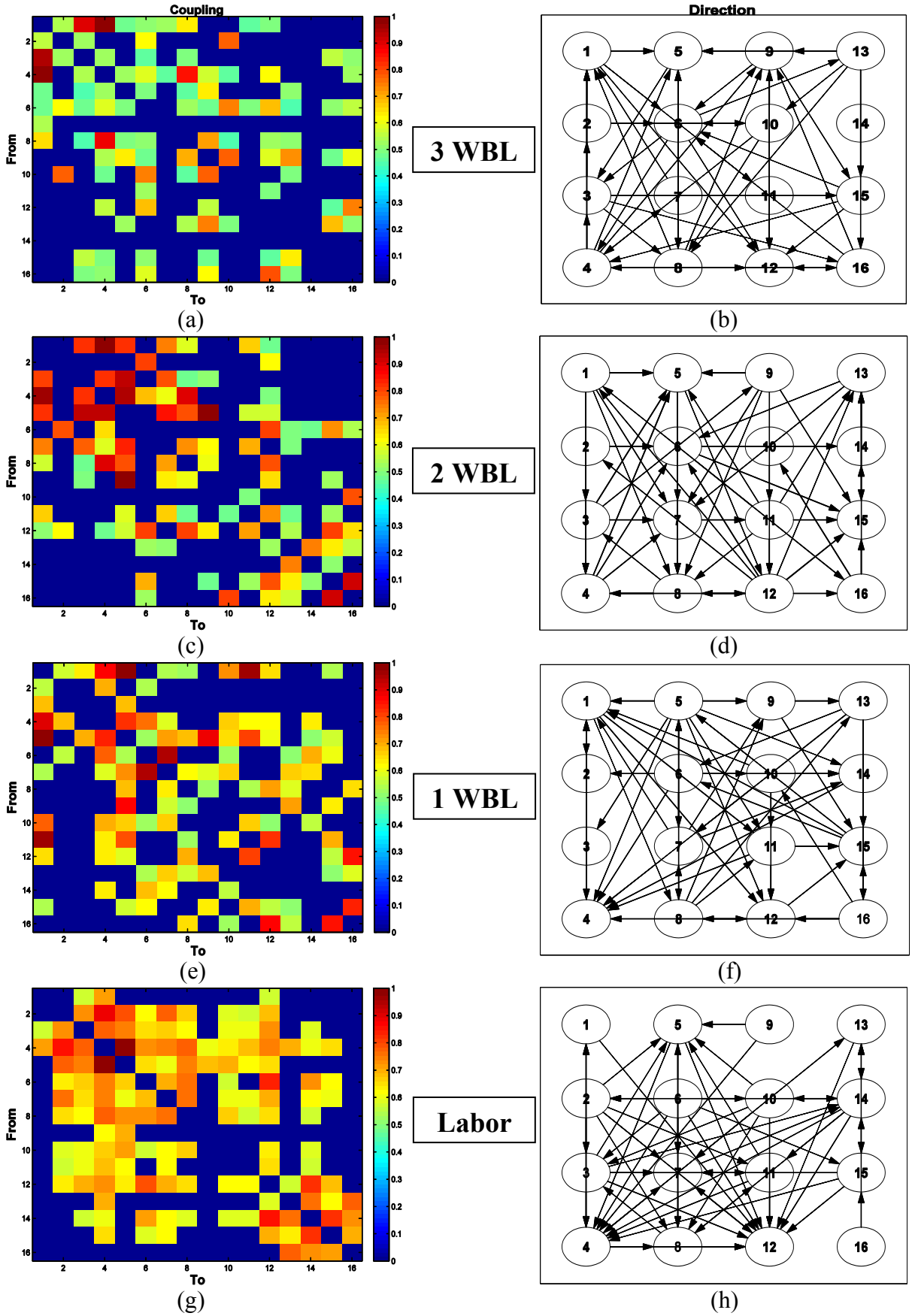

Figure 3.7: Quantity (a-c-e-g) and direction (b-d-f-h) of information flow recorded at 3 WBL (a-b), 2 WBL (c-d), 1 WBL (e-f) and Labor (g-h), between the 16 monopolar channels of EHG by using the h^2 method. Each coupling graph is normalized by its maximum.

3.3.2 Part 2: Sensitivity to signal characteristics and recording type

3.3.2.1 Results on synthetic signals

After doing the comparison of methods in the first part, in this part, we test the sensitivity of these methods to some of the signal"s characteristics by using both synthetic and real signals. We investigate here the effect of the application of the *bPSP* method on the four dimensional NLNS Rössler synthetic model mentioned above (2).

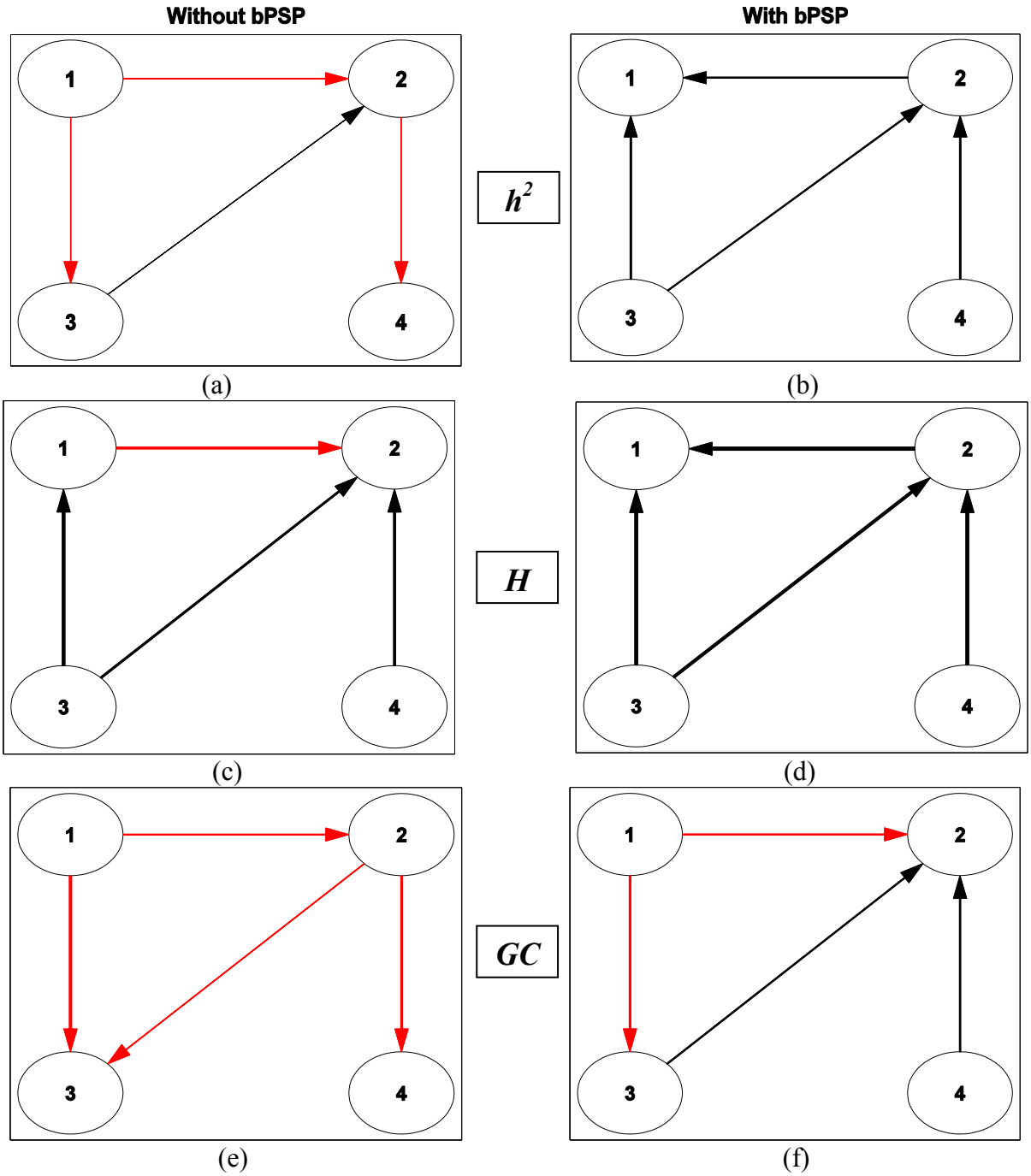

Figure 3.8: Direction of information flow without (a-c-e) and with *bPSP* (b-d-f), obtained between the nodes of NLNS Rössler model by using the h^2 (a-b), H (c-d), and GC (e-f) methods. Red arrows indicate erroneous direction.

We plot in **Figure 3.8** the map of coupling directions (node with arrows) between all the combination of simulated time series in two cases, with and without *bPSP,* for h^2, *H*, and *GC* **Figure 3.8** (a-b), **Figure 3.8** (c-d), and **Figure 3.8** (e-f) respectively. The arrows indicate the coupling directions, black arrows indicate the detection of a correct direction and red arrows indicates a wrong direction. We see in **Figure 3.8** (a-b) that h^2 applied without *bPSP* has 3 out of 4 direction errors (red), whereas its *bPSP* application rectifies all the errors by correctly detecting all four directions. It is clear from **Figure 3.8** (c-d) that *H* works better than h^2 when it is applied without *bPSP* since it has just 1 out of 4 direction error. This one error is corrected by using *bPSP* before *H*. **Figure 3.8** (e-f) show that *GC* is the worst method since it has 4 out of 4 direction errors when applied without *bPSP*. Using *bPSP*, the GC direction error rate improves a little and reaches 2 out of 4. According to results on synthetic signals we can confirm that the *bPSP* approach improves the detection of correct coupling direction. We therefore apply our methods to real EHG signals using the with *bPSP* approach as we estimate that the above results conclusively show that this generally helps with the nonstationarity issue.

3.3.2.2 Results on real signals

We investigate in this section the ability of the methods to differentiate between pregnancy and labor contraction groups. We apply our methods with bPSP to all the available bipolar and monopolar EHG bursts (**Figure 3.9** (a-b)). Then we apply the same methods to the same signals after bPSP, but with filtering to isolate the lower EHG frequency band (FWL) as additional pretreatment (**Figure 3.9** (c-d)). **Figure 3.9** presents the mean and standard deviations of the method results applied for each kind of measurement type and each group of EHG signals (labor and pregnancy).

In **Figure 3.9** (a-b), *GC* gives higher coupling for labor than for pregnancy in both cases (monopolar and bipolar). But we obtain higher standard deviation in the monopolar case than in the bipolar case. h^2 gives higher coupling values for labor than for pregnancy, only in the monopolar case, with low standard deviation in both cases. The *H* method shows a higher coupling for pregnancy than for the labor group with relatively low standard deviations in both monopolar and bipolar cases. All methods give lower coupling in the bipolar (**Figure 3.9** (a)) than the monopolar (**Figure 3.9** (b)) case for both groups.

It is not surprising to obtain such results for *GC* since this linear method cannot deal with the non linear non stationary characteristics of the EHG signal, as shown by the work on synthetic

signals (**Figure 3.8** (e-f)). On the other hand we are surprised by the results obtained when using h^2. Indeed h^2 did not demonstrate a significant difference between labor and pregnancy, even if it increases slightly from pregnancy to labor. *H* gave the most unexpected result, since its value decreases from pregnancy to labor.

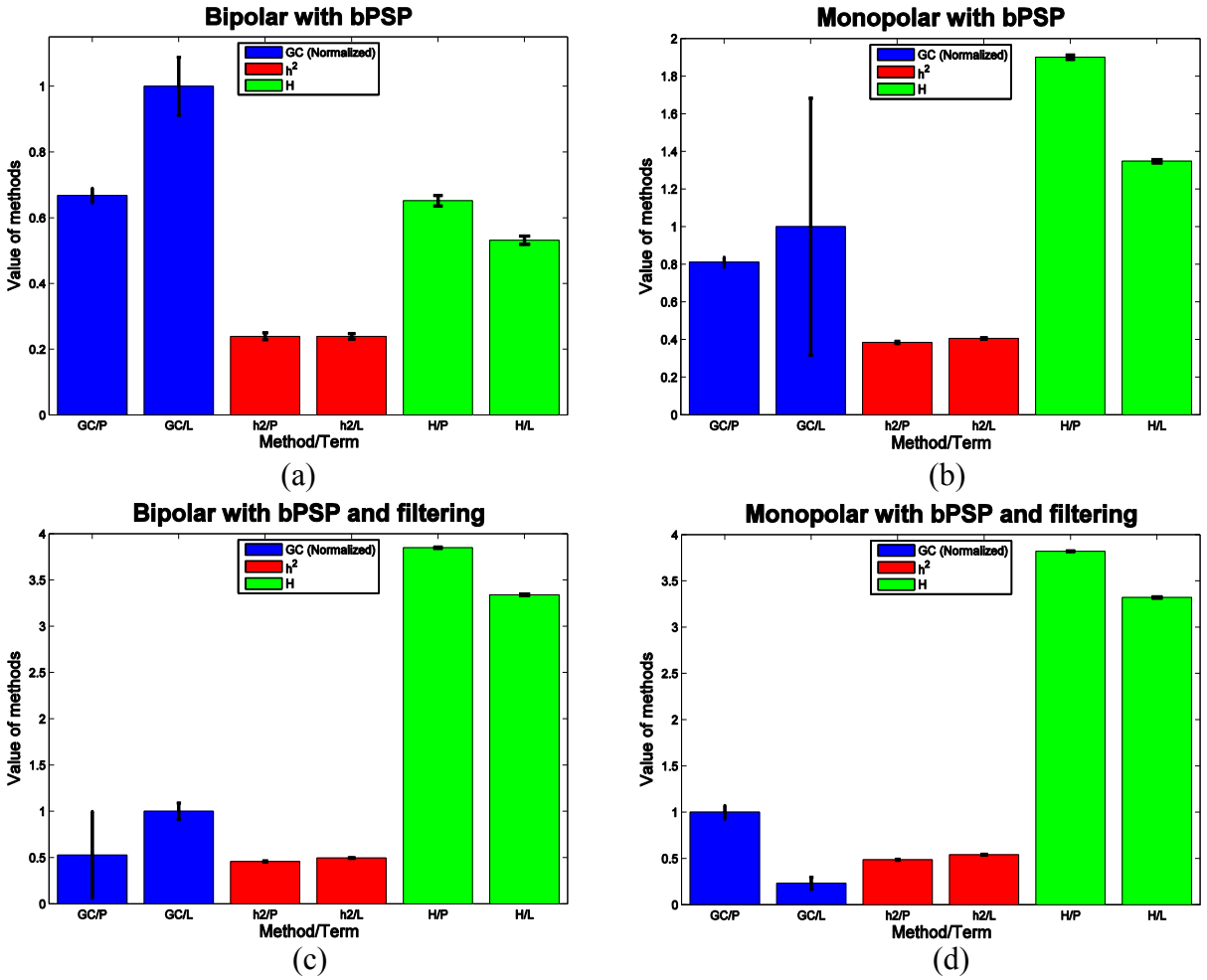

Figure 3.9: Estimated coupling difference between pregnancy and labor contractions estimated by h^2, *H*, and *GC* applied with *bPSP* using bipolar (a) and monopolar (b) uterine EMG signals. And with *bPSP* and filtering together using bipolar (c) and monopolar (d) uterine EMG signals; method/P (method/L) means results obtained for a given method on pregnancy (respectively Labor) group.

A well-known hypothesis is that the propagation of EHG is more related to the low frequency components (FWL) of the EHG signal [42]. Therefore, in an attempt to improve the results, we try to filter the EHG to isolate the low frequency band (0.1Hz-0.3Hz) by using a Butterworth filter, as a preprocessing step, before applying our methods with *bPSP*. The results obtained are shown for bipolar (**Figure 3.9** (c)) and monopolar (**Figure 3.9** (d)) signals.

In general, the estimated coupling values increase after filtering when compared to results in **Figure 3.9** (a-b). We note that the filtering reversed the result for *GC* for monopolar signals (**Figure 3.9** (d)), since its value now decreases from pregnancy to labor. For the h^2 method, the difference between pregnancy and labor increases when compared to **Figure 3.9** (a-b). To test the statistical significance of the obtained differences, we apply a simple two tails student t-test for h^2 results with and without filtering, but with *bPSP*, in bipolar and monopolar cases. It is clear from **Table 3.3** that filtering makes pregnancy/labor difference more significant, for both monopolar and bipolar cases (**: p<1%). It is also clear that the use of monopolar measurement type is better than the bipolar one, since h^2 yields better significant difference both with and without filtering in the monopolar case.

Table 3.3: *P*-VALUE Obtained by Student t-test for h^2 Method

	Without filtering		With Filtering	
Method	Bipolar	Monopolar	Bipolar	Monopolar
h^2	0.9796	0.1873	0.0068^{**}	$9.7105e^{-05**}$

H always decreases from pregnancy to labor even after filtering, in both the bipolar and monopolar cases. We know that *H* computes the synchronization in a phase space (detailed in chapter 2), which is highly influenced by the nonlinearity (chaotic characteristic) and the complexity of the signals. We know also that the complexity and nonlinearity of the EHG signals increase when going from pregnancy to labor [43]. To explain the unexpected results given by *H,* we then go back to synthetic signals. We apply the three methods on coupled signals generated using a bivariate version of the same NLNS Rössler model, but by changing the dissipative parameter *c* that controls the model chaotic characteristics.

Figure 3.10 presents the evolution of all the methods with changing chaoticity degree *c* from 2 to 10. We notice that *H* decreases when the chaoticity of signals increases, opposite to h^2 behavior as shown in **Figure 3.10**. *GC* does not show any monotonic evolution. This result could explain why *H* method always decreases from pregnancy associated to non-chaotic EHG (almost linear, non complex), to labor associated to chaotic EHG (nonlinear, complex), even when using *bPSP* and filtering.

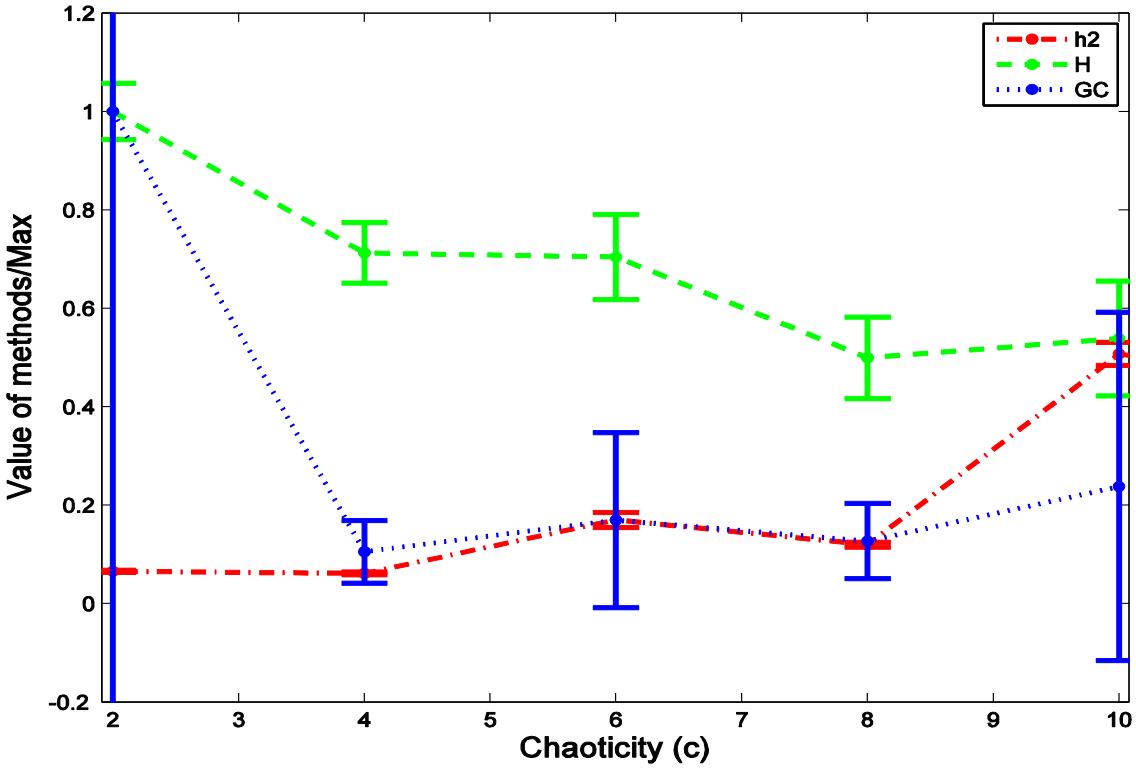

Figure 3.10: Evolution of h^2, H, and GC methods with variable chaoticity of signals generated from bivariate Rössler model. Bars represent the standard deviation.

Figure 3.11 presents the connectivity matrices and the direction maps, for the results obtained by averaging the coupling estimated using Filtered Windowed h^2 (FW-h^2) between all channel combinations of all monopolar EHG signals obtained from 18 women, in both pregnancy (mean of FW-h^2 results on all WBL) and labor groups. After verification of their Gaussian distributions, a threshold of $m+2\sigma$ was applied to the result in order to remove insignificant coupling, where m is the mean of the correlation matrix and σ its standard deviation. We did not use bipolar EHG due to the direction bias induced by bipolarization [38].

We can make the same observation as in **Figure 3.7** when comparing the 3 WBL to labor using h^2, but with no preprocessing. We can notice that the correlation for the pregnancy group (**Figure 3.11** (a)) appears to be random, whereas the correlation matrix during labor (**Figure 3.11** (b)) is more regular. The row and the column associated to channel 9 divide the matrix in four more or less active regions. We can notice, for each region, a high interaction and correlation between the channels, with in general, a higher connectivity for labor than for pregnancy.

In terms of direction, we see in **Figure 3.11** (c) that for pregnancy the arrows point in all directions (propagation in the entire matrix) without any dominant direction. During labor in

Figure 3.11 (d), the arrows also point in all the directions but with a dominant direction towards the bottom (node 3, 4, 7, 8, 11, and 12) of the matrix (towards the cervix), compared to a lower concentration toward the top of the matrix (node 5, 9 and 13). A higher graph density is also obvious for labor than pregnancy using FW-h^2 method, which means a more complex connectivity for labor than pregnancy.

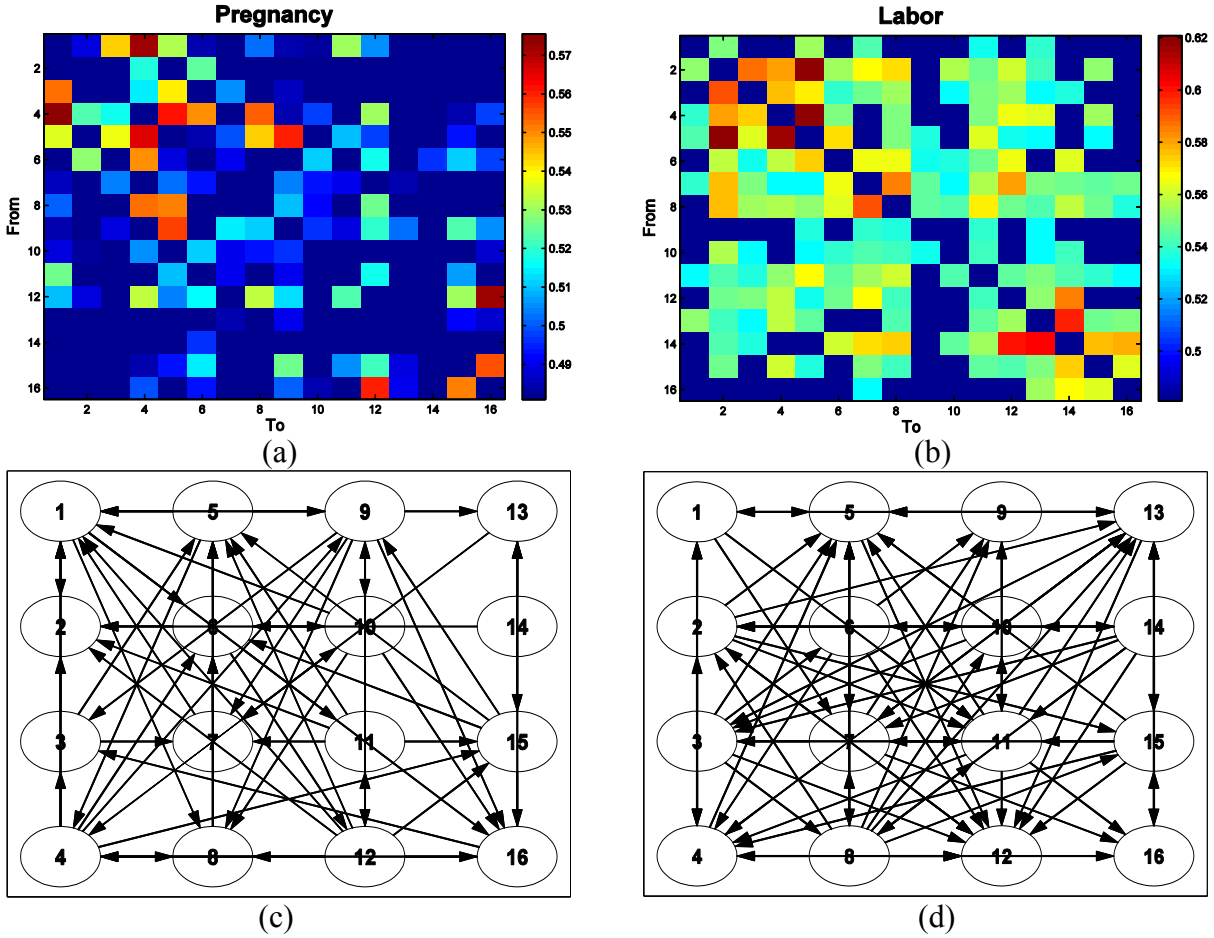

Figure 3.11: Quantity (a) and direction (c) of information flow for pregnancy, and quantity (b) and direction (d) of information flow for labor, obtained between all combinations of EHG channels by using the FW-h^2 method.

3.4 Discussion

In the first part of the study in this chapter, three widely known connectivity and directionality measures (h^2, H and GC) were tested on synthetic signals generated by a two-dimensional coupled nonlinear stationary Rössler model. We analyzed quantitatively these three different methods in order to test their sensitivity to the change in coupling and direction of propagation.

These measures were first applied to the synthetic Rössler model with increasing coupling to test their abilities to follow the coupling variation. h^2 was the best method among the three to detect and follow the coupling. However, *GC* shows poor evolution for low coupling values and then decreases after $C = 0.7$. *H* did demonstrated no evolution with increasing coupling value. Our results confirm those obtained by Ansari et al. [44] who found that h^2 is the best method for evaluating coupling variation among all the studied methods. However Ansari measured only the strength of coupling whereas, in our study we also estimated the ability of the methods to correctly indicate the direction of coupling. The performance of *GC* is expected since its linear characteristics cannot deal with the nonlinearity of signal model. At the opposite, the performance of *H* method was not expected. They may be due to *H* high dependency on the chaotic characteristics of the model, as shown in the results of Part 2. All methods presented similar variability regarding their standard deviation.

The h^2 and *GC* methods were able to estimate the correlation between the signals x_1 and y_1 (**Figure 3.4** (top)) with respect to the direction change (**Figure 3.4** (middle)), as well as to indicate the correct direction (**Figure 3.4** (bottom)). The *H* method, however, failed to detect the correct direction and indicated the opposite of the true direction, when the methods were applied to the same model with an inversion of the coupling direction of a part of the signal, with a given level of coupling (section 2.3.1.1).

To summarize our findings on the stationary bivariate Rössler synthetic signals, h^2 was found to be sensitive to both coupling and direction variation whereas *GC* was found to be sensitive to direction changes and slightly sensitive to coupling changes. *H* was insensitive to both coupling and direction changes. We therefore selected h^2 as the most robust and appropriate method to be applied to simulated signals generated by the physiological model of EHG developed by our team.

The new physiological model is supposed to simulate real signals better than the Rössler model. However the coupling degree between its output signals cannot be controlled as for Rössler model. In case of a simulated planar propagation, h^2 evidenced the correct direction related to the signal propagation, but with a bi-directionality between adjacent channels. This is due to the simultaneous presence of two propagating waves under the electrode matrix. In the circular propagation case, the direction of arrows is towards the center with some shifting to the left and the top. This concentration to the center is related to the presence of 2 AP waves inducing that the previous action potential should explain the next one generated at the

center (**Figure 3.5** (b)). The shifting comes from the edge effects. Indeed, the action potential encounters the left and the top edges before the right and the bottom ones (**Figure 3.5** (b)). Hence the previous action potential explains the top and the left of the new action potential before the bottom and the right one. This phenomenon is expressed by a shifting in the direction map.

The synchronization between channels is restricted to the diagonal in the planar case because the propagation is only longitudinal. Thus the connection is only in one direction (between electrodes on the same line). In the case of circular propagation, the synchronization is propagated through the whole matrix. In this case, the electrodes are recruited by the waves in all the directions at the same time; so the synchronization simultaneously spreads to the whole matrix. The conclusion is that h^2 permitted to evidence properly the main characteristics of the signals propagated by this physiological model.

h^2 was then applied to a dataset of uterine EMG signals. We first studied the evolution of coupling with the term of gestation (WBL). h^2 presented some increase at the beginning, then lost this trend after 3 WBL. This is to be expected since the closer we are to labor, the closer the characteristics of pregnancy contractions will be to labor contractions, and the more difficult the differentiation between them will be. Results of a Kruskal-Wallis statistical test applied to the h^2 results between the different WBL and labor, evidenced a significant difference only between 1, 2, 3, 4 WBL and labor. This could be due to the inter-individual variability of the women included in this study (**Figure 3.12**).

Figure 3.12 show the variability in the behavior of h^2 applied individually to each of the 6 women measured longitudinally that is at different pregnancy terms. Therefore when we take the mean of all contractions measured on all women at each WBL we cannot find the expected increase due to the huge inter-individual variability evidenced **Figure 3.12**.

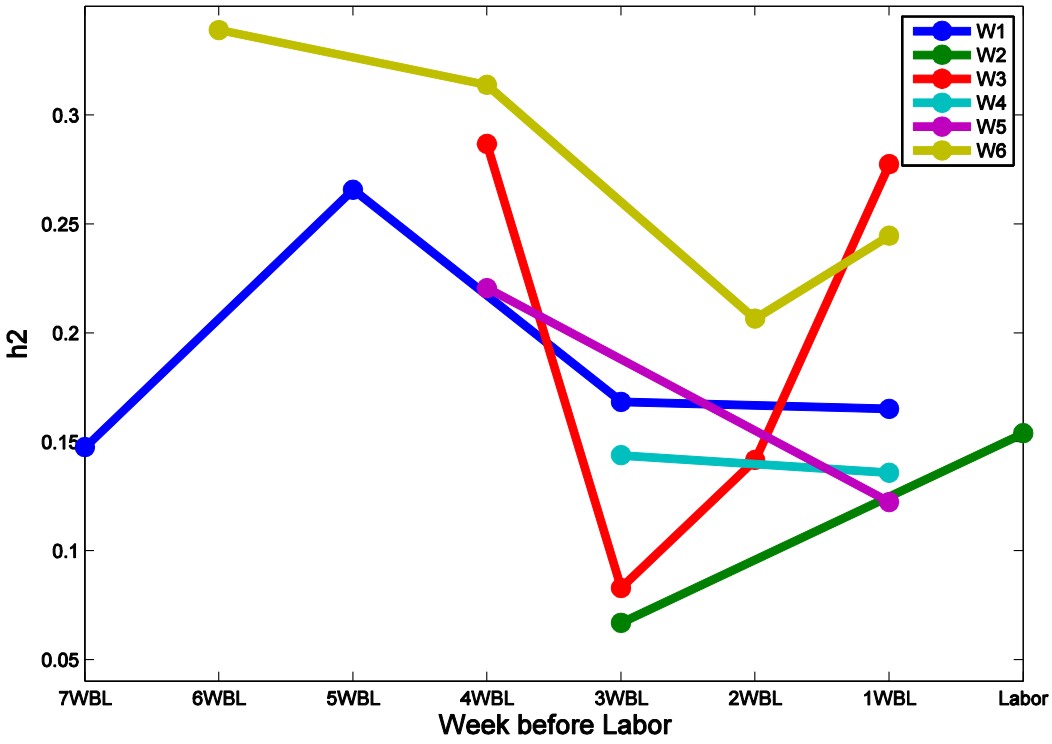

Figure 3.12: Evolution of h^2 applied on the 6 women, who were measured longitudinally on more than one term, in function of WBL.

Finally, we monitor the pregnancy by following the changes in the matrix of synchronization and in the map of direction for signals recorded at 3 WBL, 2 WBL, 1 WBL and during labor by using h^2. Results demonstrated an increase in synchronization and a more regular pattern of synchronization (4 highly correlated regions), as well as a higher concentration of direction toward the cervix, when going from pregnancy to labor. This is in agreement to our previous results [10, 17, 45].

To sum up, the main findings of the first part of this study are the following: (i) the H method is insensitive to varying signal coupling and varying coupling direction, whereas GC is sensitive to direction variation and slightly sensitive to coupling variation; (ii) h^2 reveals the right coupling and direction when used with the physiological model; (iii) h^2 did not display a significant increase related to term; (iv) the evolution of h^2 with WBL is highly affected by the inter-individual variability; (v) in general there is an increase in the regularity of coupling and the direction is more focused toward the cervix when going from pregnancy to labor.

Our next aim in the Part 2 of this study was to improve the performance of the methods used by compensating for the nonstationarity of the signals (such as computing methods in

predefined segments), and by focusing on FWL component, which is supposed to be more related to the propagation of EHG signals.

Therefore, the same connectivity measures (h^2, H and GC) as used in the first part, were tested in the second part on synthetic signals generated this time by a four-dimensional coupled NLNS Rössler model. We analyzed quantitatively these three different methods in order to test the effect of nonstationarity on direction estimation, and the improvement induced by *bPSP* approach effect on direction estimation for these NLNS signals.

The general synchronization (H) method was shown to be the most efficient method without using *bPSP* among the 3 methods since it has the lowest direction error (1 out of 4), **Figure 3.8** (c). h^2 has an intermediate performance since it has 3 out of 4 direction errors. GC is the worst method since it did not detect any of the correct direction (4 out of 4 direction errors). The bPSP approach corrected the errors in the estimations of directions for h^2 and H thus giving same performance for both methods, whereas GC still have a 2 out of 4 direction errors, even after *bPSP*.

On real signals Hassan et al. [45] used h^2 to process bipolar signals recorded on one pregnancy contraction and one labor contraction, and on one women measured longitudinally at 3 terms. They obtained a good pregnancy/labor differentiation with an increase from pregnancy to labor. When we apply our three methods including h^2 on our bigger database, h^2 and GC did not demonstrate any monotonic increasing behavior from pregnancy to labor. H methods decreased when going from pregnancy to labor, as shown in **Figure 3.13**.

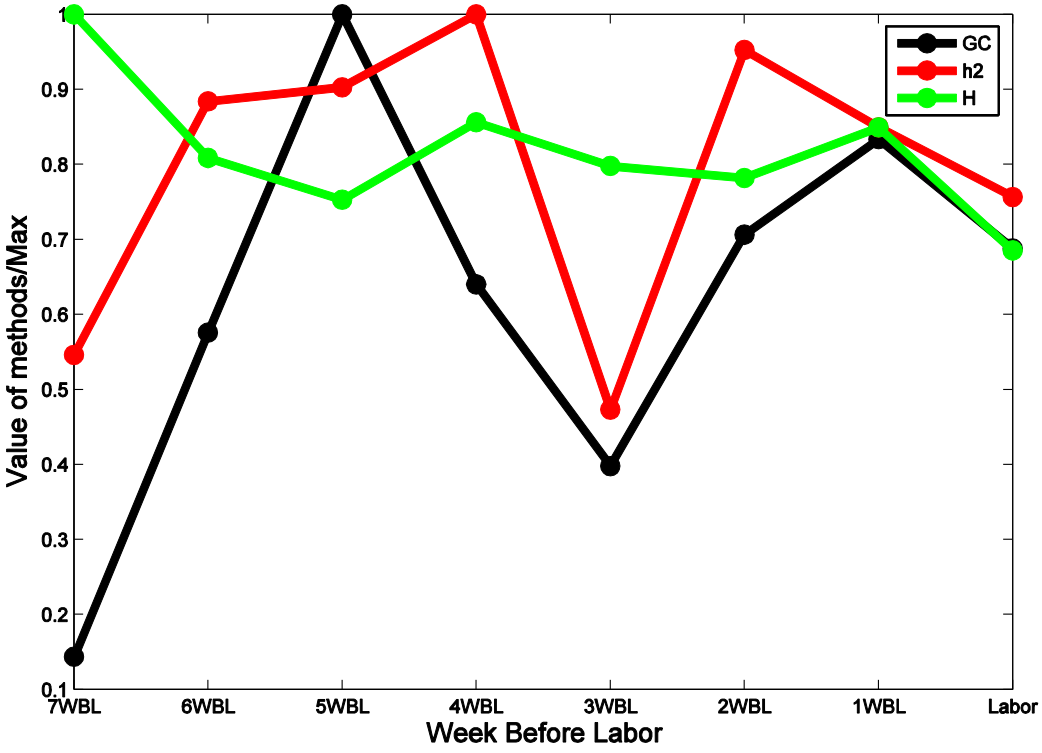

Figure 3.13: Evolution of methods with WBL on our bigger database without any pre-processing.

Terrien et al. applied the *bPSP* segmentation algorithm on monkey EHG signals. They also investigated the filtering of the monkey signals into higher frequency band (FWH), but their aim was to see the effect on h^2 results inside the contractions not to study any pregnancy/labor differentiation [29]. However, Terrien et al. investigated in another study the effect of filtering into low frequency band (FWL) on the pregnancy/labor classification rate by using h^2. Whereas in this study they use the filtering solely without *bPSP* and on bipolar signals, not on monopolar signals as in our case [11]. Their results are in agreement with our results since, after filtering, they found that the significance of pregnancy/labor differentiation increases. Finally, Terrien et al. [46] presented a way to correct the bias of h^2 by using surrogates. This approach worked very well on monkey EHG signals. Using surrogates is however very time consuming in terms of computation. Furthermore, using surrogates did not improve our results (evolution with WBL) on human EHG signals (**Figure 3.14**).

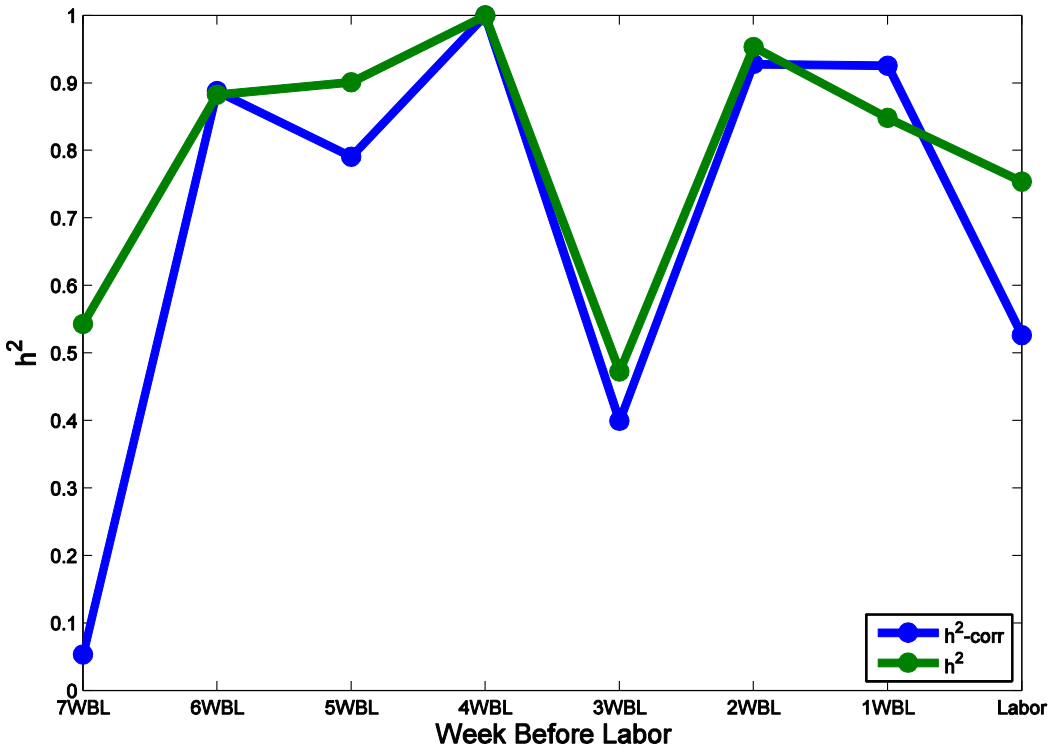

Figure 3.14: Evolution of h^2 without (green) and with (blue) correction in function of WBL.

Therefore, we propose a Filtering-Windowing approach as a suitable method for this signal, since the EHG is a non-stationary signal with propagation mainly related to low frequencies. These two characteristics should be taken into account by *bPSP* and FWL filtering respectively. We apply our approach on bipolar as well as monopolar signals, since, as we know, the way of measuring signals affects the detection and the quality of these signals and consequently the results of the applied methods [30]. Indeed, the bipolarization of signals induces some bias for the direction computation.

As we see in **Figure 3.9**, the *bPSP* approach did not improve the results of *GC* as it still gives non-significant difference between pregnancy and labor due to the high variance (especially for the monopolar case). The results of h^2 was improved slightly by *bPSP* alone, since it increased instead of decreasing (without *bPSP*), when going from pregnancy to labor. But the difference was non-significant and small especially in bipolar case. *H* was not improved by *bPSP* since it still decreased in both monopolar and bipolar cases. These results are in agreement with the ones obtained on synthetic signals.

The second step of our approach was filtering signals between 0.1 and 0.3 Hz (low frequency) associated with the segmentation of signals. This step makes the difference between pregnancy and labor more significant (see **Figure 3.9** and **Table 3.3**). We suppose that this is

due to the fact that filtering reducing the EHG frequency content to FWL band, we focus on the more propagated part of this signal [42]. Furthermore, when we checked the PSD of our EHG signals, we noticed that their frequency content is strongly affected by the women‟s weight or body mass index. For example **Figure 3.15**, since the fat in the abdomen for a heavy woman has a strong low pass filtering effect (**Figure 3.15** (right)), for a thin women the EHG frequency band is larger (**Figure 3.15** (left)).

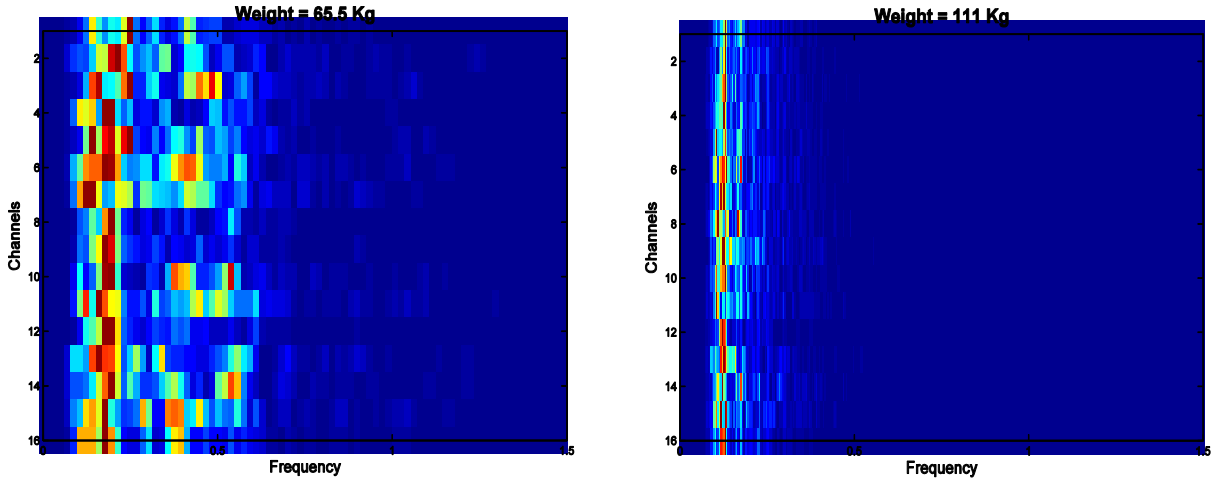

Figure 3.15: Channel-frequency plot for one contraction of thin women (65.5 Kg) at 38 week of gestation (left), and for another contraction of heavy women (111 Kg) at 40 week of gestation with weight = 111 Kg (right).

This fat filtering effect is bypassed by reducing and thus homogenizing the bands for all the EHG measurements (FWL filtering), and making the measure independent of the woman‟s weight. This filtering thus increased the significance difference between pregnancy and labor groups.

The use of monopolar recordings is better than bipolar ones according to **Table 3.3**, since the significance difference between pregnancy and labor group with and without filtering is better for monopolar than bipolar recordings.

H always decreased in all cases from pregnancy to labor. This could be due to the fact that *H* is highly influenced by chaoticity (nonlinearity and complexity) of the signals. Using simulation, we demonstrated (**Figure 3.10**) that *H* decreases when chaoticity increases opposite to h^2. This evolution of EHG from almost linear (pregnancy) to complex (labor) characteristics has been evidenced on real signals. Indeed, uterus goes from an almost

deterministic state during pregnancy to a chaotic (nonlinear and complex) state during labor as shown in [43].

Finally we compared the matrix of connectivity and the map of direction for signals recorded during pregnancy and labor by using FW-h^2. Results show an increase in coupling and a more regular pattern of synchronization between the 16 unipolar nonlinear, complexsignals (4 highly correlated regions) as well as a higher concentration of direction towards the cervix for labor than for pregnancy which is coherent with our previous studies. We identify also a higher graph density (number of arrows) for labor than pregnancy, which represents a more complex pattern in labor than in pregnancy which agrees well with results in [43]. This increase in coupling and synchronization during labor induces fast contractions of the whole uterus. The concentration of coupling direction towards the cervix may help in pushing the baby out.

3.5 Conclusion and perspectives

The above results permit us to conclude that the h^2 method is a good candidate for measuring EHG coupling and direction as it is able to correctly detect them for synthetic and simulated EHG signals. Due to subject variability, h^2 did not show a monotonic increasing behavior along with WBL. But when we perform a longitudinal study from 3 WBL to labor, the coupling matrix show more regular pattern for labor than for pregnancy. An interesting evolution happens to the direction when going from pregnancy to labor: it becomes more highly concentrated toward the cervix as labor progresses.

We can also conclude that in our case (application to EHG) two preprocessing steps (FW-h^2) permit to increase significantly h^2 performance. When using FW-h^2, labor group demonstrates higher coupling than pregnancy, which is in agreement with the literature. Also, when using FW-h^2, the density of the direction map is higher for the labor than for the pregnancy group. The H method performance is highly influenced by the nonlinearity of EHG signals and therefore it requires further investigation. Monopolar recordings are better than bipolar one. We think that these findings are likely to be valuable to help us to solve the problem of the preterm labor detection.

A promising next step of the work would be to extract parameters from the connectivity graphs by using a graph theory based approach (considering the electrodes as nodes and the

connectivity lines as edges of the graph). Different parameters such as density of graphs and ingoing and outgoing edges for each node, can be used to quantify the uterine connectivity, and thus help us to get new parameters to discriminate between pregnancy and labor contractions, which is the ultimate goal of our project.

References

[1] M. Rosenblum, and J. Kurths, "Analysing synchronization phenomena from bivariate data by means of the Hilbert transform". in *Nonlinear analysis of physiological data*. Springer Berlin: Heidelberg, 1998: pp. 91-99.

[2] J. Sun, X. Hong, and S. Tong, "Phase synchronization analysis of EEG signals: an evaluation based on surrogate tests," *IEEE Trans. Biomed. Eng.*, vol. 59, no. 8, pp. 2254-2263, Aug. 2012.

[3] K. Majumdar, "Constraining minimum-norm inverse by phase synchronization and signal power of the scalp EEG channels," *IEEE Trans. Biomed. Eng.*, vol. 56, no. 4, pp. 1228-1235, Apr. 2009.

[4] A. Porta, V. Bari, F. Badilini, E. Tobaldini, T. Gnecchi-Ruscone, and N. Montano, "Frequency domain assessment of the coupling strength between ventricular repolarization duration and heart period during graded head-up tilt," *Journal of Electrocardiology*, vol. 44, no. 6, pp. 662-668, Nov.-Dec. 2011.

[5] E. Oczeretko, J. Swiatecka, A. Kitlas, T. Laudanski, and P. Pierzynski, "Visualization of synchronization of the uterine contraction signals: running cross-correlation and wavelet running cross-correlation methods," *Medical engineering & physics*, vol. 28, no. 1, pp. 75, 2006.

[6] A. Diab, M. Hassan, J. Laforet, B. Karlsson, and C. Marque, "Estimation of Coupling and Directionality between Signals Applied to Physiological Uterine EMG Model and Real EHG Signals," in *Proc. XIIIMediterranean Conference on Medical and Biological Engineering and Computing 2013*, Sevilla, Spain, Sep. 2014, pp. 718-721.

[7] A. Diab, M. Hassan, B. Karlsson, and C. Marque, "Effect of decimation on the classification rate of nonlinear analysis methods applied to uterine EMG signals," *IRBM*, vol. 34, no. 4-5, pp. 326-329, Oct. 2013.

[8] B. Karlsson, M. Hassan, and C. Marque, "Windowed multivariate autoregressive model improving classification of labor vs. pregnancy contractions," in *Proc. IEEE Eng. Med. Biol. Soc. Conf.* 2013, Osaka, Japan, Jul. 2013, pp. 7444-7447.

[9] P. F. Panter, "Modulation, noise, and spectral analysis: applied to information transmission," New York: *McGraw-Hill*, 1965, pp. 767.

[10] M. Hassan, J. Terrien, C. Muszynski, A. Alexandersson, C. Marque, and B. Karlsson, "Better pregnancy monitoring using nonlinear propagation analysis of external uterine electromyography," *IEEE Trans. Biomed. Eng.*, vol. 60, no. 4, pp. 1160-1166, Apr. 2013.

[11] J. Terrien, T. Steingrimsdottir, C. Marque, and B. Karlsson, "Synchronization between EMG at Different Uterine Locations Investigated Using Time-Frequency Ridge Reconstruction: Comparison of Pregnancy and Labor Contractions," *EURASIP J. Adv. Signal Process.*, vol. 2010, pp. 1-10, Jun. 2010.

[12] C. Alvarez, and S. Reynolds, "A better understanding of uterine contractility through simultaneous recording with an internal and a seven channel external method," *Surgery, gynecology & obstetrics*, vol. 91, no. 6, pp. 641-650, Dec. 1950.

[13] T. Y. Euliano, D. Marossero, M. T. Nguyen, N. R. Euliano, J. Principe, and R. K. Edwards, "Spatiotemporal electrohysterography patterns in normal and arrested labor," *Amer. J. Obstet. Gynecol.*, vol. 200, no. 1, pp. 54 e1–54 e7, Jan. 2009.

[14] W.J. Lammers, H. Mirghani, B. Stephen, S. Dhanasekaran, A. Wahab, M.A.H. Al Sultan, and F. Abazer, "Patterns of electrical propagation in the intact pregnant guinea pig uterus," *Am. J. Physiol. Regul. Integr. Comp. Physiol.*, vol. 294, no. 3, pp. R919-28, Mar. 2008.

[15] C. Rabotti, M. Mischi, J.O.E.H van Laar, G.S Oei, and J.W.M Bergmans, "Inter-electrode delay estimators for electrohysterographic propagation analysis," *Physiol. Meas.*, vol. 30, no.8, pp. 745-61, Jun. 2009.

[16] E. Mikkelsen, P. Johansen, A. Fuglsang-Frederiksen, and N. Uldbjerg, "O452 propagation direction and velocity of uterine EMG signals during labor," *International Journal of Gynecology & Obstetrics*, vol. 119, pp. S421, Oct. 2012.

[17] A. Diab, M. Hassan, S. Boudaoud, C. Marque, and B. Karlsson, "Nonlinear estimation of coupling and directionality between signals: Application to uterine EMG propagation," in *Proc. IEEE Eng. Med. Biol. Soc. Conf. 2013*, Osaka, Japan, Jul. 2013, pp. 4366-4369.

[18] E. Mikkelsen, P. Johansen, A. Fuglsang-Frederiksen, and N. Uldbjerg, "Electrohysterography of labor contractions: propagation velocity and direction," *Acta obstetricia et gynecologica Scandinavica*, vol. 92, no. 9, pp. 1070-1078, Sept. 2013.

[19] L. Lange, A. Vaeggemose, P. Kidmose, E. Mikkelsen, N. Uldbjerg, and P. Johansen, "Velocity and Directionality of the Electrohysterographic Signal Propagation," *PLoS ONE*, vol. 9, no. 1, pp. e86775, Jan. 2014.

[20] J. Pijn, and F. Lopes Da Silva, "Propagation of electrical activity: nonlinear associations and time delays between EEG signals," in *Basic Mechanisms of the EEG*. Birkhäuser Boston, 1993, pp. 41-61.

[21] J. Arnhold, P. Grassberger, K. Lehnertz, and C.E. Elger, "A robust method for detecting interdependences: application to intracranially recorded EEG," *Phys D: Nonlin Phen*, vol. 134, no. 4, pp. 419-30, Dec. 1999.

[22] C. W. J. Granger, "Investigating causal relations by econometric models and cross-spectral methods," *Econometrica: Journal of the Econometric Society*, vol.37, no. 3, pp. 424-438, Jul. 1969.

[23] J. Laforet, C. Rabotti, J. Terrien, M. Mischi, C. Marque, “Toward a Multiscale Model of the Uterine Electrical Activity,” *IEEE Trans. Biomed. Eng.*, vol. 58, no. 12, pp. 3487-3490, Dec. 2011.

[24] C. Marque and J. Duchêne, “Human abdominal EHG processing for uterine contraction monitoring,” in *Applied Sensors*. Boston, MA: Butterworth, 1989, pp. 187–226.

[25] M. Hassan, J. Terrien, B. Karlsson, and C. Marque, “Interactions between Uterine EMG at different sites investigated using wavelet analysis: Comparison of pregnancy and labor contractions,” *EURASIP J. Adv. Signal Process.*, vol. 2010, no. 17, pp. 1–10, Feb. 2010.

[26] J. G. Planes, J. P. Morucci, H. Grandjean, and R. Favretto, “External recording and processing of fast electrical activity of the uterus in human parturition,” *Med. Biol. Eng. Comput.*, vol. 22, no. 6, pp. 585–591, Nov. 1984.

[27] M. Lucovnik, W. L. Maner, L. R. Chambliss, R. Blumrick, J. Balducci, Z. Novak-Antolic, and R. E. Garfield, “Noninvasive uterine electromyography for prediction of preterm delivery,” *Amer. J. Obstet. Gynecol.*, vol. 204, no. 3, pp. 228–238, Mar. 2011.

[28] J. Terrien, M. Hassan, C. Marque, and B. Karlsson, “Use of piecewise stationary segmentation as a pre-treatment for synchronization measures,” in *Proc. IEEE Eng. Med. Biol. Soc. Conf.* 2008, Vancouver, BC, Aug. 2008, pp. 2661-2664.

[29] J. Terrien, G. Germain, C. Marque, and B. Karlsson, “Bivariate piecewise stationary segmentation; improved pre-treatment for synchronization measures used on non-stationary biological signals,” *Medical engineering & physics*, vol. 35, no. 8, pp. 1188-96, Aug. 2013.

[30] J. Alberola-Rubio, G. Prats-Boluda, Y. Ye-Lina, J. Valerob, A. Peralesb, and J. Garcia-Casado, “Comparison of non-invasive electrohysterographic recording techniques for monitoring uterine dynamics,” *Medical engineering & physics*, vol. 35, no. 12, pp. 1736-1743, Dec. 2013.

[31] M. G. Rosenblum, A. S. Pikovsky, and J. Kurths, “Phase synchronization of chaotic oscillators,” *Phys Rev Lett*, vol. 76, no. 11, pp. 1804-1807, Mar. 1996.

[32] P. Borgnat, P. Flandrin, P. Honeine, and C. Richard, “Testing stationarity with surrogates: A time-frequency approach,” *IEEE Trans. Sig. Process*., vol. 58, no. 7, pp. 3459-3470, Jul. 2010.

[33] M. Winterhalder, B. Schelter, W. Hesse, K. Schwab, L. Leistritz, D. Klan, R. Bauer, J. Timmer, and H. Witte, “Comparison of linear signal processing techniques to infer directed interactions in multivariate neural systems,” *Signal Process.*, vol. 85, no. 11, pp. 2137-60, Nov. 2005.

[34] C. Rabotti, M. Mischi, L. Beulen, S. Oei, and J. Bergmans, “Modeling and identification of the electrohysterographic volume conductor by highdensity electrodes,” *IEEE Trans. Biomed. Eng.*, vol. 57, no. 3, pp. 519–527, Mar. 2010.

[35] L. Mesin and R. Merletti, “Distribution of electrical stimulation current in a planar multilayer anisotropic tissue,” *IEEE Trans. Biomed. Eng.*, vol. 55, no. 2, pp. 660–670, Feb. 2008.

[36] S. Gabriel, R. Lau, and C. Gabriel, "The dielectric properties of biological tissues: II. Measurements in the frequency range 10 Hz to 20 GHz," *Phys. Med. Biol.*, vol. 41, pp. 2251–2269, Nov. 1996.

[37] B. Karlsson, J. Terrien, V. Gudmundsson, T. Steingrimsdottir, and C. Marque, "Abdominal EHG on a 4 by 4 grid: mapping and presenting the propagation of uterine contractions," in *Proc. 11th Mediterranean Conference on Medical and Biological Engineering and Computing*, 2007, Ljubljana, Slovenia, 2007, pp. 139-143.

[38] M. Hassan, S. Boudaoud, J. Terrien, B. Karlsson, and C. Marque, "Combination of Canonical Correlation Analysis and Empirical Mode Decomposition applied to denoise the labor electrohysterogram," *IEEE Trans. Biomed. Eng.*, vol. 85, no. 9, pp. 2441-2447, Sep. 2011.

[39] E. Pereda, R.Q. Quiroga, and J. Bhattacharya, "Nonlinear multivariate analysis of neurophysiological signals," *Progress in Neurobiology*, vol. 77, no. 1-2, pp. 1-37, Sep.-Oct. 2005.

[40] F. Wendling, F. Bartolomei, J. J. Bellanger, and P. Chauvel, "Interpretation of interdependencies in epileptic signals using a macroscopic physiological model of the EEG," *Clin Neurophysiol*, vol. 112, no. 7, pp. 1201-1218, Jul. 2001.

[41] P. Carré, and C. Fernandez, "Research of stationary partitions in nonstationary processes by measurement of spectral distance with the help of nondyadic Malvar's decomposition," in *IEEE-SP International Symposium on Time-Frequency and Time-Scale Analysis*, Pittsburgh, PA, USA, Oct. 1998, pp. 429 - 432.

[42] D. Devedeux, C. Marque, S. Mansour, G. Germain, and J. Duchêne, "Uterine electromyography: a critical review," *Am J Obstet Gynecol*, vol. 169, no. 6, pp. 1636-53, Dec. 1993.

[43] M. Hassan, J. Terrien, B. Karlsson, and C. Marque, "Comparison between approximate entropy, correntropy and time reversibility: Application to uterine electromyogram signals," *Medical engineering & physics*, vol. 33, no. 8, pp. 980-986, oct. 2011.

[44] K. Ansari-Asl, L. Senhadji, J. J. Bellanger, and F. Wendling, "Quantitative evaluation of linear and nonlinear methods characterizing interdependencies between brain signals," *Physical review E*, vol. 74, no. 3, pp. 031916, Sept. 2006.

[45] M. Hassan, J. Terrien, B. Karlsson, and C. Marque, "Spatial analysis of uterine EMG signals: evidence of increased in synchronization with term," in *Proc. IEEE Eng. Med. Biol. Soc. Conf.* 2009, Minneapolis, USA, Sep. 2009, pp. 6296-6299.

[46] J. Terrien, M. Hassan, G. Germain, C. Marque, and B. Karlsson, "Nonlinearity testing in the case of non Gaussian surrogates, applied to improving analysis of synchronicity in uterine contraction," *Proc. IEEE Eng. Med. Biol. Soc. Conf.*, Minneapolis, USA, Sep. 2009, pp. 3477-80.

Chapter 4: Uterine EMG source localization

One of the primary concerns in electrophysiology is the non-invasive localization of the origin of the measured uterine EMG (electrohysterogram, EHG) activity. Methods for localization of unknown sources from their effect far away are termed inverse methods and the solutions that they provide inverse solutions. We tackle in this chapter the problem of uterine source localization. Source localization has been widely applied to EEG [1-4], MEG [5-7], but to our knowledge it has never been applied to EHG signal. The work presented in this chapter is therefore the first attempt to localize uterine EMG sources. The methods which were developed to solve the inverse problem are divided into two main families, mainly the non parametric (over-determined) and parametric (under-determined) methods [8]. For non-parametric methods, we find various techniques including minimum norm estimates and their generalizations (LORETA, sLORETA, VARETA, S-MAP, ST-MAP, Backus-Gilbert, LAURA, Shrinking LORETA FOCUSS (SLF), SSLOFO and ALF). For the parametric methods, there are the beamforming techniques, BESA, the subspace techniques such as MUSIC and methods derived from it, the FINES, simulated annealing and computational intelligence algorithms [8]. The main difference between the two is whether a fixed number of dipoles is a priori assumed (parametric) or not (non-parametric).

4.1 Introduction

In our application to EHG, we do not have a priori information on source number, strength and location. Therefore we focused on the non-parametric methods. We begin by testing the basic method of this family, which is the minimum norm estimate (MNE) method.

Source estimation is a general tool for analyzing spatiotemporal dynamics of organs or system. Uterine EMG stand out among the different non-invasive techniques that can be used to study the functionality of the uterus, due to its high temporal resolution. It could permit to observe the dynamics of uterine contractile activity on a time-scale of milliseconds, reflecting synchronous activity of cells within the uterus muscle. EHG can therefore provide a dynamic characterization of uterus activity which is not possible with other direct and indirect modalities presented in chapter 1. Therefore, in this work, we implemented source estimation tool for the uterus electrical activity, using the FieldTrip open-source software [9]. Simulated

Electrohysterogram (EHG) signals were generated with a known source location by using the same electrophysiological multiscale model [10] as used in the previous chapter, in order to validate our implemented source estimation tool. We also tested our source estimation tool, after this validation, on real EHG with unknown uterine sources, recorded with the 4x4 electrode matrix.

The procedure of the EHG source localization deals with two problems: 1) a *forward problem* to find the skin potentials for the current source(s) inside the uterus muscle (definition of the lead-field), 2) an *inverse problem* to estimate the source(s) that fit with the given potential distribution at the skin electrodes [11]. In our case, uterine activity can be estimated from EHG by solving an ill-conditioned inverse problem that is regularized using neuroanatomical, computational, and dynamic constraints [12].

For the forward problem, the boundary element method (BEM) implemented in the FieldTrip open-source software, we needed to define a four compartment model (uterus muscle, abdominal muscle, fat, and skin), based on triangular mesh to represent the geometrical part of the volume conductor. We then used the EHG channels simulated with the multiscale model, with different sources locations, as well as the EHG signals, recorded during different uterus physiological situation (pregnancy, labor), to inversely reconstruct the sources (inverse problem) by using minimum norm estimate method [13, 14] and the lead-field extracted from the forward problem step. Estimated source locations and strengths were reconstructed, and their error was calculated to evaluate this FieldTrip-based source localization algorithm.

4.2 Materials and methods

4.2.1 Data

4.2.1.1 Signals simulated from the EHG multiscale electrophysiological model

We use in this chapter the same electrophysiological model as used in the previous chapter [10]. But in the previous chapter, we were only interested in the signal obtained at the electrodes level to compute the coupling and the directionality between them. In this chapter we are interested in these simulated signals not only as inputs of the inverse problem, but also in the position of their source(s) to validate the source localization process.

The electrical source is a volume current source density. For the volume conductor, we adopt the description in [15]. The volume conductor is considered as made of parallel interfaces

separating the four different abdominal tissues, namely: the myometrium (where the source is located) with conductivity = 0.2 S/m and depth = 0; the abdominal muscle with conductivity 0.2 S/m and 0.4 S/m respectively in the X and Y directions, and thickness = 0.936 cm; fat with conductivity = 0.04 S/m and thickness = 1.132 cm; and skin with conductivity = 0.5 S/m and thickness = 0.2 cm. To limit computation time we only simulate a square of 10x10 cm divided into 204x204 computational elements, of the uterus muscle and the above abdomen conductor volume is simulated. This area is supposed to be near the median axis of the uterus, where the surfaces are supposed to be more or less flat and parallel.

Figure 4.1 presents a representation of the model including the 4 tissue layers, the electrodes placement, and an example for placement of one source at the center of the uterine muscle layer. The volume conductor effect depends on the tissue thicknesses, their conductivities, and the source depth. All the tissues are assumed to be isotropic with the exception of the abdominal muscle. Finally, we assume the source to be close to the myometrium–abdominal muscle interface.

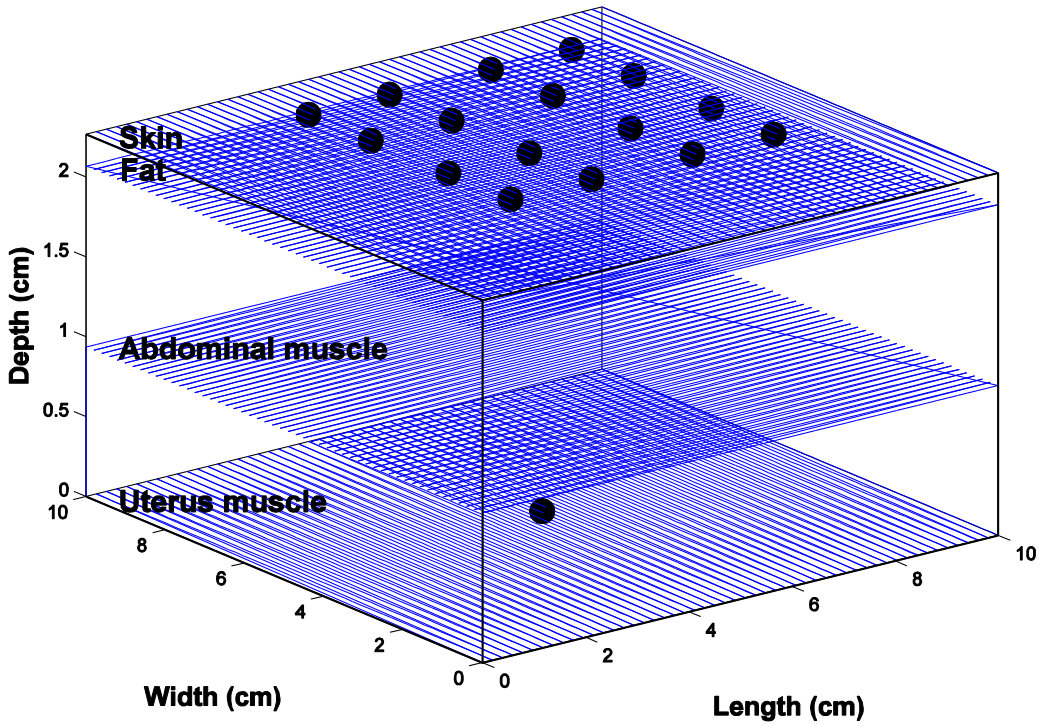

Figure 4.1: The uterus EHG model representation of the volume conductor for the physiological multiscale model, with the four layers (uterine and abdominal muscle, fat and skin). The 16 black disks above the skin layer represent the electrodes. The black disk in the uterus muscle layer represents an example for a source at the center of the uterine muscle.

4.2.1.2 Real signals

As in the previous chapter we use signals recorded by the experimental protocol described in chapter 1. The signals are recorded using 16 monopolar channels of a 4x4 recording matrix

located on the women's abdomen (see [16] for details), and filtered using the CCA-EMD method [17]. We tested our source localization tool on pregnancy and labor signals to see what might be the difference between these two physiological situations in terms of uterine dynamic. Understanding what happens to this uterine dynamic when going from pregnancy to labor has been a question of great interest for a long time.

4.2.2 Methods

4.2.2.1 Forward problem (BEM)

In order to locate the source for the specific activity seen on the abdomen skin, we first have to solve the forward problem [18]. This problem is to define the rules of the signal propagation from the source to the recorded site (here the abdominal skin) [18]. This problem involves calculating the electric potentials generated by known current sources for a given anatomical model.

Forward modeling is done in our case based on a volume-conduction model that describes the geometrical and electrical properties of the tissue in the abdomen above the uterus. The volume conduction often requires a geometrical description of tissue boundaries in the abdomen [19]. The uterus model used in this chapter for EHG analysis assumes that the abdomen above the uterus consists of a set of meshes, triangulated surfaces in 3D-space, representing the uterine muscle, abdomen muscle, fat, and skin. If the conductivities within each of these regions are isotropic and constant, the electric potentials can be expressed in terms of surface integrals. The forward EHG problems can then be solved numerically using a boundary-element method (BEM) [20-22]. We used in this step the same geometrical and electrical definitions that the ones used for the physiological multiscale model (illustrated figure 4.1). The mesh is done with a precision of 51x51 elements.

BEM calculates the potentials/fields of the non-intersecting homogeneous regions bounded by the uterine muscle, abdominal muscle, fat, and skin surface boundaries, each one having a conductivity (σ) values of 0.2, 0.2 and 0.4, 0.04 and 0.33 S/m respectively.

To solve the forward problem we should compute the lead field matrix represented by the following equation:

$$L_{ij} = \frac{1}{4\pi\sigma} \frac{\left(r_{\phi_i} - r_{j_j}\right)}{\left\| r_{\phi_i} - r_{j_j} \right\|^3}$$

where $r_{\Phi i}$, $r_{ji} \in R^{1\times 3}$ are position vectors for the i-th electrode and for the j-th source respectively and $\|\cdot\|$ designates the classical 2-norm. Of course, these relations can be used to compute the potentials in every chosen point of the 3D space. This leadfield (L) matrix which is the result of the forward problem solution is then used to solve the inverse problem.

4.2.2.2 Inverse problem (MNE)

An increasing interest in current-density reconstruction algorithms has occurred during the past few years. All these algorithms have in common that elementary dipoles are distributed on regular grids [23]. The calculation of the strengths and position of these dipoles usually leads to a highly under-determined system of equations - the number of unknown dipole components is greater than the number of electrodes and sensors. Thus, it requires additional mathematical constraints (e.g., minimum norm and variance-weighted minimum-norm) to yield to a unique solution.

A generalized formulation for the minimum-norm solution of the inverse problem with a squared deviation, Δ^2, and the dipole component vector, J, can be written as follows [18]:

$$\Delta^2 = \left|D\left(M - L*J\right)\right|^2 + \lambda^2 \left|C*J\right|^2$$

The data term, $\left|D(M - L*J)\right|^2$, (measuring the closeness of the solution obtained to the data) and the constraining model term, $|C*J|^2$, (measuring the closeness to a given source model) are optimized simultaneously. Both are linked using a regularization parameter, $\lambda = 1e^{-1}$. M is the spatiotemporal measured data matrix (m x n), lead-field matrix L coming from the forward problem (m x c current dipole components), D is an (m x m) weighting matrix of the sensors, and C is a (c x c) weighting matrix of the current dipole components; where m is the channels number, n is signal point number, and c is the number of sources.

Thus, within the minimum norm least-squares (MNLS) framework, the solution that has the minimum power is chosen from the non-unique solution set. This standard solution is known to generate very smooth solutions and favors superficial source distributions, even if the true source is a deeper, more focal, current generator. This is due to the reason that small currents close to the detectors can produce fields of similar strengths than larger currents at greater depths. To compensate for the undesired depth dependency of this approach, the currents can be weighted to account for the lower gains of deeper dipole components (lead-field normalization), which leads to the second method known as sLORETA. However in our case we consider that the myometrium layer to contain only one cell layer and we assume the

source to be close to the myometrium–abdominal muscle interface. Therefore we are not interested in the source depth.

4.3 Results

The same strategy used in the previous chapter is also used here. We will validate our methods on simulated signals in different cases using the electrophysiological model before applying the methods to real signals. In our application to real signal we localize the sources of one pregnancy contraction and one labor contraction recorded on the same woman, to see how the uterine dynamic evolves from pregnancy to labor. In all the figures below we plot the obtained localization on the mesh of the myometrial muscle.

4.3.1 Results on simulated signals

We have simulated three cases of source generation: i) two synchronous sources with circle propagation waveform; ii) two asynchronous sources with circle propagation waveform; iii) a longitudinal bar of sources that propagates longitudinally. This "plane wave" type propagation corresponds to a source similar to the ones in case i), but viewed from a point distant from the source. The results of sources localization are presented **Figure 4.2**(a-b) for the first case (synchronous sources that begin at the same time), **Figure 4.2**(c-d) for the second case (asynchronous sources which have a delay between their onset), and **Figure 4.2**(e-f) for the third case (bar of sources that propagate longitudinally). Each picture of **Figure 4.2** represents the source localization result for a single instant of the signal generated in each case. Subfigures (a), (c) and (e) represent the original sources generated by the multiscale physiological model; subfigures (b), (d) and (f) represent the corresponding sources estimated by our algorithm.

It is clear from **Figure 4.2** that our implemented forward/inverse algorithm is able to localize the given sources in all cases. We can see in **Figure 4.2**(a) and (b) approximately the same wave front shapes, after the collision of the two circle waves generated by the two synchronous sources. After the collision of the original wave fronts, the resulting wave fronts propagate to the corners with no source, **Figure 4.2**(b).

Figure 4.2(c) and (d) also present similar shapes. In **Figure 4.2**(d) a yellow circle shape is first generated by the source propagating from the bottom left corner, represented by the blue disk. The second source generated at the top right corner (**Figure 4.2**(c)), represented by the magenta disk, is also well localized with some error in its position (**Figure 4.2**(d)).

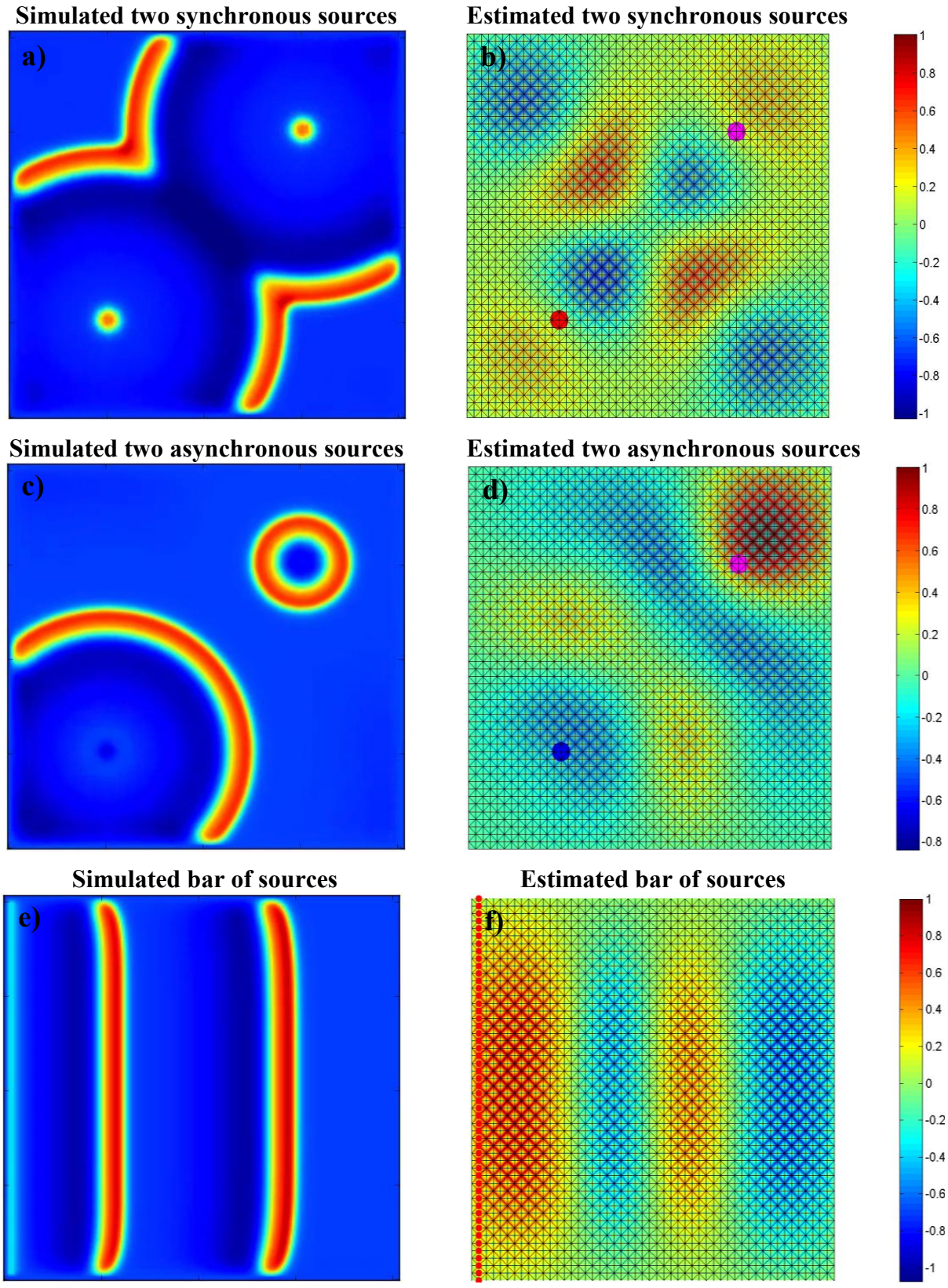

Figure 4.2: Simulation of two synchronous (a), asynchronous (c) and vertical bars (e) sources, and their estimated localization and propagation (b), (d) and (f) respectively, for a single instant. The colored disks in (b) and (d) and the red bar in (f) represent the position of the original source.

In **Figure 4.2**(e) and (f), our method was also able to detect the waves fronts generated at the left of the mesh and their propagation.

However, the estimated wave fronts are always thicker than the actual simulated source ones introduced into the physiological multiscale model. We can also notice a precision error in the localization, as well as a smaller power for the estimated wave front than for the initial simulated sources.

We thus computed the localisation error for one time instant of the synchronous case and for two time instants of the asynchronous sources presented in **Figure 4.3**. We computed the absolute and the relative (relative to the reference postion) errors on both, x and y, dimensions of the mesh, as well as the euclidian distance between the simulated and the estimated sources (**Table 4.1**). The position of the estimated source(s) is the one(s) of the maximum value(s) for each instant.

As we see in all figures the localization is done with some error. We should notice here that the dimension of one element in the original mesh is 0.049 cm whereas in the decimated mesh it is 0.196 cm. For the case of synchronous sources (**Figure 4.3**(a-b)), the absolute error on x for the estimated source 1 is equal to the absolute error on y for the estimated source 2 and vice versa. The relative error of source 2 is smaller than the relative error of source 1. Both estimated sources have the same distances from the original sources, which is equal to 1.2 cm (**Table 4.1**).

In the case of asynchronous sources the absolute error is the same for the estimated sources 1 (**Figure 4.3**(c-d)) and 2 (**Figure 4.3**(e-f)). As in the case of synchronous source, the relative error of the estimated source 2 is smaller than the estimated error of source 1 for the case of asynchronous sources. Both estimated sources have the same distances from the original sources, which is equal to 0.9 cm (**Table 4.1**).

We can see also from **Table 4.1** that the localization is better for the asynchronous cases (which are more realistic) then for the synchronous case, since the absolute and relative errors in asynchronous cases are smaller than for the synchronous case. The distance between the original and estimated sources is also smaller for asynchronous cases than for the synchronous case.

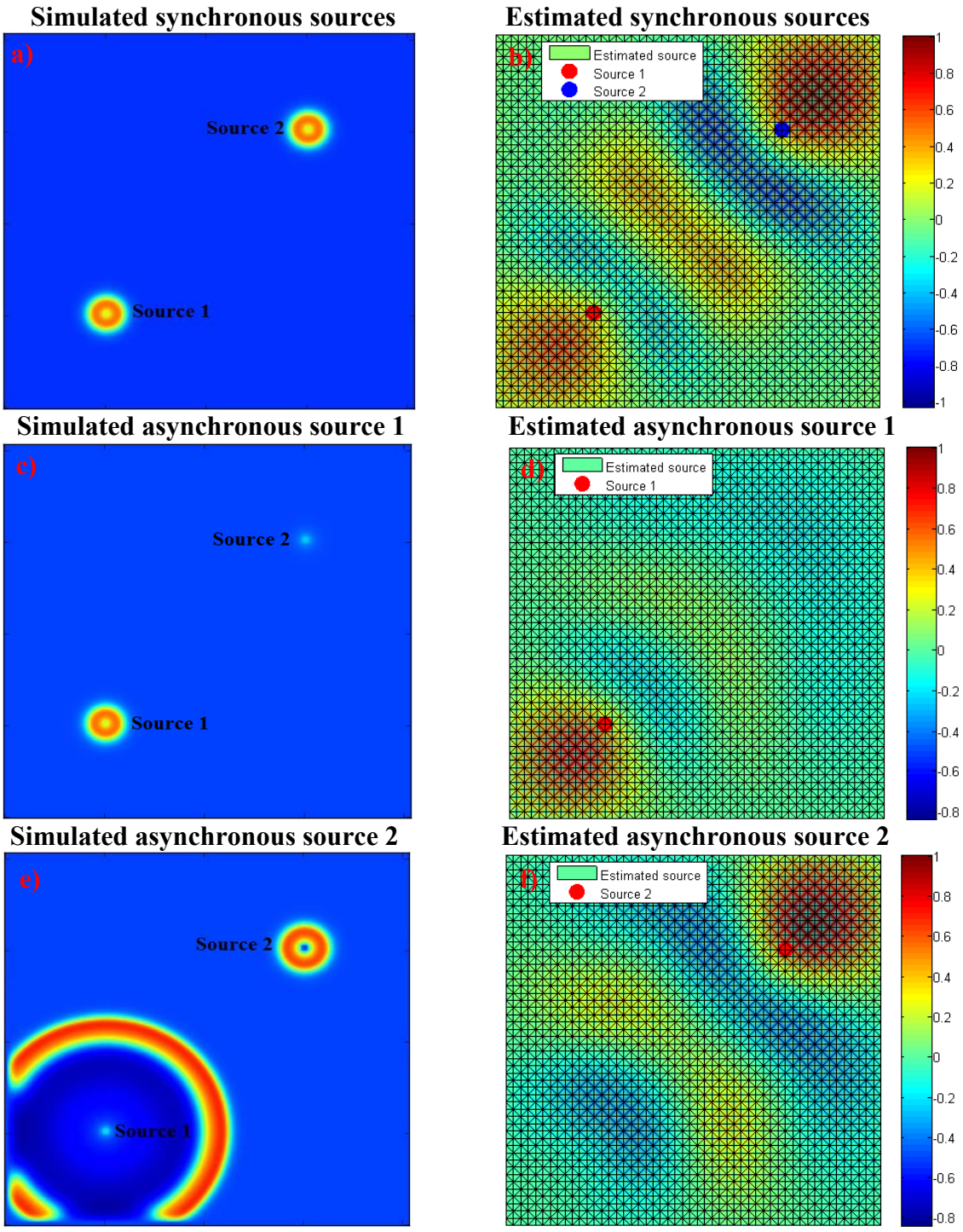

Figure 4.3: Simulation of two synchronous (a) and asynchronous (c-e) sources, and their estimated localisation (b) and (d-f) respectively.

Table 4.1: PRECISION ERROR AND DISTANCE BETWEEN THE SIMULATED AND THE ESTIMATED SOURCES.

		Synchronous sources	Asynchronous sources
Source 1	Absolute error-x	0.9 cm	0.5 cm
	Absolute error-y	0.7 cm	0.7 cm
	Relative error-x	30 %	19 %
	Relative error-y	27 %	27 %
	Distance	1.2 cm	0.9 cm
Source 2	Absolute error-x	0.7 cm	0.5 cm
	Absolute error-y	0.9 cm	0.7 cm
	Relative error-x	9 %	6 %
	Relative error-y	12 %	9 %
	Distance	1.2 cm	0.9 cm

4.3.2 Results on real signals

After validation of the implemented source localization tool, based on EHG signals simulated by using an electrophysiological multiscale model, we applied our source localization algorithm to real uterine EHG signals in order to study the uterine dynamic. We do the localization for one pregnancy contraction (recorded 3 weeks before labor, 3WBL) and one labor contraction recorded on the same woman, in order to get free from anatomical changes. To be able to represent the results we plot in **Figure 4.4** the mean of the estimated localization on the total samples of the real uterine EHG bursts. A video of figures obtained at each time sample would be more representative and could give us more information on the dynamic of the uterine contractility.

It is clear from **Figure 4.4** that the power of the estimated source is lower at 3 WBL than during Labor. During labor we can notice 3 spots in the plot (red maxima) where the sources are estimated in most of the time samples of the contraction (**Figure 4.4** presents the mean on all the time samples of the EHG burst). The yellow color zones can originate from the propagated waves summated during the whole contraction duration. They can also be related to the "shadow effect" that we already noticed it in our study on simulated signals (**Figure 4.2**, thickening of the sources).

For the contraction recorded at 3 WBL we can just notice one spot of high power, where the source is estimated frequently during the whole contraction duration. As we said previously, the yellow color zones can also originate from the propagation and the shadow effect.

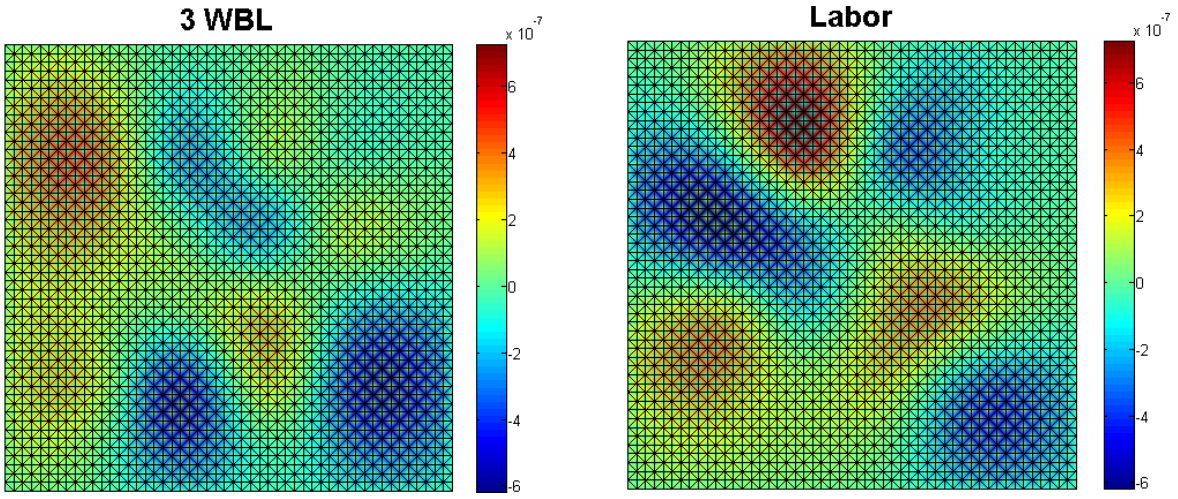

Figure 4.4: Mean of source localization on all samples of one pregnancy contraction (left) and one labor contraction (right).

Furthermore, if we plot one instant representative of the maximal activation for each contraction, this difference between the two situations (pregnancy and labor) is even more noticeable, **Figure 4.5**. The pregnancy contraction is associated with low active and local sources (78 sources with activity greater than 50% of the maximal source intensity of the whole contraction) whereas the labor contraction presents multiple very active sources present in most of the tissue at the same time (346 sources with activity greater than 50% of the maximal source intensity of the whole contraction).

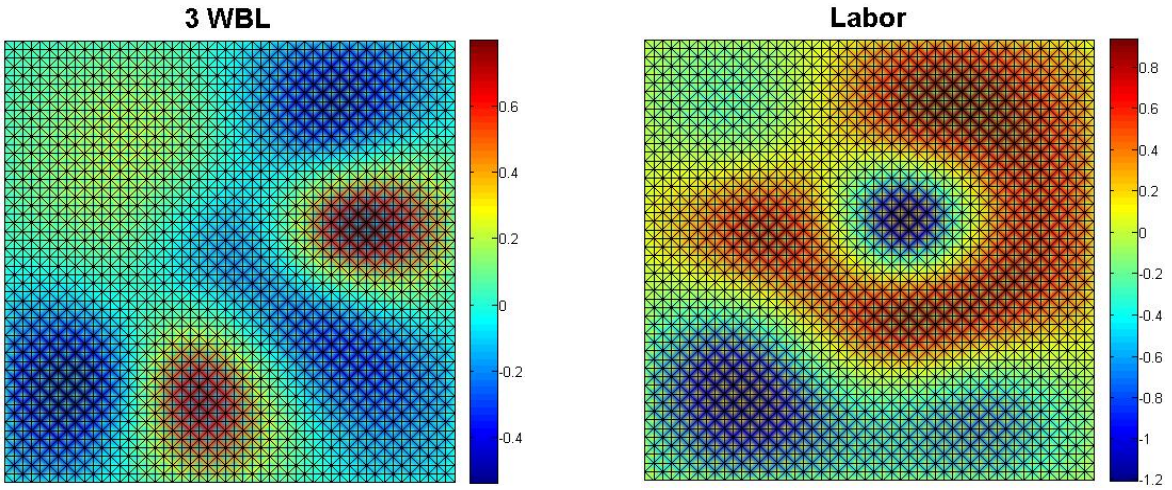

Figure 4.5: Source localization for one sample selected as representative of the maximum activity for the pregnancy contraction recorded at 3 weeks before labor (left) and the labor contraction (right) recorded on the same woman.

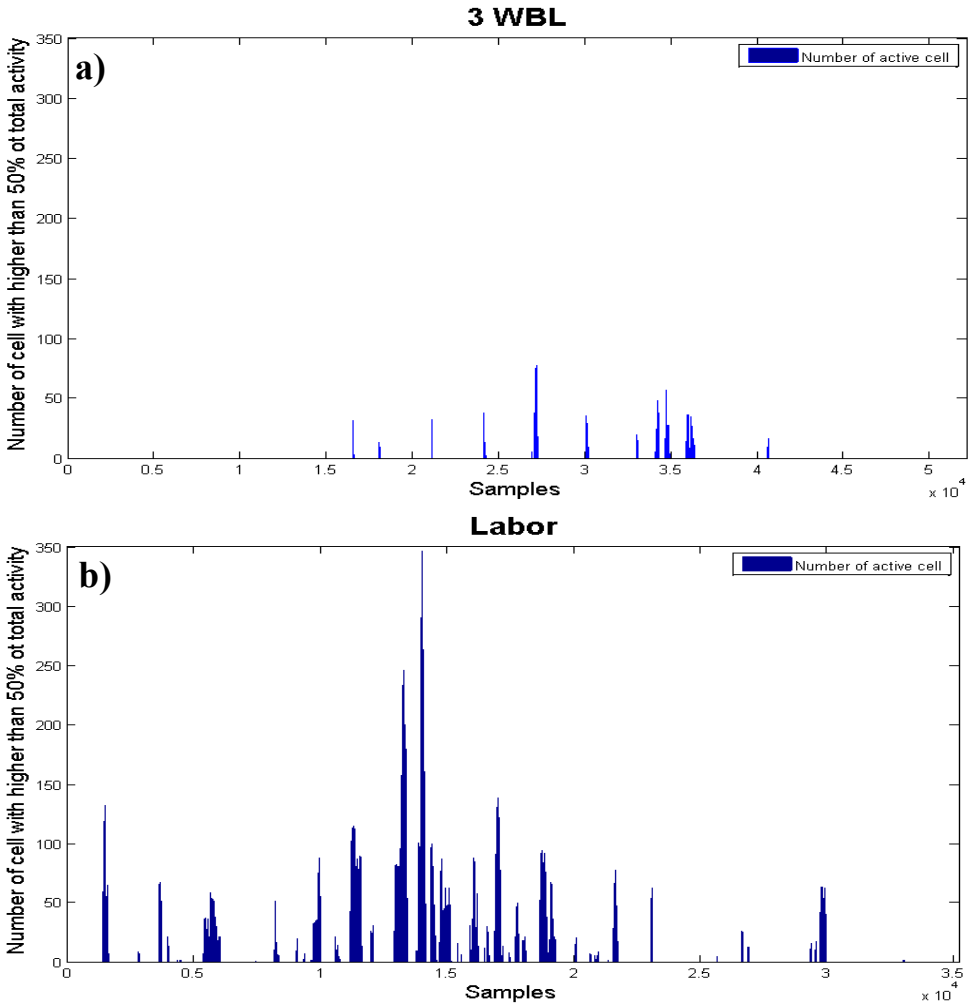

Figure 4.6: Evolution of the number of active elements along the contraction duration for a contraction recorded at 3 weeks before labor (a) and one labor contraction (b) recorded on the same woman.

We then compute, for each time sample, the number of elements which activity is greater than 50% of the maximal source intensity, identified for each whole contraction. The results (**Figure 4.6**) present an indicator of the contraction dynamic. We can see that the number of active elements is always greater and more frequent (6414 identified time sample where the elements activity is greater than 50% of the maximal source intensity) for the labor contraction than for the pregnancy one (1674 identified time sample where the elements activity is greater than 50% of the maximal source intensity), indicating a more synchronous activity of the whole uterine tissue investigated by our electrode grid.

4.4 Discussion

In this work, we solved the first step of source localization, the forward problem, by using the BEM method for a 10x10 cm uterus model with four tissue layers. Simulated and real signals were then used as inputs of the inverse problem by using MNE method. The study on simulated signals presented three cases: two synchronous sources, two asynchronous sources, and a bar of sources. Results show that MNE is able to localize the sources and to detect their propagation with some minor precision error. We computed the localization error for the first two cases and we found that source 2 is better localized than source 1. Furthermore, the more realistic case, asynchronous sources, gave better precision than the synchronous one. We think that most of the localization error comes from the down sampling of the mesh (to limit memory usage), since the mesh is decimated by factor of 4. Therefore the localization error could perhaps better be termed "resolution" as it is closely related to the sampling of the space under investigation. Also for all the cases of simulated signals, the wave front is detected thicker than its actually size. This could be due to the high velocity of wave propagation in the model and to the well known „cone shape" of the volume seen by the electrodes. It looks like a shadow following the wave front.

After validation of the forward and inverse problem on simulated signals, we applied these methods to a pregnancy and a labor contractions, in order to attempt to localize the origin of the contractions and to detect its propagation. This information would permit us to better understand the functioning of uterus during pregnancy and labor, which may eventually help us in preterm labor prediction. We found that the sources intensity of labor contraction is higher than for pregnancy one. We clearly evidenced three sources for the labor contraction whereas pregnancy contraction presented only one source. This appears to be logical since as we know labor contractions are more efficient then pregnancy ones. We expect labor contractions to be more global (propagating fast to the whole uterus) whereas pregnancy contraction remains more or less localized (smaller propagation).

But the localized sources did not demonstrate any "propagation like" behavior. Indeed, the dynamic of the sources evidenced for each time sample of each contraction appeared more like a blowing or an erupting one than a propagated one. This could be in agreement with the hypothesis proposed by Young [24] who stated that the mechanism of global organ-level communication is probably not via action potential propagation, but may be via a

hydrodynamic-stretch activation mechanism, including a coupling between the electrical and the mechanical properties of the uterine organ.

However in the application on real signals we were limited by the geometry of the model (cube containing parallel plane surfaces), which is far from a real uterus. Also we are limited by the electrodes configuration, since the signals in our database are measured by 16 electrodes arranged in a plan matrix placed on a small part of the abdomen, near the vertical median axis of the uterus. These 16 electrodes are spatially localized and do not cover the whole uterus. So they do not provide us with a global image of the uterus. In this case some regions of interest may be missed if they are far from the recording site. In this case, the electrodes are collinear and the localization problem is undetermined, regardless of the number of available signals. The dipole component orthogonal to the plane determined by the electrode and the origin of the dipole cannot be seen by any of the sensors [25]. These issues can affect our results and contribute to the source estimation error.

In all cases however, the intensity of the identified sources remained very small for real signal. This problem could come from the characteristic of the MNLS method itself (minimum norm least-squares) that searches for the solution that presents the minimum power. We could solve this drawback by using another method, such as sLOTERA, that gives also information on the depth of the source.

4.5 Conclusion and perspectives

A first preliminary study on EHG source localization problem was presented in this chapter. A validation of forward and inverse methods was done on simulated signals in different cases. Then we applied these methods on real uterine EHG bursts, corresponding to contractions recorded during pregnancy and labor. The methods were able to identify the sources injected in the model for the simulated signals, with some error, related to the mesh decimation. On real EHG signals, the methods gave logical results that fit with the well-known hypothesis in the literature, which says that during labor the contraction is efficient and propagated to the whole uterus, whereas during pregnancy, the contraction is inefficient and local.

In a future work, we will study the effect of varying the velocity and of the regularization parameter λ on the results. We will also attempt to use the whole mesh in order to see the effect of mesh resolution on the localization error. We will also compare different inverse methods to see which one is most suited to our particular (EHG) source localization problem.

We will also compare the results obtained on more real EHG signals, in different situations (normal and risk pregnancies, labor). An improvement in the model that would make it electrically and geometrically closer to the real uterus is very important to future work, as well as an extension of the electrode matrix configuration to cover bigger part of the uterus. Possibly the sensors could be placed to cover the whole uterus except of course for the dorsal part, to obtain a complete image of the electrical propagation of the uterus.

References

[1] H. Becker, L. Alberab, P. Comon, M. Haardt, G. Birot, F. Wendling, M. Gavaret, C.G. Bénar, and I. Merlet, "EEG extended source localization: Tensor-based vs. conventional methods," *NeuroImage*, In press, available online March 2014.

[2] J.D. López, V. Litvak, J.J. Espinosa, K. Friston, and G.R. Barnes, "Algorithmic procedures for Bayesian MEG/EEG source reconstruction in SPM," *NeuroImage*, vol. 48, pp. 476-487, Jan. 2014.

[3] V. Montes-Restrepo, P. van Mierlo, G. Strobbe, S. Staelens, S. Vandenberghe, and H. Hallez, "Influence of Skull Modeling Approaches on EEG Source Localization," *Brain Topography*, vol. 27, no. 1, pp. 95-111, Jan. 2014.

[4] O. Hauk, "Keep it simple: a case for using classical minimum norm estimation in the analysis of EEG and MEG data," *NeuroImage*, vol. 21, no. 4, pp. 1612-1621, Apr. 2004.

[5] J. Mattout, C. Phillips, W.D. Penny, M.D. Rugg, and K.J. Friston, "MEG source localization under multiple constraints: An extended Bayesian framework," *NeuroImage*, vol. 30, no. 3, pp. 753-767, Apr. 2006.

[6] A.M. Dale and M.I. Sereno, "Improved localizadon of cortical activity by combining eeg and meg with mri cortical surface reconstruction: A linear approach," *Journal of cognitive neuroscience*, vol. 5, no. 2, pp. 162-176, spring 1993.

[7] O. Hauk, D.G. Wakeman, and R. Henson, "Comparison of noise-normalized minimum norm estimates for MEG analysis using multiple resolution metrics," *NeuroImage*, vol. 54, no. 3, pp. 1966-1974, Feb. 2011.

[8] R. Grech, T. Cassar, J. Muscat, K.P. Camilleri, S.G Fabri, M. Zervakis, P. Xanthopoulos, V. Sakkalis, and B. Vanrumste, "Review on solving the inverse problem in EEG source analysis," *Journal of neuroengineering and rehabilitation*, vol. 5, no. 1, pp. 25-58, Nov. 2008.

[9] R. Oostenveld, P. Fries, Eric Maris, and J.-M. Schoffelen, "FieldTrip: open source software for advanced analysis of MEG, EEG, and invasive electrophysiological data," *Computational intelligence and neuroscience*, vol. 2011, pp. 9, Oct. 2011.

[10] J. Laforet, C. Rabotti, J. Terrien, M. Mischi, and C. Marque, “Toward a Multiscale Model of the Uterine Electrical Activity,” *IEEE Trans. Biomed. Eng.*, vol. 58, no. 12, pp. 3487-3490, Dec. 2011.

[11] Y. Shirvany, F. Edelvik, and M. Persson, “Multi-dipole EEG source localization using particle swarm optimization,” in *Proc. 35th Annual International Conference of the IEEE Eng. Med. Biol. Soc. Conf. 2013*, Osaka, Japan, Jul. 2013, pp. 6357 - 6360.

[12] E. Pirondini, B. Babadi, C. Lamus, E.N. Brown, and P.L. Purdon,“A spatially-regularized dynamic source localization algorithm for EEG,” in *Proc. 34th Annual International Conference of the IEEE Eng. Med. Biol. Soc. Conf. 2012*, San Diego, California, Aug-Sep. 2012, pp. 6752 - 6755.

[13] M.S. Hämäläinen, S. Matti, and R.J. Ilmoniemi, “Interpreting measured magnetic fields of the brain: estimates of current distributions,” Helsinki University of Technology, Department of Technical Physics, 1984.

[14] M.S. Hämäläinen, and R.J. Ilmoniemi, “Interpreting magnetic fields of the brain: minimum norm estimates,” *Medical & biological engineering & computing*, vol. 32, no. 1, pp. 35-42, Jan. 1994.

[15] C. Rabotti, M. Mischi, L. Beulen, S. Oei, and J. Bergmans, “Modeling and identification of the electrohysterographic volume conductor by highdensity electrodes,” *IEEE Trans. Biomed. Eng.*, vol. 57, no. 3, pp. 519–527, Mar. 2010.

[16] B. Karlsson, J. Terrien, V. Gudmundsson, T. Steingrimsdottir, and C. Marque, “Abdominal EHG on a 4 by 4 grid: mapping and presenting the propagation of uterine contractions,” in *Proc. 11th Mediterranean Conference on Medical and Biological Engineering and Computing*, 2007, Ljubljana, Slovenia, 2007, pp. 139-143.

[17] M. Hassan, S. Boudaoud, J. Terrien, B. Karlsson, and C. Marque, “Combination of Canonical Correlation Analysis and Empirical Mode Decomposition applied to denoise the labor electrohysterogram,” *IEEE Trans. Biomed. Eng.*, vol. 85, no. 9, pp. 2441-2447, Sep. 2011.

[18] K.G. Mideksa, H. Hellriegel, N. Hoogenboom, H. Krause, A. Schnitzler, G. Deuschl, J. Raethjen, U. Heute, and M. Muthuraman, “Source analysis of median nerve stimulated somatosensory evoked potentials and fields using simultaneously measured EEG and MEG signals,” in *Proc. 34th Annual International Conference of the IEEE Eng. Med. Biol. Soc. Conf. 2012*, San Diego, California, Aug-Sep. 2012, pp. 4903 - 4906.

[19] K.G. Mideksa, H. Hellriegel, N. Hoogenboom, H. Krause, A. Schnitzler, G. Deuschl, J. Raethjen, U. Heute, and M. Muthuraman, “Dipole source analysis for readiness potential and field using simultaneously measured EEG and MEG signals,” in *Proc. 35th Annual International Conference of the IEEE Eng. Med. Biol. Soc. Conf. 2013*, Osaka, Japan, Jul. 2013, pp. 1362 - 1365.

[20] W.S. Hall, “Boundary Element Method,” in *The Boundary Element Method*, Netherlands:Springer, 1994, pp. 61-83.

[21] J. Kybic, M. Clerc, T. Abboud, O. Faugeras, R. Keriven, and T. Papadopoulo, “A common formalism for the integral formulations of the forward EEG problem,” *IEEE Transactions on Medical Imaging*, vol. 24, no. 1, pp. 12-28, Jan. 2005.

[22] A. Gramfort, T. Papadopoulo, E. Olivi, and M. Clerc, “OpenMEEG: opensource software for quasistatic bioelectromagnetics,” *Biomedical engineering online*, vol. 9, no. 1, pp. 45-65, sep. 2010.

[23] M. Fuchs, M. Wagner, T. Köhler, and H.-A. Wischmann, “Linear and nonlinear current density reconstructions,” *Journal of clinical neurophysiology*, vol. 16, no. 3, pp. 267-295, 1999.

[24] R.C. Young, Myocytes, “myometrium, and uterine contractions,” *Annals of the New York Academy of Sciences*, vol. 1101, no. 1, pp. 72-84, Apr. 2007.

[25] V. Caune, S. Le Cam, R. Ranta, L. Maillard, and V. Louis-Dorr, “Dipolar source localization from intracerebral SEEG recordings,” in *Proc. 35th Annual International Conference of the IEEE Eng. Med. Biol. Soc. Conf. 2013*, Osaka, Japan, Jul. 2013, pp: 41-44.

General conclusion and perspectives

Many improvement have been done during this thesis on the way of reaching the thesis objective of early prediction of term or preterm labor as well as making better prediction of when premature labor is not imminent. We developed in this thesis several new approaches to uterine EMG (Electrohysterogramme, EHG) processing. They were based on either improving the previously studied parameters or extracting and evaluating new parameters from the EHG signals, in order to bring us closer to our ultimate goal, which is to improve preterm labor prediction and diagnosis.

For many years, the uterine excitability and the propagation of activity have been the subject of a lot of EHG processing studies, in different fields (time, frequency, time/frequency, linear, nonlinear...). Whereas most of these studies have been done on bipolar signals coming from a small number of electrodes. And when using multiple electrode leads, they were based on small databases of bipolar signals. This work has mainly addressed five original points:

i) using a larger database than ever before of bipolar as well as monopolar signals (recorded with a 4x4 electrode matrix) to obtain a more global image of the dynamics of the uterus along pregnancy and labor, with a good spatial resolution, and high number of longitudinal recordings;

ii) using the new electrophysiological multiscale EHG model to validate our processing techniques;

iii) extracting the map of propagation direction of uterine EHG, based on the asymmetry of the available methods of coupling between the 16 monopolar EHG channels;

iv) introducing for the first time source localization analysis of the EHG to characterize the dynamic of the origin of EHG signals;

v) developing new suction electrodes for measuring EHG signals on pregnant rat uterus using the already developed "*ex-vivo*" experimental protocol in our laboratory.

These new and innovative results of thesis work are presented in the second, third, and fourth chapter that investigated respectively the monovariate nonlinear analysis, the direction of propagation, and the source localization analysis of the EHG. The suction electrode matrix development for the rat experimental protocol is presented in the Appendix.

For the monovariate analysis, we first studied, on synthetic signals, the performances of nonlinear methods relatively to different experimental and/or processing situations (noise, sampling frequency, signal filtering) as well as the effect of using surrogates. After testing and validating the nonlinear methods on synthetic signals, we compared (using ROC curves) their performances with the linear methods on real signals, in terms of classification rate for pregnancy vs. labor classification. Results on synthetic signals show that no method was found to be the best method in all the cases studied (with and without noise, with and without surrogates). Time reversibility was found to be the method that works well in most of the above-mentioned cases. Results on bipolar real signals show that Time reversibility and Sample entropy methods gave the highest area under curve in case of using surrogates and not using surrogates respectively. However, the use of surrogates does not bring any improvement in the classification rate, and unexpectedly it decreased it for some methods in some cases. Sample entropy method gave better results, improved when using surrogates rather that when not using them. However, its AUC remained lower than the AUC of Time reversibility applied without using surrogates. This leads us to the conclusion that there is no need to use the surrogates and the related z-scores to evaluate non-linearity, because surrogate computation is a highly computational expensive technique. Furthermore, the results indicated that the nonlinear methods, applied without using surrogates, overcame the linear ones since Time reversibility have the highest AUC. This also justifies the choice of the nonlinear coupling methods used later in chapter 3.

Then we presented results concerning the sensitivity to sampling frequency and to the frequency content of the signals of all of the nonlinear methods we used. We found that decimation reduces the computational time with no noticeable reduction of the methods performances, and even with a noticeable increase in the performance of some methods such as Sample entropy. Filtering signals into three frequency bands demonstrated that Time reversibility method is the method least dependent on the frequency content of the signal. The performance of Sample entropy is also improved here, by filtering signals into the low frequency band (FWL).

We conclude from this sensitivity analysis that Time reversibility is the best performing and robust method to sampling frequency and frequency content of the signals. Furthermore, one should take care in choosing the sampling frequency and the signal filtering before applying Sample entropy, in order to optimize this method performance.

We suggest the following point as perspectives in this direction:

- Comparing Time reversibility method to new nonlinear methods, in order to further increase the actual performance of Time reversibility for pregnancy monitoring. Indeed, the non-linear characteristics of EHG seem to evolve between pregnancy and labor. A close and precise monitoring of this evolution along term could be a good predictor of preterm labor.
- Doing a sensitivity study of nonlinear methods to several sampling frequency in order to find the optimal sampling frequency that should be used to increase the classification rate.
- Studying the effect of the nonstationarity on the methods performances in order to adapt them to the non stationary characteristics of EHG signals, by using for example the *bPSP* algorithm presented in chapter 3.
- Comparing the performances of nonlinear methods when applied to bipolar and monopolar signals (as was done for the synchronization method in chapter 3).

Chapter 3 presents the study done on the relation between signals coming from the multichannel electrode matrix (bivariate analysis). In this chapter we tested the performances of the methods on pure synthetic signals using the classical Rössler model. But we also validated, for the first time, the selected methods on more realistic signals simulated by a new EHG physiological multiscale model developed in our Lab. We then studied, on real EHG, the evolution of methods with increasing WBL (decreasing time before delivery), not just in terms of coupling but also in terms of direction of the propagation evidenced. Then we tried in a second step, to improve the performances of the methods on real EHG since the first attempts to characterize the real EHG did not give expected results. We thus implemented a "Filtering-Windowing" version of the methods that permits to suit the nonstationarity of EHG signals, and also to get free from the inter-individual filtering effect of the fat, very variable in our database, by unifying the frequency band of all the signals. In a second part of this study, we compared the results obtained by this method on bipolar and monopolar signals.

Results show that h^2 gives the best results on stationary synthetic signals. It also managed to detect the coupling and direction injected in the multiscale EHG model for simulation of EHG signals. Results on real signals also demonstrated that, by taking the mean of the 16x16 coupling matrix on all the contractions of each WBL, no clear evolution of coupling is evidenced with decreasing WBL, even if some statistical difference appear between some

terms. By plotting the resulting coupling matrix as well as the direction map, we found some patterns changing when going from pregnancy to labor. The correlation matrix went from a random distribution pattern during pregnancy to a more organized pattern during labor. The direction map presented a multidirection pattern for pregnancy. It kept this multidirection aspect but more concentrated down towards the cervix when approaching labor.

When trying to improve the performances of methods, we focused on overcoming some of the weaknesses in the methodology, as well as on getting free from the natural filtering effect due to inter-individual varying fat thickness during signal recording. We found that making our methods time varying clearly improved the performance of methods for the direction detection in a modified nonstationary version of a fourth order Rössler model. Therefore, we applied the methods on real EHGs segmented by using the *bPSP* algorithm. This preprocessing technique improved slightly the performance of the method. But the difference obtained between pregnancy and labor remain non significant. We decided to retain only the low frequency band of the EHG (FWL), which is supposed to be more related to the propagation of EHG, with keeping the windowing-preprocessing step. We found that using a combination of these two preprocessing steps, the obtained Filtered-Windowed- h^2 (FW-h^2) yielded the best results with a clear increase from pregnancy to labor. The coupling matrix and direction map of all pregnancy and all labor contractions obtained using this methods showed an increasing in coupling, when going from pregnancy to labor, as well as an increase in the density of the direction map, in addition to the patterns seen in the previous part of this chapter. Results further demonstrated that using monopolar signals is better for coupling analysis than using bipolar signals, since the difference between pregnancy and labor classes is more significant when using monopolar signals. This is an expected result, since in our protocol, bipolar lead computing induced a bias between two adjacent bipolar leads. Inversely monopolar signals do not present such a bias.

We should mention that the other methods tested (H, GC) did not give good results, for the classification of EHGs, due to some EHG characteristics: increasing EHG nonlinearity when approaching to labor, variability of women in the database, increasing frequency content along term, the effect of fat... which are discussed in the chapter 3. As H and GC are sensitive to these characteristics, they should be adapted before being used for EHG characterization.

A lot of work can be done in the future for the study of propagation, for example:

- Using high density electrode recordings with a larger surface. This may provide us with more information (better spatial resolution, larger view of the uterine contractility) and thus give a better image of the dynamics of the uterus, than the small 4x4 matrix just located near the vertical median axis of the uterus.
- In this thesis we obtain a qualitative results for the direction map analysis. In order to obtain quantitative results we may apply "graph theory" on the map of direction by considering the electrodes as nodes and the coupling values and directions as edges.
- Including new methods in the study such as Phase Locking Value (PLV) method, which has been widely applied on EEG signals, which study the correlation of contractions for the same lead not between different signals as we do in this thesis.

Finally, we tackled for the first time in this work, the EHG source localization problem. We implemented a tool for solving the forward and the inverse problem based on the Fieldtrip open source toolbox. We tested our approach for validation, on simulated signal from our new electrophysiological multiscale EHG model. Then we apply it on one real pregnancy and one real labor EHG bursts, in order to see how the dynamic of the uterus evolves from pregnancy to labor, at source level not at the abdominal surface electrode level, as all researcher in the EHG field did.

We found that MNE method succeeded in localizing the sources and detecting their propagation, when applied to signals simulated with different positions and different propagation patterns. However, we obtained some position errors that could be related to different factors such as propagation velocity and down sampling of the mesh. On real signals we found that the strength of the EHG source evidenced at 3WBL is lower than the strength of sources evidenced during labor. The number of sources detected during labor is greater than the number of sources detected during pregnancy. We should mention that this is the first and preliminary results concerning uterine source localization, which opens the road for a new platform of EHG processing. Many improvement remain to be done to this first attempt to source localization and this new EHG processing technique opens many perspectives, such as:

- Use of the whole mesh (no down sampling) to minimize the localization error and precision.
- Study the effect of varying the propagation velocity of the simulated signals.
- Study the effect of the regularization parameter of the MNE method.

- Comparing the MNE methods with other methods such as sLOTERA, residual variance..., to find which method suits the most the EHG source localization.
- Selecting regions of interests (ROI) in the mesh where the sources seems to be localized in most of times during the contraction and computing the coupling between the sources in these ROI (Intra-coupling estimation) and between these ROI (Inter-coupling estimation). Thus we could get rid of the effect of volume conductor and noise encountered when studying the relationship at the electrode level.
- Use electrode matrices that cover the larger possible area of the abdomen above the uterus, to get a more global image of the contractility and to be not limited in localizing the sources that are not below of the recording matrix.
- Improve the multiscale model and go towards a generic uterus model then towards a personalized model to obtain more precise results.

The Appendix of this manuscript describes our contribution to the rat experimental protocol improvement. I developed during this work a new suction electrode matrix that may help in reducing the interferences between the electrodes and in overcoming the problem of the contact between the uterus and the electrodes related to the uterus curved surface. As no results have been obtained yet by using these electrodes, the description of the protocol is only reported in the appendix. The signals recorded by using this device should permit to validate the coupling/direction analysis methods, as, for rat uterus, the anatomy permits to select either longitudinal or transverse propagation (longitudinal external muscular layer, circular internal muscular layer). This is not possible on woman‟s uterus.

Finally the work presented in this thesis may have important implications in studying the genesis of human labor. It opened many doors for the investigation of uterine contractions coupling and propagation study, which may help to develop a reliable way of predicting preterm labor.

Appendix:

This annex describes the work performed in parallel with the main thrust of the thesis. Originally this work was undertaken in the aim of obtaining recordings from rats to compare to the recording made on human subjects. However due to technical difficulties, time limits and the fact that in the meantime the very useful physiological model came to maturity in our laboratory, it was not possible to finish this work.

Here we present the part of the work that was realized, namely the modifications made to the so-called "*ex-vivo*" experimental protocol previously developed within our laboratory. This experimental protocol is dedicated to record uterine EMG signals on pregnant rats. These signals can potentially be used to map the electrical activity of the uterus. They could also provide data useful to validate our signal processing methods developed in chapter two, three and four. The data obtained can also be used to validate the electrophysiological model. The benefit of using a rat uterus is that it contains two well organized layers of muscle fibers, structure that is not present in the human uterus: a longitudinal superficial layer and an internal cylindrical layer. In light of this simpler structure, validation of the model and methods can be done more easily, because we can predict the expected direction of propagation of action potentials in the rat uterus, which is not possible with a human uterus and certainly not with external non-invasive techniques.

The aim of this protocol is to measure multiple monopolar uterine EMG signals, with electrodes placed directly on the intact pregnant rat uterus, at different terms of pregnancy and during spontaneous contractions. We modified the "*ex-vivo*" protocol developed by Chkeir et al. [1] who previously improved the "*in-vitro*" protocol developed by Rihana et al. [2] based on the study by Lammers et al. [3], [4]. The *in-vitro* protocol gave signals contaminated by a lot of noise, mainly from the pump ensuring the circulation of the physiological liquid, but also from all the other classical noise sources such as, electronic, physiologic, high frequency...

The *ex-vivo* protocol sidesteps the problem of the pump noise by keeping the uterus connected to the rat, so there is no need for the physiological liquid circulation. However the *ex-vivo* protocol is not without presenting its own problems; since the uterus is kept intact, we have a problem with the contact between the uterus and the electrodes matrix. Indeed, the intact uterus presents successive humps (one for each baby rat) and therefore a multiple curved

surface that does not fit well with the rigid support of the electrode grid. Also we noticed some interference between adjacent electrodes because they were too close one to each other. The modifications of the protocol and setup presented here solve these problems.

Ethical approval and certification:

One of laws on animal protection prescribes that "no one by a unjustified way must impose pain, suffer, damage to animals or put them in a state of anxiety" (art. 2, paragraph 3, law of 9 march 1978 on animals protection, LPA, RS 455). This study has received the approval of the animal care laboratory of the Université de Technologie de Compiègne. Our animal facilities are approved under No. B60-60159-001. Furthermore, our experimental protocol has been approved by the regional ethical committee of Picardie for animal experimentation (CREMEAP in French) under the number 96, certified by the Ministry of higher education and research (MESR in French). I have been also given a training course on animal experimentation, level 1, to be permitted to perform these animal experiments.

Materials and methods:

The experimentation were done on Wistar rats. All the rats were weighed using precision balance, their weights varied between 300 g and 450 g. A rat has a gestation period of about 21 days. The population on which we worked contains 4 rats recorded at 4 terms of pregnancy (17 days, 19 days, 20 days and 21 days), with one rat recorded for each term.

The procedures does not differ from the previous protocol [1] and are performed under sterile conditions. The modifications done to this protocol mainly concern the equipment. The Wister rat is first anaesthetized by Pentobarbital for surgery and recordings. A mid-abdominal incision permits to access the two uterine horns, which can contain an average of 5 to 8 fetuses each. Only one of the horns is used for the experiment. Two strings are quickly tied around the end of the selected horn (**Figure 1**) keeping a distance of 5 mm between the ties.

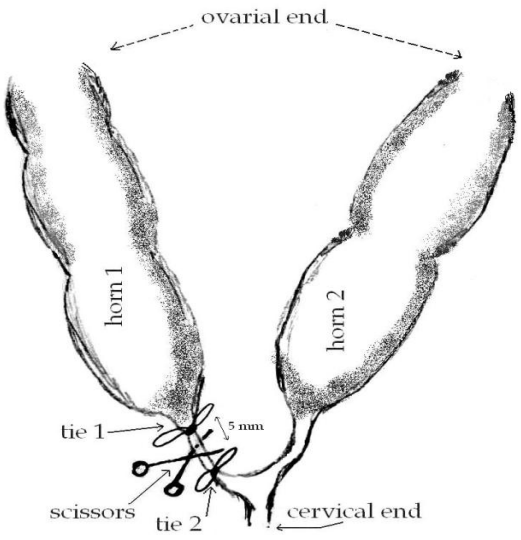

Figure 1: Presentation of how to make the two ties and to cut the horn [1].

The aim of the ties is to prevent the bleeding and the release of the fetuses. After cutting the selected horn between the two ties, we excise the horn of the uterus keeping its opposite end connected to the ovary. Then we place the horn in a custom-made support (**Figure 2**). Water heated at 37 ^{o}C passes inside this support thanks to gravity, without using a pump, and with no contact with the uterus, to maintain the temperature of the uterus. The uterus is also irrigated with a physiological liquid (ringer). The string is then attached to a flexion transducer (range between 0 and 2 N). In order to obtain a good extended horn, we pin and hook the horn at the ovarian end. This procedure permits us to record simultaneously the electrical and the mechanical activities during uterine contraction.

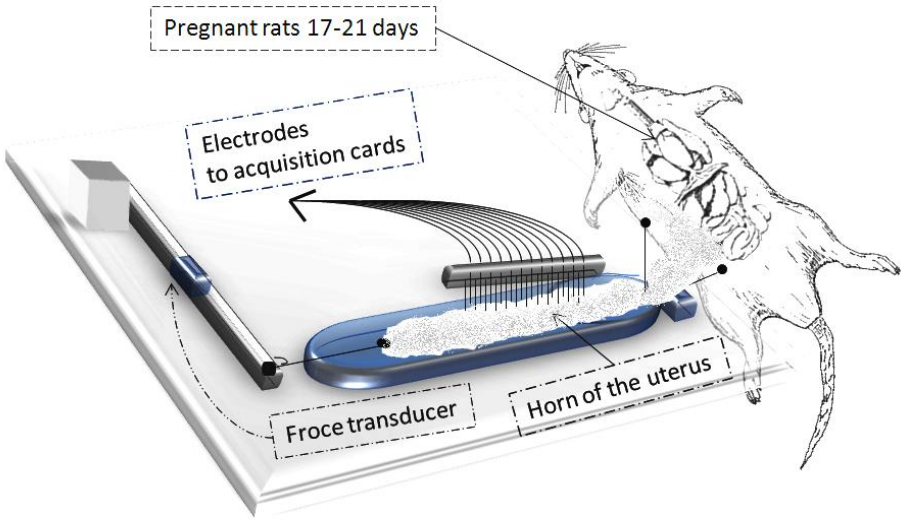

Figure 2: Illustration of the whole experimental protocol used to record the electrical activity using 30 electrode pins [1].

In order to be able to record the electrical and mechanical activity simultaneously, great care was taken in the positioning of the horn of the uterus and of the electrode. We thus developed an adapted suction electrode device. A cuboid of length = 12 cm, width = 4 cm, and height = 5 cm was made by 6 faces of Plexiglas glued carefully to make it waterproof. 32 holes were perforated in the bottom and the top faces of the cuboid, 30 holes for the uterine EMG electrodes and 2 for the reference electrodes (**Figure 3**).

Two other holes were perforated also on one side face of the cuboid, one connected to a syringe for suction and a second that could be connected to an intra-cuboid pressure sensor. As we did not use the pressure sensor for the first experiments we sealed it as shown in **Figure 4** to avoid leakage.

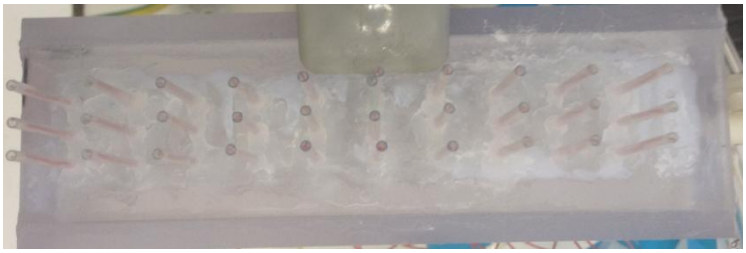

Figure 3: Bottom face of the electrode matrix, we can see the 32 holes.

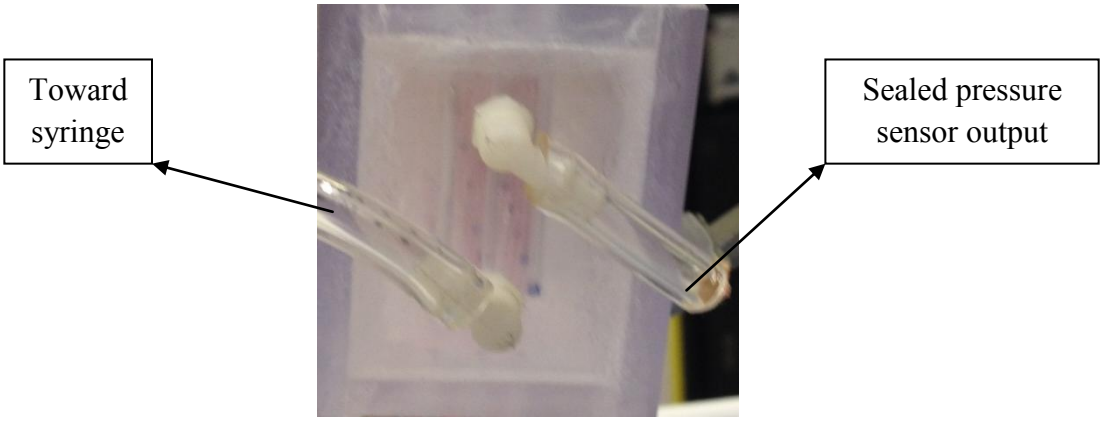

Figure 4: Side of the electrode matrix, we can see the connectors for the syringe and the pressure sensor, which is sealed, being unused for these first experiments.

Then we inserted 32 glass capillaries into the holes of the bottom face by keeping space between the introduced capillaries and the upper face, and we glued them around the holes to keep the cuboid waterproof. After that we introduce the electrodes wires (red wires in **Figure 5**-left) from the holes of the upper face into the capillaries until they reach the end of the capillaries. We them glued around the holes to prevent leakage. The outside parts of the capillaries were wrapped at the end by rubber (**Figure 5**-right), to protect them.

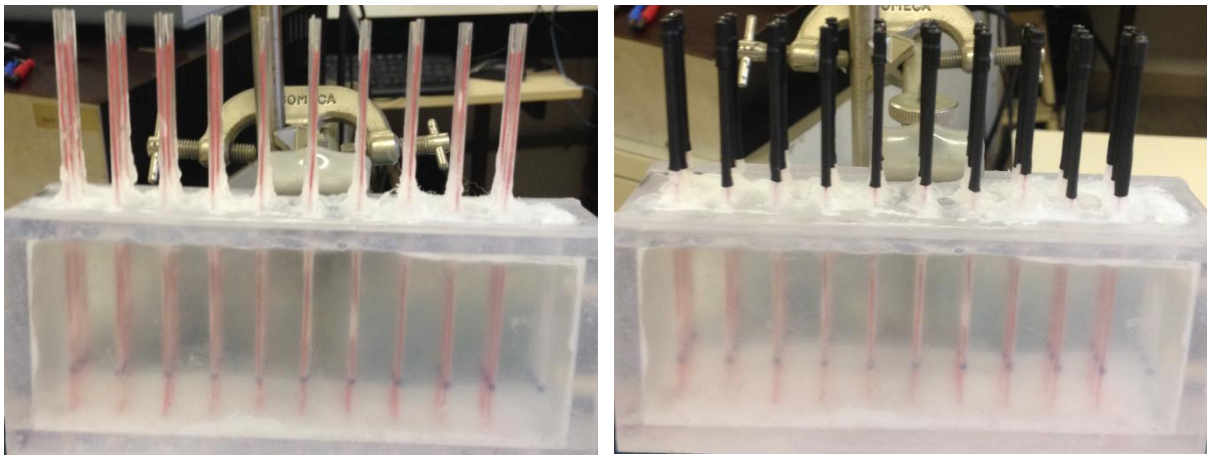

Figure 5: Glass capillaries with the red wire electrodes (left), then capillaries wrapped with black rubber (right).

A hand-made connector (**Figure 6**) was soldered to connect the 32 electrodes and the flexion sensor to the A/D Biosemi active-one box.

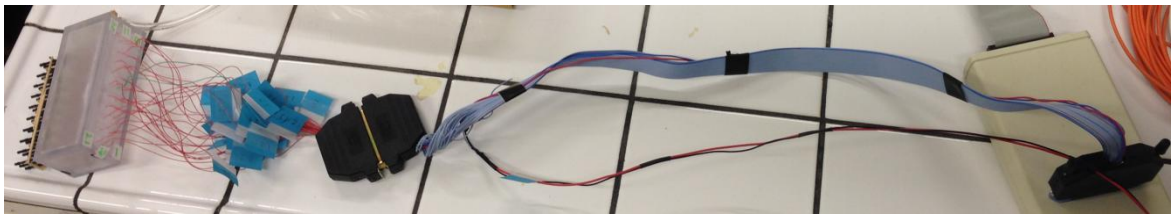

Figure 6: Hand-made connector from the electrodes matrix to the BIOSEMI adapter.

To perform the measurements, the 30-electrodes matrix (cuboid with capillaries and electrodes, pin of 0.3 mm diameter and 1 cm inter-electrode distance), is gently positioned along the length of the selected horn and maintained by using a stand. Then we use the syringe to suck up the uterus tissue to make it stick to the whole electrodes. Recorded signals are amplified between 0.16 and 256 Hz by the BioSemi Active-One amplifiers and sampled at 512 Hz.

So our complete system (**Figure 7**) contains:

- The cuboid with the capillary electrode of 3 columns x 10 lines. All electrodes are distant of 1 cm (lines and columns). Two reference electrodes (CMS / DRL) placed in the middle of the grid (full description at http://www.biosemi.com/faq/cms,drl.htm).
- A flexion sensor (strain gauge technology), measuring the strength of the mechanical contraction of the uterine horn (ref. F1200, 0 to 2N, MEIRI: http://www.meiri.com).

- The amplification is provided by a BIOSEMI A/D box, with sampling accuracy of 24 bits and sampling frequency of 512 Hz. These signals are transmitted by optical fiber to the computer.
- The Actiview software (BIOSEMI) allows the collection and the storage of signals.

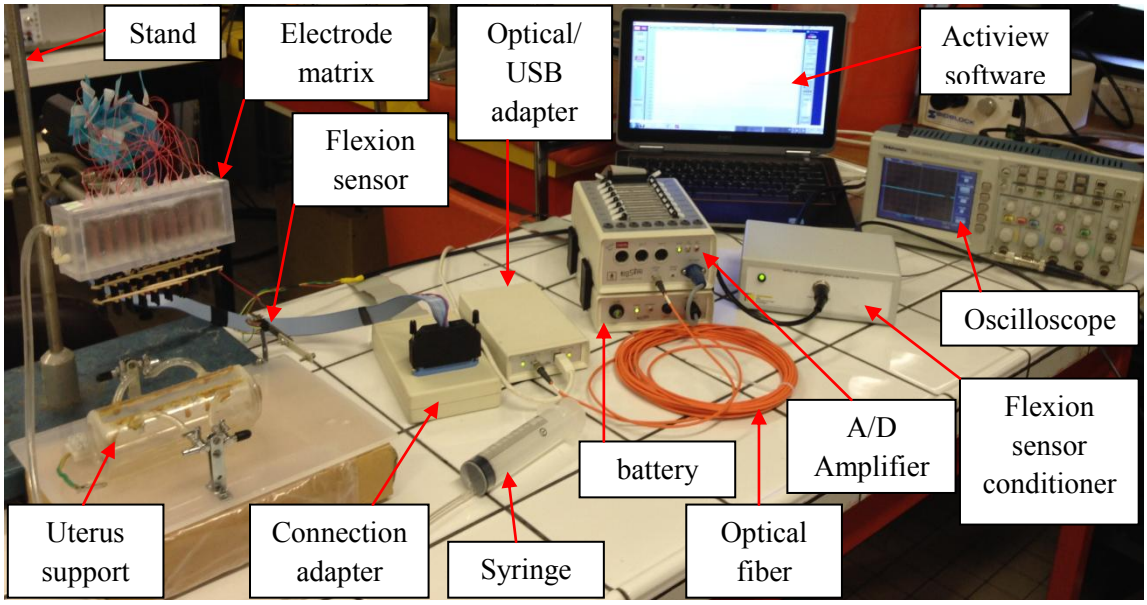

Figure 7: Description of the entire system.

Discussion

The new *ex-vivo* experimental protocol and the improved instrumentation should allow the recording of the electrical activity of the uterus while keeping it connected to the rat. This permits to maintain vascularization of the uterus tissue and then to prevent the use of a pump for oxygenation of the tissue. Our modification to the measurement matrix overcomes the problem of the curvature of the uterus horn by using a suction system. It also overcomes the problem of interference between the electrodes due to the capillaries covered by rubber.

By using this system, we measured 4 rats at 17, 19, 20 and 21 days of gestation. But unfortunately no rat exhibited spontaneous contraction during these experiments. After verification of the system functioning and the all connections, we concluded that the problem might come from the anesthetic product. In fact the rats were anesthetized by intraperitoneal injection into the left part of the abdomen. We thus suspect that the uterine muscle, which certainly comes in to contact with the anesthetic during this injection, could be inhibited in its contractile activity. We tried with the last rat to take the horn that is in the right part of the

abdomen, but unfortunately this horn was not as developed as the left horn and was too small for manipulation.

Many improvements should be done in the anesthesia protocol in the future, since we are limited in materials and time. For example making a pre-anesthesia under hood by gas then doing the anesthesia by intravenous in the vein of the tail. Thus the anesthesia will not affect the uterine muscle. Furthermore, a study [5] has shown that an appropriate cocktail of anesthetic should be used to prevent the paralysis of smooth muscle.

Another reason should be the maintenance of the progesterone block, which is very strong for rat uterus during all pregnancy. As vascularization is maintained in our protocol, this progesterone block is present through the maternal blood. Indeed, progesterone withdrawal has been widely recognized as needed for the initiation of labor in rat uterus. But we were unable to induce this progesterone withdrawal in our last attempt, even by giving RU486 (strong progesterone inhibitor) to the rat. This protocol has to be refined in further studies.

References:

[1] A. Chkeir, M-J. Fleury, B. Karlsson, M. Hassan, and C. Marque, “Patterns of electrical activity synchronization in the pregnant rat uterus,” BioMedicine, vol. 3, no. 3, pp. 140-144, Sep. 2013.

[2] S. Rihana, “Modélisation de l'activité électrique utérine,” Phd. dissertation, Université de technologie de Compiègne, 2008, Compiègne.

[3] W.J. Lammers, B. Stephen, R. Hamid, and D.W.G. Harron, “The effects of oxytocin on the pattern of electrical propagation in the isolated pregnant uterus of the rat,” Pflügers Archiv, vol 437, no. 3, pp. 363-370, Jan. 1999.

[4] W.J. Lammers, E. El-Kays, K. Arafat, and T.Y. El-Sharkawy, “Wave mapping: detection of coexisting multiple wavefronts in high-resolution electrical mapping,” Med. Biol. Eng. Comput., vol. 33, no. 3, pp. 476-81, May. 1995.

[5] J. Laforet, D. Guiraud, D. Andreu, H. Taillades, and C.A. Coste, “Smooth muscle modeling and experimental identification: application to bladder isometric contraction,” *Journal of neural engineering*, vol. 8, no. 3, pp. 036024, May. 2011.

Summary:

The uterine EMG -called Electrohysterogramme (EHG)- temporal, frequency, and time-frequency characteristics have been used for a long time for the prediction of preterm labor. However, the investigation of its propagation is rare. All the results of the previous studies did not show a satisfactory potential for clinical application. The objective of this thesis is the analysis of the propagation as well as of the nonlinear characteristics of EHG signals during pregnancy and labor for clinical application. A monovariate analysis was done to investigate the nonlinearity and the sensibility of methods to different characteristics of the signals. A bivariate analysis was then done for the investigation of the propagation of EHG by measuring the coupling between channels, as well as the direction of coupling, which is an innovative part of our thesis. In this analysis we propose a new approach to improve the coupling and direction estimation methods. Another innovation of this thesis is the implementation of a tool for EHG source localization to investigate the dynamic of the uterus at the source level, not at electrodes level as previously done. Results show that nonlinear methods are more able to classify pregnancy and labor contractions than linear ones, and that time reversibility method is the least sensitive to sampling frequency and frequency content of the signal. Results also indicate an increase in coupling and a concentration of coupling direction toward the cervix when going from pregnancy to labor. We also proposed to respect the nonstationarity of EHG signal and to recover the effect of variable fat filtering along pregnancy, by segmenting and filtering the EHG in its FWL component. This filtering-windowing approach permits to improve the performances of connectivity methods. Finally, the intensity of localized sources and their number is higher in labor than in pregnancy contractions. The identified sources are more active and more propagated in labor whereas in pregnancy they remain weak and local. An improvement in the electrode matrix of the rat experimental protocol has also been done by developing a suction electrode. This protocol can then be used for the validation of our methods and of the electrophysiological model.

Keywords:

Prediction of preterm labor, nonlinearity analysis, coupling and direction analysis, source localization.

Résumé:

L'EMG utérin appelé Electrohystérogramme (EHG) a été exploité depuis longtemps par ses caractéristiques temporelles, fréquentielles, et temps-fréquence, pour la prédiction de l'accouchement prématuré, tandis que l'étude de sa propagation est rare. Tous les résultats des études antérieures n'ont pas montré un potentiel satisfaisant pour une application clinique. L'objectif de cette thèse est l'analyse de la propagation ainsi que de la non-linéarité des signaux EHG pendant la grossesse et le travail en vue d'une application clinique. Une analyse monovariée a été faite pour étudier la non-linéarité et la sensibilité des méthodes aux différentes caractéristiques des signaux. Une analyse bivariée a ensuite été menée pour l'étude de la propagation de l'EHG, en mesurant le couplage entre les voies ainsi que la direction de couplage, ce qui est une nouveauté de notre thèse. Dans cette analyse, nous proposons une approche de filtrage-fenêtrage pour améliorer les méthodes d'estimation du couplage et de sa direction. Une autre nouveauté de cette thèse est l'implantation d'un outil de localisation de source d'EHG pour étudier la dynamique de l'utérus au niveau de la source, et non pas au niveau des électrodes comme fait dans les études précédentes. Les résultats montrent que les méthodes non linéaires sont plus capables que les méthodes linéaires, de classifier les contractions de grossesse et de travail. La méthode de réversibilité de temps est la moins sensible à la fréquence d'échantillonnage et au contenu fréquentiel du signal. Les résultats indiquent également une augmentation de couplage et une concentration des directions vers le col de l'utérus, en allant de la grossesse vers le travail. En respectant la non-stationnarité des signaux EHG et en se libérant de l'effet de filtrage de la graisse, très variable durant la grossesse et entre les différentes femmes, notre méthode de filtrage-fenêtrage (segmentation et filtrage du signal EHG pour ne garder que la composant FWL), améliore les performances des méthodes de connectivité. L'intensité des sources localisées et leur nombre sont plus élevés durant le travail que durant la grossesse. Les sources localisées sont actives et propagées durant le travail alors que durant la grossesse elles restent faibles et localisées. Une amélioration de la matrice d'électrodes du protocole expérimental de rat a été effectuée par le développement d'une électrode à succion. Ce protocole pourra ensuite être utilisé pour la validation de nos méthodes et celle du modèle électrophysiologique.

Mots clés:

Prédiction d'accouchement prématuré, analyse non linéaire, analyse de couplage et de directionalité, localisation de source.